**Sedimentology, stratigraphy, and chronology of the Northwestern Outlet of glacial Lake Agassiz, northeastern Alberta**

by

Joseph M. Young

A thesis submitted in partial fulfillment of the requirements for the degree of

Master of Science

Department of Earth and Atmospheric Sciences
University of Alberta

## Abstract

Lake Agassiz was dammed on the retreating southern and western margins of the Laurentide Ice Sheet during the end of the last Ice Age. Periodic discharges of freshwater from the lake basin have been implicated in altering oceanic circulation and impacting global climate. Meltwater from a rapid decrease in lake level at the start of the Moorhead Phase has been hypothesized as the initiation mechanism for the Younger Dryas cold reversal (~12.9 to 11.5 ka yr BP). However, the timing and routing of this event is still disputed, as there is evidence for both easterly and northwestward drainage during this time. This thesis presents a twofold contribution to understanding the timing, dynamics, and significance of glacial Lake Agassiz meltwater centred on the Moorhead Phase.

Radiocarbon data pertaining to the Moorhead and subsequent Emerson Phases from the Lake Agassiz basin was collated and assessed using manual and statistical filters to vet the dataset. Approximately one third of existing dates were found to be inadequate chronological constraints. A Bayesian model was then applied to the filtered dataset to produce refined age ranges for the start and end of each lake phase. The modelled onset of the Moorhead Phase suggests a lack of contemporaneity to the onset of the Younger Dryas. We suggest further high-quality radiocarbon dates are needed in the Lake Agassiz basin to more robustly constrain lake dynamics during this time. This does not necessarily preclude Lake Agassiz from being the forcing mechanism but underlies the need for further high-quality radiocarbon dates in the lake basin.

Sediments associated with the northwestern outlet of Lake Agassiz were examined in the lower Athabasca River valley north of Fort McMurray, Alberta. Three distinct sedimentological reaches are identified, containing eleven principal units that bracket catastrophic Lake Agassiz during the Moorhead Phase. Our data permit the development of a new depositional model that suggests catastrophic drainage occurred into a lower stage of glacial Lake McConnell, with a subsequent transgression and deposition of a distal braided delta. Bitumen-mitigated radiocarbon ages from the distal braided delta complex indicate the northwestern outlet was well operational by at least 10.2 $^{14}C$ ka yr BP until 9.6 $^{14}C$ ka yr BP.

## Preface

Quaternary geology is a highly diverse field of science that often requires collective efforts to unravel the mysteries of an Earth that once was. As such, sections of this thesis represent collaborative works as reflected in the authorship of chapters in preparation for publication. D.G. Froese was the supervisory author and was involved with concept formation and manuscript composition of Chapters 2 and 3.

Chapter 2 of this thesis is a manuscript in preparation for publication as: Young, J.M., Reyes, A.V., and Froese, D.G. *Age evaluation of the Moorhead and Emerson Phases of glacial Lake Agassiz and their temporal connection to the Younger Dryas cold reversal*. J.M.Y, A.V.R, and D.G.F designed the research. J.M.Y collated and filtered the data, designed and implemented the Bayesian model, and wrote the manuscript with input from all authors.

Chapter 3 of this thesis is a manuscript in preparation for publication as: Young, J.M., Reyes, A.V., Woywitka, R.J., and Froese, D.G. *The Northwestern Outlet Stratigraphy of Glacial Lake Agassiz in the Fort McMurray Area, Alberta, Canada*. D.G.F designed the research. J.M.Y collected field samples, conducted laboratory analyses, and analysed data. J.M.Y., A.V.R., R.J.W. and D.G.F. interpreted sedimentological units and developed depositional models. A.V.R. devised radiocarbon pre-treatment methods for bituminous organic samples. R.J.W. applied LiDAR imaging to infer flood sedimentation profiles. J.M.Y wrote the manuscript with input from all authors.

## Acknowledgements

I owe an indescribable amount of gratitude to Duane Froese for the mentorship through the inception, progression, and completion of this project. Thank you, Duane, for having the seemingly magical ability of giving reassurance that may have saved my sanity on more than one occasion. I also thank Alberto Reyes for being readily approachable for a conversation and having an endless supply of enthusiasm for this thesis.

Thanks to Martin Margold for a countless daily discussions on all things Quaternary and showing me how a well-constructed figure can make all the difference. Special thanks to Colin Cooke for helpful comments and logistical support. Additional thanks to Murray Gingras for being a dynamic part of the supervisory committee and final defense.

Funding and support for this research in graciously acknowledged from the Northern Scientific Training Program (NSTP), University of Alberta Northern Research Awards (UANRA), the Geological Society of America, University of Alberta Graduate Students' Association, Natural Sciences and Engineering Research Council of Canada (NSERC) and Canada Research Chairs program to Duane Froese, and Alberta Environment and Parks grants to Colin Cooke and Duane Froese.

A special thanks to those who assisted in the field and lab, including Casey Buchanan, Robin Woywitka, Martin Margold, Sophie Norris, Sasiri Bandara, Lauren Davies, Joel Pumple, and Alvin Kwan. Thanks also to the hockey guys and gals and the barley-based beverage appreciating crib gang for providing much needed distractions over the course of this project.

Last, but farthest from least, a sincere thank you to my family for a continued source of love, support, and inspiration. None of this would have been possible without you all.

## Table of Contents

## List of Tables

## List of Figures

# Chapter 1: Introduction

## 1.1 Regional Overview

The end of the last glaciation in North America was characterized by the rapid diminishing of the continental-sized Laurentide Ice Sheet (LIS). Continued retreat of the LIS enabled the formation of enormous proglacial lakes in recently depressed areas along its southern and western margins. Glacial Lakes Agassiz and McConnell were the largest of these proglacial lakes, encompassing a total area of over 1.7 x $10^6$ $km^2$ throughout their ca. 5000 year histories (Fig. 1.1) (Smith, 1994; Teller and Leverington, 2004). Freshwater derived from Lake Agassiz periodically discharged into surrounding oceans through three main outlets: 1) southward into the Gulf of Mexico via the Mississippi River system; 2) eastward to the north Atlantic via the St. Lawrence River system; and 3) to the northwest, through the Clearwater and Athabasca Rivers into glacial Lake McConnell and the Mackenzie River valley, en route to the Arctic Ocean (Fig. 1.1). Much research has been conducted on the complex evolution and routing of glacial Lake Agassiz (e.g. (Upham, 1895; Elson, 1967; Klassen, 1983; Teller and Clayton, 1983; Smith and Fisher, 1993; Fisher and Smith, 1994; Leverington, Mann and Teller, 2000; Teller and Leverington, 2004; Fisher et al., 2008; Lepper et al., 2013; Teller, 2013; Breckenridge, 2015) and to a lesser extent, Lake McConnell (McConnell, 1890; Craig, 1965; Lemmen et al., 1994; Smith, 1994). Reconstructions of Lake Agassiz extents are largely based on strandline analysis and are punctuated by a rapid decrease in lake level around 13 ka yr BP, coincident with the abandonment of the southern outlet (Broecker et al., 1989). This period of low-water is termed the Moorhead Phase, lasting approximately 1000 years until a transgression in the Agassiz basin – from differential isostatic rebounding and/or a LIS re-advance (e.g. Clayton, 1983; Teller, 2001; Breckenridge, 2015) – increased the lake volume to the Campbell Beach level.


Figure 1.1. Routing of glacial lake meltwater from North America to the 1) south through the Mississippi River system; 2) east through the St. Lawrence River system; and 3) northwest through the Mackenzie River system. Laurentide Ice Sheet extent and glacial lake distribution from Dyke (2004). Location of Figure 1.3 highlighted in purple box. Modified from Murton et al. (2010).

The dynamics of glacial Lake McConnell are less documented however. Smith (1994) inferred that the lake formed ca. 13.5 ka yr BP along the northwestern margin of the LIS in the Great Bear Lake basin. Lemmen et al. (1994) suggest development started later, around 13.0 ka yr BP, before expanding southward and eventually encompassing ~ $2.4 \times 10^5$ km$^2$ across west-central Northwest Territories and northern Alberta (Fig. 1.1). The extent and distribution of the lake is evidenced in strandline complexes, raised deltas, wave-cut scarps, and silt to clay deposits (e.g. Wolfe et al., 2014). The demise of Lake McConnell occurred around 8.5-8.1 ka yr BP when isostatic adjustment uplifted and isolated the basin into the modern Lakes of Great Bear, Great Slave, and Athabasca (Smith, 1994; Lemmen et al., 1994).

### 1.2 Meltwater routing and its link to abrupt climate change

The transition from cold glacial to warmer interglacial climatic conditions at the end of the last Ice Age was not linear. The most severe climatic perturbation during this time (ca. 12.9-11.5 ka yr BP) was the Younger Dryas (YD) chronozone, where global temperatures abruptly reversed back to glacial-like conditions.

The causation of this cold reversal period has long been hypothesized to be the result of large fluxes of Lake Agassiz freshwater delivered into the Atlantic Ocean from interior North America (Johnson and McClure, 1976), supressing thermohaline circulation (THC) (Rooth, 1982). A landmark paper by Broecker et al. (1989) used oxygen isotope records from the Gulf of Mexico and radiocarbon dates from the Agassiz basin to link the abandonment of the southern outlet with the initiation of the Moorhead Low Phase and the initiation of the Younger Dryas. They inferred that Agassiz runoff was diverted from the southern to the eastern outlet at the onset of the YD, in agreement with Rooth's (1982) hypothesis. Indeed, succeeding research has noted supplemental evidence for eastward drainage of meltwater during the YD, such as oxygen isotope records (Brand and McCarthy, 2005; Cronin et al., 2012; Keigwin and Jones, 1995), micropaleontological assemblages (Levac et al., 2015; Rayburn et al., 2011), and detrital rock geochemistry (Carlson et al., 2007). However, these data disagree with similar studies on isotopic trends from microfossil assemblages in sediment cores. For example, Rodrigues and Vilks, (1994) and de Vernal et al. (1996) conclude that a large freshwater influx into the Gulf of St. Lawrence was not concurrent with the onset of the YD at ~12.9 ka yr BP.

An alternative hypothesis suggests that Lake Agassiz catastrophically drained though its northwestern outlet, into glacial Lake McConnell and eventually into the Arctic Ocean at the start of the Younger Dryas. Teller et al., (2005) note that characteristic flood deposits and geomorphological features (i.e. steep-walled, straight-trending meltwater spillway(s)) are noticeably absent from the eastern outlet. Further, radiocarbon ages constraining retreat of the LIS over the eastern outlet show the area to be ice free only after Younger Dryas time (Lowell et al., 2009; Teller et al., 2005). These dates contrast more recent $^{10}$Be surface exposure ages on boulder samples however, which display ice retreat from the eastern outlet from ca. 14.6 ± 0.6 ka yr BP to 11.9 ± 0.4 ka yr BP, suggestive that the outlet may have been ice-free before and during the YD and that Lake Agassiz overflow could have been routed into the St. Lawrence River system throughout this time (Leydet et al., 2018).

Murton et al. (2010) identify a regional flood surface near the mouth of the Mackenzie River delta demarcated by gravels unconformably overlying aeolian sands. Optically stimulated luminescence (OSL) dates on the lower sand unit range from 13.4 ± 0.9 ka yr BP to 12.8 ± 0.8 ka yr BP, with OSL dates overlying the lower flood gravels at 11.9 ± 1.0 ka yr BP and 11.8 ± 1.0 ka yr BP, respectively. Murton et al. (2010) attribute this flooding event to the routing of Lake Agassiz runoff through its northwestern outlet and suggest it was the trigger mechanism for the Younger Dryas. Likewise, Keigwin et al. (2018) produce AMS ages from depleted $\delta O^{18}$ planktonic foraminifera in sediment cores indicating an influx of freshwater into the Arctic Ocean starting around 12.9 ± 0.15 ka yr BP, consistent with magnetic susceptibility logs showing increase sedimentation rates. However, the nearest documented evidence of unequivocal Lake Agassiz flooding is >2000 km south of their study area in the Fort McMurray region (c.f. Smith and Fisher, 1993; Fisher and Smith, 1993). Further sedimentological work in the Mackenzie River valley is required to elucidate the severity and timing of Lake Agassiz discharge into Arctic Ocean. In addition, freshwater simulation studies by Tarasov and Peltier, (2005) show that an influx of freshwater into the Arctic Ocean is the most probable mechanism for triggering the Younger Dryas cold reversal, as it reduces the Atlantic THC more severely than an injection through the St. Lawrence River system (Condron and Winsor, 2012).

Lowell et al. (2005; 2009; 2013) advocate for an alternative explanation to the eastward or northwestward drainage hypotheses for the drop in Lake Agassiz during the Younger Dryas. They argue instead that a significant increase in evaporative conditions within the lake basin resulted in a negative hydrological budget, rapidly decreasing the lake extent to Moorhead Phase levels. This theory is not without objectors however. Teller, (2013) reviews paleoclimatic and paleoecological studies from the Agassiz basin and concludes that these datasets do not support the drought-driven drawdown model; rather further support drawdown from opening of a lower outlet. Similarly, Carlson et al., (2009) note that the evaporation rates required to sustain such a model are an order of magnitude greater than the highest evaporation rates recorded in modern settings. Nonetheless, Lowell et al. (2013) outline a series of theoretical and inferred hydrological and climatic parameters that enable Lake Agassiz to become a closed basin lake before and during the Younger Dryas.

### 1.3 Initiation of the Moorhead low-water Phase

The Moorhead Phase is characterized by a rapid lake level drawdown in glacial Lake Agassiz of up to ~90 m (Breckenridge, 2015) (Fig. 1.2) coinciding with the abandonment of the southern outlet around 13.0 ka yr BP (11.0 $^{14}$C ka yr BP) (Broecker et al., 1989). Constraining the onset of the Moorhead Phase has largely been attributed to the radiocarbon date of 10.96 ± 300 $^{14}$C ka yr BP (W-723) as it is the oldest seemingly reliable wood age within the Lake Agassiz basin (Moran et al., 1973; Clayton, 1983). The sample was first dated in 1960 (Rubin and Alexander, 1960) and re-dated a few years later as TAM-1, measuring 10.82 ± 190 $^{14}$C ka yr BP (Noakes et al., 1964).

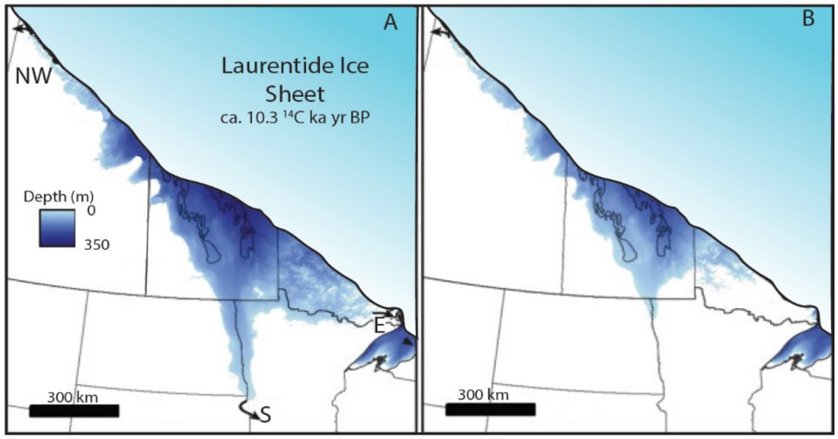


Figure 1.2. (a) Reconstructed extent of glacial Lake Agassiz at pre-Moorhead Phase levels and (b) post-Moorhead Phase levels. Estimated difference of 17000 km$^3$ of water between the two lake stages. Ice margin extent from Dyke (2004). Lake stages modified from Breckenridge (2015).

However, some researchers have since contested the use of this date for defining the onset of lake level drop. Fisher and Lowell, (2006) suggest the sample may be of reworked, or anomalously old material that was transported into the Lake Agassiz basin from paleo-river systems. They also contend that organics from similar stratigraphic horizons and depositional environments yield ages much younger than the W-723 sample (e.g. 10.08 ± 280 $^{14}$C ka yr BP; W-900 (Moran et al., 1973). Additional radiocarbon dates obtained by Fisher et al., (2008) from Moorhead beach deposits resulted in an age range from ca. 10.71 to 10.0 $^{14}$C ka yr BP. According to Fisher et al. (2008), the oldest reliable date for constraining the onset of the Moorhead Phase is ca. 10.47 $^{14}$C ka yr BP, near the end of the YD, as older samples were interpreted not *in situ* and therefore an inadequate water-level constraint. An alternative chronology is proposed by Breckenridge (2015) based on an isostatic rebound model of Lake Agassiz strandlines to calculate the beginning of the Moorhead Phase at ca. 12.1 ka yr BP, almost 1000 calendar years after the onset of the YD at ca. 13.0 ka yr BP.

Other researchers support the radiocarbon correlation linking the Moorhead drop with the abandonment of the southern outlet and the onset of the Younger

Dryas. Carlson and Clark, (2012)instead interpret the >10.5 $^{14}$C ka yr BP radiocarbon dates of Fisher et al. (2008) as an adequate lake-level constraint as 1) multiple wood ages older than 10.5 $^{14}$C ka yr BP exist on Lake Agassiz sediment, and 2) the 'older' radiocarbon dates are within error of distal Lake Agassiz runoff and proxy records of the YD. Bajc et al., (2000) note a wood date of 10.8 $^{14}$C ka yr BP in the Eastern portion of the Lake Agassiz basin that could only be used to define the beginning of the low-water phase only if the organics were not affected by long-distance transport and reworking.

### 1.4 The Northwestern Outlet

The Northwestern Outlet did not prominently fit into the early works on the history of glacial Lake Agassiz (e.g. Upham, 1895; Elson, 1967; Teller and Thorleifson, 1983). The outlet was first documented by Sproule, (1939), who suggested that increased meltwater from the retreating LIS carved out the Clearwater lower Athabasca Spillway (CLAS) (Fig. 1.3). Christiansen (1979) and Schreiner (1983) later speculated that a westward flow from the regional glacial Lake Meadow was responsible for carving out the spillway. It was not until Smith and Fisher (1993) documented extensive sheets of boulder gravel in the Fort McMurray region that the northwestern outlet garnered significant interest in the scientific community. Eastward trending paleocurrent measurements on boulder gravel deposits coupled with strandline complexes and glaciolacustrine deposits at the head of the spillway linked a highstand of Lake Agassiz with catastrophic drainage through the area (Smith and Fisher, 1993). The paleoflood model presented by Smith and Fisher (1993) suggested that floodwaters carved out the CLAS and deposited a large, Late Pleistocene braid delta along the Athabasca River (Rhine and Smith, 1988) into glacial Lake McConnell at approximately 300 m elevation. Chronology for this event was approximate at the time, as Smith and Fisher (1993) averaged 6 radiocarbon dates (ranging from 10.3 ka yr BP to 9.4 ka yr BP) associated with flood and delta deposits to infer that the outlet facilitated catastrophic Lake Agassiz drainage around 9.9 ka yr BP.

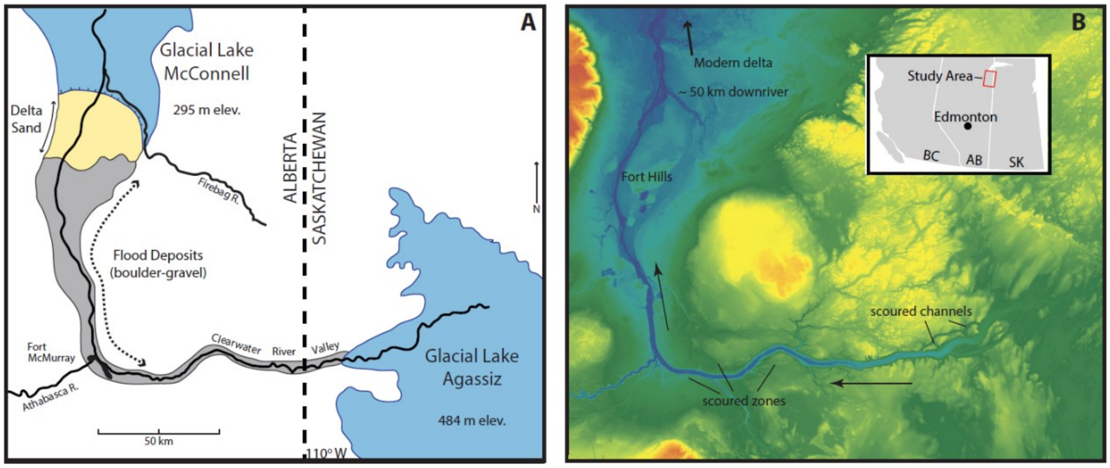


Figure 1.3. The northwestern outlet of glacial Lake Agassiz. (A) Depositional model in the lower Clearwater and Athabasca River valleys consisting of proximal flood gravels abruptly transitioning into deltaic sands built into glacial Lake McConnell at 295 m elevation. Lake Agassiz represented at maximum extent at the head of the Clearwater spillway. Modified from Smith and Fisher (1993). (B) Digital elevation model of the northwestern outlet with scoured zones and direction of catastrophic flooding (black arrows) denoted.

Fisher et al. (2009) and Fisher and Lowell (2012) aimed to further constrain the timing of outlet availability by obtaining >70 radiocarbon dates from >30 lakes sediment cores associated with deglacial moraines in the Fort McMurray region. They content that the LIS vacated the lower Athabasca valley – therefore permitting northward meltwater drainage – around 9.8 – 9.6 $^{14}$C ka yr BP based on these minimum-limiting ages. However, as Teller (2013) notes, the base of the clastic (glacial) to organic (deglacial) transition in >70% of the cores was not reached, questioning the viability of using such ages to constrain ice retreat. In addition, dates >10 ka yr BP have been obtained from the lower Athabasca River valley (c.f. Murton et al., 2010), which Murton et al. (2010) use further suggest a connection between the Younger Dryas and northwestward drainage of Lake Agassiz into the Arctic Ocean. The lone optically stimulated luminescence (OSL) date within the Fort McMurray region is from deltaic sands just west of Fort McMurray, with an age of 14.0 ± 1.0 ka yr BP, as reported by (Munyikwa et al. , 2017).

### 1.5 Thesis Objectives and Outline

The overarching objective of this thesis is to investigate the drainage of glacial Lake Agassiz through its northwestern outlet. Specifically, the timing and dynamics of meltwater drainage are investigated using a combination of sedimentology, stratigraphy, geomorphology, and statistical modelling. This is accomplished through two paper-based chapters in this thesis.

Chapter 2 of this thesis is a paper titled: *Age evaluation of the Moorhead and Emerson Phases of glacial Lake Agassiz and their Temporal Connection to the Younger Dryas Cold Reversal*. This chapter is a critical synthesis and re-assessment of the radiocarbon ages associated with the Moorhead and Emerson phases in the southern glacial Lake Agassiz basin. Existing radiocarbon ages are vetted through manual and statistical methods to produce a robust chronological dataset. The vetted dataset is then subject to a Bayesian model that produces refined age probability ranges for the onset and demise of the Moorhead and Emerson Phases respectively. Resultant probability age determinations are then related to glacial Lake Agassiz drainage and shifts in Pleistocene climate, most notably the Younger Dryas.

Chapter 3 of this thesis is a paper titled: *The Northwestern Outlet Stratigraphy of Glacial Lake Agassiz in the Fort McMurray Area, Alberta, Canada*. This chapter presents stratigraphic descriptions from river-cut and mining exposures in the lower Athabasca River Valley, which provide insight into the dynamics associated with northwestward drainage from glacial Lake Agassiz into glacial Lake McConnell. Sedimentological units relating to the retreat of the Laurentide Ice Sheet, Lake Agassiz flooding, and post-flood stages of the region are defined. An absence of clear flood sedimentation in the medial to distal reaches of the valley coupled with a steeply-grading flood profile prompt the development of a conceptual depositional model, which suggests flooding occurred during a low-stand elevation of glacial Lake McConnell and pre-dates the deposition of the distal braid delta at ca. 10.2 ka yr BP. Results from Chapter 3 show that the northwestern outlet facilitated meltwater to the Arctic Ocean at least during the later part of the Younger Dryas cold period, but possibly earlier if flooding preceded braided delta formation. Chapter 4 summarizes the results of Chapters 2 and 3 and relates the key findings to the thesis objectives. Future avenues of research relating to meltwater routing into the Arctic Ocean and the relation to abrupt climate change are also discussed.

**References**

Bajc, A.F., Schwert, D.P., Warner, B.G., Williams, N.E., 2000. A reconstruction of Moorhead and Emerson Phase environments along the eastern margin of glacial Lake Agassiz, Rainy River basin, northwestern Ontario. Can. J. Earth Sci. 37, 1335–1353. https://doi.org/10.1139/e00-051

Brand, U., McCarthy, F.M.G., 2005. The Allerød-Younger Dryas-Holocene sequence in the west-central Champlain Sea, eastern Ontario: A record of glacial, oceanographic, and climatic changes. Quat. Sci. Rev. 24, 1463–1478. https://doi.org/10.1016/j.quascirev.2004.11.002

Breckenridge, A., 2015. The Tintah-Campbell gap and implications for glacial Lake Agassiz drainage during the Younger Dryas cold interval. Quat. Sci. Rev. 117, 124–134. https://doi.org/10.1016/j.quascirev.2015.04.009

Broecker, W.S., Kennett, J.P., Flower, B.P., Teller, J.T., Trumbore, S., Bonani, G., Wolfli, W., 1989. Routing of meltwater from the Laurentide Ice Sheet during the Younger Dryas cold episode. Nature 341, 318–321. https://doi.org/10.1038/341318a0

Carlson, A.E., Clark, P.U., 2012. Ice Sheet Sources of Sea Level Rise and Freshwater Discharge During the Last Deglaciation. Rev. Geophys. 50, https://doi:10.1029/2011RG000371.

Carlson, A.E., Clark, P.U., Haley, B.A., Klinkhammer, G.P., Simmons, K., Brook, E.J., Meissner, K.J., 2007. Geochemical proxies of North American freshwater routing during the Younger Dryas cold event. Proc. Natl. Acad. Sci. 104, 6556-6561. https://doi.org/10.1073/pnas.0611313104

Carlson, A.E., Clark, P.U., Hostetler, S.W., 2009. Comment : Radiocarbon deglaciation chronology of the Thunder Bay , Ontario area and implications for ice sheet retreat patterns. Quat. Sci. Rev. 28, 2546–2547.

https://doi.org/10.1016/j.quascirev.2009.05.005

Christiansen, E.A., 1979. The Wisconsinan deglaciation of southern Saskatchewan and adjacent areas. Can. J. Earth Sci. 17, 913–938. https://doi.org/10.1139/e80-052

Clayton, L., 1983. Chronology of Lake Agassiz drainage to Lake Superior, in: Teller, J. T. and Clayton, L. Eds, Glacial Lake Agassiz. 291–307. Geolgical Survey of Canada Special Paper 26.

Condron, A., Winsor, P., 2012. Meltwater routing and the Younger Dryas. Proc. Natl. Acad. Sci. 109, 1–6. https://doi.org/10.1073/pnas.1207381109

Cronin, T.M., Rayburn, J.A., Guilbault, J.P., Thunell, R., Franzi, D.A., 2012. Stable isotope evidence for glacial lake drainage through the St. Lawrence Estuary, eastern Canada, ~13.1-12.9 ka. Quat. Int. 260, 55–65. https://doi.org/10.1016/j.quaint.2011.08.041

de Vernal, A., Hillaire-Marcel, C., Bilodeau, G., 1996. Reduced meltwater outflow from the Laurentide ice margin during the Younger Dryas. Nature 381, 774.

Dyke, A.S., 2004. An outline of North American deglaciation with emphasis on central and northern Canada. Dev. Quat. Sci. 2, 373–424. https://doi.org/10.1016/S1571-0866(04)80209-4

Elson, J.A., 1967. Geology of glacial Lake Agassiz. In: Mayer-Oakes, W.J. (ed.), Life, Land, and Water. University of Manitoba Press, Winnipeg, pp. 37-95. 1967.

Fisher, T.G., Lowell, T. V., 2012. Testing northwest drainage from Lake Agassiz using extant ice margin and strandline data. Quat. Int. 260, 106–114. https://doi.org/10.1016/j.quaint.2011.09.018

Fisher, T.G., Lowell, T. V, 2006. Questioning the age of the Moorhead Phase in the glacial Lake Agassiz basin. Quat. Sci. Rev. 25, 2688–2691. https://doi.org/10.1016/j.quascirev.2006.05.007

Fisher, T.G., Smith, D.G., 1994. Glacial Lake Agassiz: Its northwest maximum extent and outlet in Saskatchewan (Emerson Phase). Quat. Sci. Rev. 13, 845–858. https://doi.org/10.1016/0277-3791(94)90005-1

Fisher, T.G., Smith, D.G., 1993. Exploration for Pleistocene aggregate resources using process-depositional models in the Fort Mcmurray region, Ne Alberta, Canada. Quat. Int. 20, 71–80. https://doi.org/10.1016/1040-6182(93)90037-G

Fisher, T.G., Waterson, N., Lowell, T. V., Hajdas, I., 2009. Deglaciation ages and meltwater routing in the Fort McMurray region, northeastern Alberta and northwestern Saskatchewan, Canada. Quat. Sci. Rev. 28, 1608–1624. https://doi.org/10.1016/j.quascirev.2009.02.003

Fisher, T.G., Yansa, C.H., Lowell, T. V., Lepper, K., Hajdas, I., Ashworth, A., 2008. The chronology, climate, and confusion of the Moorhead Phase of glacial Lake

Agassiz: new results from the Ojata Beach, North Dakota, USA. Quat. Sci. Rev. 27, 1124–1135. https://doi.org/10.1016/j.quascirev.2008.02.010

Johnson, R.G., McClure, B.T., 1976. A model for Northern Hemisphere continental ice sheet variation. Quat. Res. 6, 325–353. https://doi.org/10.1016/0033-5894(67)90001-4

Keigwin, L.D., Jones, G. a, 1995. The Marine Record of Deglaciation from the Continental-Margin Off Nova-Scotia. Paleoceanography 10, 973–985. https://doi.org/10.1029/95PA02643

Keigwin, L.D., Klotsko, S., Zhao, N., Reilly, B., Giosan, L., Driscoll, N.W., 2018. Deglacial floods in the Beaufort Sea preceded Younger Dryas cooling. Nat. Geosci. https://doi.org/10.1038/s41561-018-0169-6

Klassen, R.W., 1983. Lake Agassiz and the late glacial history of northern Manitoba. In: Teller, J. T. and Clayton, L. Eds, Glacial Lake Agassiz, pp. 97-115, Geological Association of Canada Special Paper 26. 97–115.

Lemmen, D.S., Duk-Rodkin, A., Bednarski, J.M., 1994. Late glacial drainage systems along the northwestern margin of the Laurentide Ice Sheet. Quat. Sci. Rev. 13, 805–828. https://doi.org/10.1016/0277-3791(94)90003-5

Lepper, K., Buell, A.W., Fisher, T.G., Lowell, T. V., 2013. A chronology for glacial Lake Agassiz shorelines along Upham's namesake transect. Quat. Res. 80, 88–98. https://doi.org/10.1016/j.yqres.2013.02.002

Levac, E., Lewis, M., Stretch, V., Duchesne, K., Neulieb, T., 2015. Evidence for meltwater drainage via the St. Lawrence River Valley in marine cores from the Laurentian Channel at the time of the Younger Dryas. Glob. Planet. Change 130, 47–65. https://doi.org/10.1016/j.gloplacha.2015.04.002

Leverington, D.W., Mann, J.D., Teller, J.T., 2000. Changes in the bathymetry and volume of glacial Lake Agassiz between 11,000 and 930014C yr B.P. Quat. Res. 54, 174–181. https://doi.org/10.1006/qres.2000.2157

Leydet, D.J., Carlson, A.E., Teller, J.T., Breckenridge, A., Barth, A.M., Ullman, D.J., Sinclair, G., Milne, G.A., Cuzzone, J.K., Caffee, M.W., 2018. Opening of glacial Lake Agassiz's eastern outlets by the start of the Younger Dryas cold period. Geology 46, 155–158. https://doi.org/10.1130/G39501.1

Lowell, T., Waterson, N., Fisher, T., Loope, H., Glover, K., Comer, G., Hajdas, I., Denton, G., Schaefer, J., Rinterknecht, V., Broecker, W., Teller, J., 2009. Reply to comments by Carlson et al ., ( 2009 ) on Radiocarbon deglaciation chronology of the Thunder Bay , Ontario area and implications for ice sheet retreat patterns 28, 2548–2550. https://doi.org/10.1016/j.quascirev.2009.06.022

Lowell, T., Waterson, N., Fisher, T., Loope, H., Glover, K., Comer, G., Hajdas, I., Denton, G., Schaefer, J., Rinterknecht, V., Broecker, W., Teller, J., 2005. Testing the Lake

Agassiz meltwater trigger for the Younger Dryas. Eos, Trans. Am. Geophys. Union 86, 365. https://doi.org/10.1029/2005EO400001

Lowell, T. V, Applegate, P.J., Fisher, T.G., Lepper, K., 2013. What caused the low-water phase of glacial Lake Agassiz ? Quat. Res. 80, 370–382. https://doi.org/10.1016/j.yqres.2013.06.002

Lowell, T. V, Fisher, T.G., Hajdas, I., Glover, K., Loope, H., Henry, T., 2009. Radiocarbon deglaciation chronology of the Thunder Bay , Ontario area and implications for ice sheet retreat patterns. Quat. Sci. Rev. 28, 1597–1607. https://doi.org/10.1016/j.quascirev.2009.02.025

Moran, S.R., Clayton, L., Scott, M., Brophy, J., 1973. Catalog of North Dakota radiocarbon dates. North Dakota Geol. Surv. Misc. Ser. 53, 1–51.

Munyikwa, K., Rittenour, T.M., Feathers, J.K., 2017. Temporal constraints for the Late Wisconsinan deglaciation of western Canada using eolian dune luminescence chronologies from Alberta. Palaeogeogr. Palaeoclimatol. Palaeoecol. 470, 147–165. https://doi.org/10.1016/j.palaeo.2016.12.034

Murton, J.B., Bateman, M.D., Dallimore, S.R., Teller, J.T., Yang, Z., 2010. Identification of Younger Dryas outburst flood path from Lake Agassiz to the Arctic Ocean. Nature 464, 740–743. https://doi.org/10.1038/nature08954

Noakes, J.E., Stipp, J.J., Hood, D.W., 1964. Texas A & M University radiocarbon dates 1. Radiocarbon 6, 189–193.

Rayburn, J.A., Cronin, T.M., Franzi, D.A., Knuepfer, P.L.K., Willard, D.A., 2011. Timing and duration of North American glacial lake discharges and the Younger Dryas climate reversal. Quat. Res. 75, 541–551. https://doi.org/10.1016/j.yqres.2011.02.004

Rhine, J.L., Smith, D.G., 1988. The late Pleistocene Athabasca braid delta of northeastern Alberta, Canada. In: W. Nemec, R. Steel Eds, Fan Deltas: Sedimentology and Tectonic Settings, Blackie and Son Ltd, Glasgow, U.K. 159-169.

Rodrigues, C.G., Vilks, G., 1994. The impact of glacial lake runoff on the goldthwait and champlain seas: The relationship between glacial lake agassiz runoff and the younger dryas. Quat. Sci. Rev. 13, 923–944. https://doi.org/10.1016/0277-3791(94)90009-4

Rooth, C., 1982. Hydrology and ocean circulation. Prog. Oceanogr. 11, 131–149. https://doi.org/10.1016/0079-6611(82)90006-4

Rubin, M., Alexander, C., 1960. U.S. Geological Survey Radiocarbon Dates V 2, 129–185.

Schreiner, B.T., 1983. Lake Agassiz in Saskatchewan, in: Teller, J.T., and Clayton, L., Glacial Lake Agassiz: Geological Association of Canada Special Paper 26. pp. 75–79.

Smith, D.G., 1994. Glacial lake McConnell: Paleogeography, age, duration, and associated river deltas, mackenzie river basin, western Canada. Quat. Sci. Rev. 13, 829–843. https://doi.org/10.1016/0277-3791(94)90004-3

Smith, D.G., Fisher, T.G., 1993. Glacial Lake Agassiz: The northwest outlet and paleoflood. Geol. 21. 9–12.

Sproule, J.C., 1939. The Pleistocene geology of the Cree Lake region, Saskatchewan. R. Soc. Canada Trans. 33, 101–109.

Tarasov, L., Peltier, W.R., 2005. Arctic freshwater forcing of the Younger Dryas cold reversal. Nature, 435, 662–665. https://doi.org/10.1038/nature03617

Teller, J.T., 2013. Lake Agassiz during the Younger Dryas. Quat. Res.80, 361–369. https://doi.org/10.1016/j.yqres.2013.06.011

Teller, J.T., 2001. Formation of large beaches in an area of rapid differential isostatic rebound: The three-outlet control of Lake Agassiz. Quat. Sci. Rev. 20, 1649–1659. https://doi.org/10.1016/S0277-3791(01)00007-5

Teller, J.T., Boyd, M., Yang, Z., Kor, P.S.G., Fard, A.M., 2005. Alternative routing of Lake Agassiz overflow during the Younger Dryas: New dates, paleotopography, and a re-evaluation. Quat. Sci. Rev. 24, 1890–1905. https://doi.org/10.1016/j.quascirev.2005.01.008

Teller, J.T., Clayton, L., 1983. Glacial Lake Agassiz. Geological Association Canada Special Paper. p. 451.

Teller, J.T., Leverington, D.W., 2004. Glacial Lake Agassiz: A 5000 yr history of change and its relationship to the δ18O record of Greenland. Bull. Geol. Soc. Am. 116, 729–742. https://doi.org/10.1130/B25316.1

Teller, J.T., Thorleifson, L.H., 1983. The Lake Agassiz – Lake Superior connection, In: Teller, J.T. and Clayton, L. Eds, Glacial Lake Agassiz, pp. 261–290.Geological Association Canada, Special Paper, 26.

Upham, W., 1895. The Glacial Lake Agassiz. U.S. Geol. Surv. Monogr. 25, 658.

# Chapter 2: Age evaluation of the Moorhead and Emerson Phases of glacial Lake Agassiz and their temporal connection to the Younger Dryas cold reversal


### Abstract

The Moorhead Phase of glacial Lake Agassiz has long been attributed to rapid drawdown in lake level contemporaneous with the onset of the Younger Dryas (YD) cold reversal. Here, we examine the radiocarbon dates associated with the Moorhead and subsequent Emerson Phase in the southern Lake Agassiz Basin. We apply manual and statistical filters to vet the radiocarbon dataset (n=99), resulting in the exclusion of about one third of existing dates. A Bayesian meta-analysis is applied on the filtered dataset (n=70) to produce a series of probability age ranges on the onset and demise of each phase. A modeled 2-sigma age range of 12,470 – 12,120 cal yr BP is attributed to the onset of the Moorhead Phase, post-dating the onset of the YD. The Emerson Phase starts 11,600 – 11,280 cal yr BP and ends 10,710 – 10,320 cal yr BP (2-sigma). At present, we find existing high-quality radiocarbon dates in the Lake Agassiz basin too few; an increase in ages are required to more robustly constrain lake-level fluctuations.


### 2.1 Introduction

Glacial Lake Agassiz formed on the southern margin of the Laurentide Ice Sheet during the last deglaciation, covering an area of around 1 million square kilometers throughout its existence (Fig. 2.1a) (Teller and Leverington, 2004). The history of Lake Agassiz is largely defined by widespread strandline complexes, recording fluctuations in lake level and shifting outlets (e.g. Elson, 1967; Teller, 2001; Breckenridge, 2015). Large discharges of freshwater sourced from Lake Agassiz have been invoked as the initiation mechanism for the Younger Dryas (YD) cold reversal via disruption of the Atlantic Meridional Overturning Circulation (AMOC) (Broecker et al., 1989; Clark et al., 2001). This inference is largely based on the apparent contemporaneity between the beginning of the YD and the onset of Lake Agassiz's Moorhead low-water Phase at 12,900 cal yr BP (Broecker et al., 1989).

The Moorhead Phase is characterized by a rapid drawdown in lake level of ~90 m (Breckenridge, 2015), whereby flow diverted from a southern outlet (to the Gulf of Mexico) to an outlet of lower elevation (Moran et al., 1973; Broecker et al., 1989)—either through the St. Lawrence Valley to the east (Carlson et al., 2007; Cronin et al., 2012; Leydet et al., 2018), or through the Mackenzie River system to the northwest (Teller et al., 2005; Murton et al., 2010; Keigwin et al., 2018). An alternative hypothesis is that meltwater drainage is not the mechanism for the low-water stage of glacial Lake Agassiz. In this scenario, climatic change resulting in a negative hydrological balance in the Lake Agassiz basin was the mechanism responsible for lake drawdown (Lowell and Fisher, 2009; Lowell et al., 2013).

In previous studies, a key radiocarbon date of 10,960 ± 300 $^{14}$C yr BP (W-723) has been used to define the onset of this drop in lake level, as it is the oldest radiocarbon determination taken from beach sediment associated with the Moorhead Phase (Moran et al., 1973; Clayton, 1983). However, there is considerable debate on this key constraint for low-stand initiation. Fisher and Lowell (2006) questioned the reliability of the W-723 radiocarbon date and suggested that it inadequately defines the start of the Moorhead Phase because: 1) the potential that the sample consists of reworked, older material that was transported into the Agassiz basin, and 2) organics from stratigraphically similar strandline sections have yielded younger age determinations (e.g. 10,080 ± 280 $^{14}$C yr BP; W-900 (Moran et al., 1973)). Building on these critiques, Fisher et al. (2008) vetted previously published radiocarbon ages not considered *in situ* and obtained additional radiocarbon dates from Moorhead beach deposits near the original W-723 section west of Grand Forks, North Dakota (Fig. 2.1), ranging from 10,710 ± 75 $^{14}$C yr BP (ETH-32674) to 10,000 ± 70 $^{14}$C yr BP (ETH-32679). Fisher et al. (2008) conclude that the oldest reliable date for the beginning of the Moorhead Phase in the Agassiz basin is 10,470 ± 75$^{14}$C yr BP (ETH-32671)—dismissing their older ETH-32674 date, and the original W-723 date, due to their apparently anomalous ages relative to other radiocarbon ages in the section.

In contrast, other researchers accepted the initial temporal correlation by Broecker et al. (1989), based on the W-723 sample, between the abrupt drop in the level of Lake Agassiz and the onset of the YD. For example, Carlson and Clark (2012) include all radiocarbon ages older than ca. 12,600 cal yr BP (11,000 $^{14}$C yr BP) in the lake basin, concluding that the W-723 and ETH-32674 dates adequately constrain the start of the Moorhead Phase because they are within the range of age uncertainty for YD initiation in proxy records of climate and distal Lake Agassiz runoff. Bajc et al. (2000) note one of the oldest wood dates of 10,810 ± 240$^{14}$C yr BP (TO-1504) in Moorhead Phase sediments in northwestern Ontario as a potential constraint for lake level drawdown—with the assumption that the wood was not a product of long-distance retransportion. In a different approach, Breckenridge (2015) constructs an isostatic rebound model from strandline isobases to estimate the timing of drawdown to the Moorhead level. By assuming the rate of rebound exponentially decayed with a relaxation time of 3500 years, and that an optically stimulated luminescence (OSL) date of 10,500 ± 300 yr BP (Lepper et al., 2013) constrains development of the Campbell strandlines, Breckenridge (2015) calculated an age of 12,180 ± 350 cal yr BP for the onset of the Moorhead Phase lake level drop.

The Moorhead Phase ended with a transgression in lake level, enabling lake drainage to return to a higher outlet and marking the start of Lake Agassiz's Emerson Phase (Clayton, 1983). Similar to the chronology of the Moorhead Phase, various interpretations for the timing of this transgression have been proposed over many years of Lake Agassiz research. Initial insights suggested the Emerson Phase started around 10,000$^{14}$C yr BP, based on radiocarbon dates on wood buried in transgressive infills of former low-water channels throughout the southern extent of the basin (Moran et al., 1971; Fenton et al., 1983; Bjorck and Keister, 1983). More recent examination of key late-glacial sites in the Lake Agassiz Basin have yielded similar conclusions (Bajc et al., 2000; Yansa and Ashworth, 2005; Boyd, 2007). An alternative hypothesis is that meltwater during the Moorhead Low was routed through the northwestern outlet at ca. 9,900 $^{14}C$ yr BP, and transgression occurred later around 9,400$^{14}C$ yr BP (Fisher et al., 2008)—in agreement with estimates for the re-activation of Agassiz's southern outlet (Fisher, 2003). Similarly, Lepper et al. (2011, 2013) argue in favour of a later transgression based on mean ages of select OSL dates from Campbell Beach strandlines. The timing of the end of the Emerson Phase—characterized by lake-level drop below the Campbell Beach shorelines and reactivation of Lake Agassiz's eastern outlet (Fig. 2.1b) (Fenton et al., 1983)—is similarly uncertain. Relatively poor chronological constraints hinder estimates on the end of this lake phase, ranging from ca. 9,600 $^{14}C$ yr BP (Fenton et al., 1983; Clayton, 1983), to ca. 9,400 $^{14}C$ yr BP (Teller, 2001).

The abundance of radiocarbon dates from various depositional environments and locales, separated by 100s of kilometers within the Lake Agassiz basin, highlights the challenge of assigning specific ages to distinct phases in the evolution and drainage history of Lake Agassiz (Fig. 2.1c). As a result, the collective Lake Agassiz $^{14}C$ dataset assembled over the last 45 years includes dates of wildly varying precision and reliability, and there is presently no consensus framework for lake chronology. In turn, it is difficult to unequivocally link events in the Lake Agassiz basin to key climatic events during deglaciation. The aim of this paper is to evaluate the radiocarbon dates associated with the Moorhead and Emerson Phases within the basin of glacial Lake Agassiz. We use Bayesian $^{14}C$ calibration methods to construct internally consistent age estimates for: 1) the onset of the Moorhead Phase, 2) the transgression between the Moorhead and Emerson Phases, and 3) the end of the Emerson Phase.

**2.2 Bayesian Modelling**

The application of Bayesian statistics to radiocarbon datasets has proven to be useful in assessing chronological robustness across a variety of geoscience disciplines. For example, Bayesian methods have been used to refine archeological inferences on the duration and temporal boundaries of culturally significant periods (e.g. Denaire et al., 2017), refine glacial chronologies (e.g. Small et al., 2017), and to better constrain the ages of tephra horizons in sedimentary sequences (e.g. Kuehn et al., 2009; Davies et al., 2016). Various Bayesian modelling software packages such as Bacon (Blaauw and Christensen, 2011), BCal (Buck et al., 1999), Datelab (Jones and Nicholls, 2011) and OxCal (Bronk Ramsey, 2009a) have been developed in conjunction with Markov Chain Monte Carlo (MCMC) analysis (Gilks et al., 1996), to assist in model development and application.

The principle difference between Bayesian and frequentist probability distribution statistics is the integration of *prior* information (i.e. knowledge on corresponding samples before calculation) into the Bayesian framework (Buck et al., 1996). With respect to radiocarbon dating, such *a priori* information can be defined as, for example: how likely an individual date is to be erroneous, the relative stratigraphic position of samples, or the magnitude of any $^{14}C$ reservoir offsets. In turn, this information is combined with individual likelihoods in the form of absolute radiocarbon dating information, producing a set of *posterior* probability density functions that represent modelled calendar age ranges.

## 2.3 Methods

### *2.3.1 Data source and selection*

We first compiled radiocarbon dates pertaining to the Moorhead and Emerson Phases of glacial Lake Agassiz. The initial database consisted of 97 radiocarbon ages on organic material throughout the Lake Agassiz basin, with 56 ages associated with the Moorhead Phase and 41 ages associated with the Emerson Phase (Table 1). Optically stimulated luminescence (OSL) dates were not included in this study; the millennia-scale uncertainty ranges associated with luminescence dating techniques render OSL dates less useful in this context. All $^{14}C$ dates, including ages that have previously been rejected or their context re-interpreted, were first calibrated using the IntCal13 radiocarbon calibration curve (Reimer et al., 2013; Table 1) using OxCal V4.3 software (Bronk Ramsey, 2009a).

The compiled dates, however, displayed large variations in overall quality, from uncertain pre-treatment methods applied to identified terrestrial macrofossils (e.g. Beta-121851; Yansa and Ashworth, 2005), to clam shells in alluvial fill dated via the solid carbon method (e.g. Y-166; Preston et al., 1955). It is therefore necessary to filter the dataset before implementation into a Bayesian model (Bronk Ramsey, 2009b). Multiple strategies have been used to vet large radiocarbon datasets, ranging from manual quality assurance tests (e.g. Kuehn et al., 2009; Blockley and Pinhasi, 2011; Reyes and Cooke, 2011) to entirely statistical detection of outliers (e.g. Small et al., 2017). The strategy employed in this study was to first manually reject dates based on criteria similar to those outlined in Kuehn et al. (2009), followed by applying a Bayesian outlier analysis to the filtered dataset. Here, we removed radiocarbon dates on materials known to be problematic for accurate radiocarbon determinations, including bulk sediments or aquatic macrofossils, because these materials are prone to hard-water effects (Shotton, 1972). We also rejected samples without a clear stratigraphic association to Moorhead or Emerson phase sediments or landforms. The lone bone sample in the compilation (BGS-617; Teller, 1980) was rejected because a reliable pre-treatment method (i.e. collagen extraction) was not specified (e.g. Brock et al., 2007). All calibrated dates are reported as calibrated years before present (cal yr BP), where BP refers to CE 1950, at the 2σ (95.4%) confidence interval.

### *2.3.2 Model Construction*

A Bayesian model consisting of two contiguous *phases* was constructed using the OxCal V4.3 software (Bronk Ramsey, 2009a). The underlying assumption in this model is that Moorhead Phase deposits directly precede those of the Emerson Phase, and that there is a transgressive sequence between the two phases (Fig. 2.1b) (Teller, 2001). Each *phase* consists of multiple radiocarbon dates in which there is no internal ordering—i.e. no prior stratigraphic or temporal relationship between individual dates is defined. The timing of these *phases* is constrained through the use of *boundary* functions that, in this model, define the endmember borders along with the transitional boundary between phases, using all of the grouped radiocarbon dates in the calculation (Bronk Ramsey, 2009a). The boundary between the Moorhead and Emerson Phases was modelled using a trapezium-based prior (Lee and Bronk Ramsey, 2012). This allows for a more gradational transition between the two phases and allows for the possibility that some organics recovered from (younger) Emerson Phase sediment may be reworked from (older) Moorhead-aged deposits. Samples that were dated multiple times were combined before calibration by using the *R_Combine* function. This function was applied to samples: BGS-1303 and WAT-1935, I-5123 and I-5123c, and to W-723 and TAM-1. All calibrated dates were subject to a temporal outlier model to statistically detect any outlying dates. The *Outlier_Model* function (c.f. Bronk Ramsey, 2009b) was implemented, with each date having a prior value of 0.05—i.e. a 5 percent probability of being an outlier, due to any potential sampling, handling, or analytical errors. The model uses a Student's t-distribution to determine outliers over a span of 10 to 10,000 years, identifying potential outliers in the time variable (Bronk Ramsey 2009b). OxCal also calculates an Agreement Index to quantify how well the posterior (modelled) distribution for a given calibrated age range overlaps with the prior (unmodelled) age range probability distribution. An Agreement Index is also calculated for the entirety of the model. The recommended Agreement Index value is >60% (Bronk Ramsey 2009a), roughly corresponding to a chi-square distribution of >95% confidence interval (Bronk Ramsey 2009a). After performing outlier testing, radiocarbon dates were statistically rejected only if they met all the following criteria: 1) being identified as a potential outlier with the outlier model; 2) an individual Agreement Index of <60%, and 3) the overall Agreement Index of the model was below the 60% threshold. Rejected dates do not influence the final Bayesian model for timing of Lake Agassiz phases and phase boundaries.

## 2.4 **Results and Discussion**

Re-examination of radiocarbon dates within the glacial Lake Agassiz basin permits a revised modelled chronology of lake development during the Moorhead and Emerson Phases.

We collated 99 radiocarbon dates associated with the Moorhead and Emerson Phases. Of these, 70 were retained and used in the construction of the multi-phased Bayesian model, while 27 were rejected due to: poor suitability of dated material, unclear stratigraphic context, unsuitable pre-treatment methods, a failed chi-squared test for multiple dates on the same sample, or non-finite ages on aquatic shells and bulk sediment (Table 1). Explicit manual filtering is a crucial step in chronological assessment, especially in the Lake Agassiz basin, where the presence of carbonate rock is a well-established source of bias in aquatic materials and bulk sediment (Grimm et al., 2009). Although the notion of error-prone material being unsuitable for constraining Lake Agassiz history is not a new concern (e.g. Fenton et al., 1983), age determinations have continued to be undertaken on questionable materials.

For the Moorhead Phase, manual vetting resulted in the acceptance of 47 ages with an unmodeled span of 13,450 - 10,790 cal yr BP (2660 cal yrs). Twenty-seven suitable radiocarbon dates for the Emerson Phase spanned a combined unmodeled range of 12640 - 10250 cal yr BP (2390 cal yrs). The wide margin and overlap in the unmodeled calibrated age ranges is the result of some samples having relatively large analytical error margins (>150 $^{14}C$ yr), along with the compounding effect of multiple plateaus in the IntCal13 calibration curve producing radiocarbon ages with large 2sigma calibrated age ranges.

Initial modelling trials in OxCal using the manually filtered data set produced an overall agreement index below the recommended 60% threshold (Bronk Ramsey, 2009b), indicating that the modelled age determinations were conflicting and suggesting the presence of outliers in the vetted compilation of radiocarbon dates. Four radiocarbon-dated samples had individual agreement indices <60% and were also flagged by OxCal's outlier analysis routine: ETH-32674; TO-1504; TO-4825; and the combined W-723/TAM-1 sample (Fig. 2.3).

The sample ETH-32674 (10,710 ± 75 $^{14}$C yr BP) (Fisher et al., 2008) is taken from a root fragment in littoral deposits below the lowstand (Ojata) strandline in the central Agassiz basin. This is the only date over 10,600 $^{14}$C yr BP from a stratigraphic section in which 18 other radiocarbon dates were taken (Fisher et al., 2008). Fisher et al. (2008) rejected this date due to its apparent old age in relation to other dates from the locale, and because it pre-dates the maximum abandonment age of the southern outlet (Fisher, 2003) at ca. 10,675 ± 60 $^{14}$C yr BP as proposed by Fisher and Lowell (2006). Furthermore, Fisher et al. (2008) note that the ETH-32674 sample contained the heaviest $^{13}$C value measured, and that the material dated (*Populus*) has a high potential for root suckering, possibly resulting in an anomalously old date.

The wood sample TO-1504 (10,810 ± 300 $^{14}$C yr BP) was recovered from a thin (~ 25 cm) silty sand layer along the eastern margin of the Lake Agassiz basin in northwestern Ontario, inferred to represent the initiation of the Moorhead Phase (Bajc et al., 2000). Wood samples in correlative borehole successions in this area produced ages of: 10,050 ± 180 $^{14}$C yr BP (WAT-1935), 10,020 ± 120 $^{14}$C yr BP (BGS-1303), and 10,100 ± 200 $^{14}$C yr BP (WAT-1689) respectively (Bajc et al., 2000). A date of 10,700 ± 140 $^{14}$C yr BP (WAT-1910) (Bajc et al., 2000) is the only comparable date to sample TO-1504 in this region. However, WAT-1910 was a bulk sediment sample of fine organic detritus from an equivocal depositional environment, and thus did not pass the manual vetting process. Bajc et al. (2000) conclude that the palynomorph morphology and assemblages across their study area are indicative of long distance transport and possible reworking. More specifically, the unit from which sample TO-1504 was retrieved contains a sizeable percentage of pre-Quaternary palynomorphs, suggesting that reworking from older deposits was prevalent (c.f. Bajc et al., 2000).

The oldest cited radiocarbon date from the Lake Agassiz basin is 10,960 ± 300 $^{14}$C yr BP (W-723), and has long been used to define the start of the Moorhead Phase (e.g. Moran et al., 1973; Clayton, 1983) and its temporal connection to the onset of the YD (Broecker et al., 1989). This wood sample was situated in ~ 3 m of silt and sand of the lowstand Ojata Beach deposits that overlie till near Grand Forks, North Dakota. The sample was initially dated by acetylene gas counting in 1959 to provide a minimum age constraint on the underlying till (Rubin and Alexander, 1960), and was later re-dated by radiometric methods as sample TAM-1 (10,820 ± 190 $^{14}$C yr BP) (Stipp et al., 1982). A collection of radiocarbon dates from a nearby exposure with similar stratigraphy to the original W-723/TAM-1 section was compiled by Fisher et al. (2008). Based on their interpretation of the new radiocarbon ages, which span 10,000 ± 70 $^{14}$C yr BP (ETH-32679) to 10,710 ± 75 $^{14}$C yr BP (ETH-32764), they infer that the Ojata Beach represents lake-level transgression at the end of the Moorhead Phase – rather than the initial interpretation of the Ojata level recording initial drawdown at the start of the low-water phase (e.g. Moran et al., 1973; Fenton et al., 1983) – and therefore reject the W-723/TAM-1 sample as being reworked in a littoral environment.

The date of 10,340 ± 100 $^{14}$C yr BP (TO 4285) is derived from the base of a 9 cm thick peat layer associated with the Emerson Phase in the eastern portion of the Agassiz basin near Wampum, Manitoba (Teller et al., 2000). This is the oldest Emerson Phase terrestrial macrofossil date in this area by ~ 300 radiocarbon years – and over 850 radiocarbon years older than another date on peat from the top of the same layer (TO 4284; 9460 ± 90 $^{14}$C yr BP) (Teller et al., 2000).

We re-ran the Bayesian age model on the vetted compilation, also excluding the four samples that identified by outlier analysis and discussed above, and obtained a well-defined age model based on the remaining dates with an overall model agreement of >90% (Fig. 2.2). Our analysis yielded an age probability model for the Moorhead Phase (Fig. 2.4) with an onset of 12,470 – 12,120 cal yr BP (2 σ), approximately 470 calibrated years younger than the previously assigned onset age based on the W-723/TAM-1 age. This modeled age for the Moorhead onset lies within the YD chronozone, albeit postdating its initiation at ~12,900 cal yr BP, suggesting that freshwater discharge associated with the Moorhead drop in lake level may not have been responsible for the initial disruption of the AMOC. It has recently been suggested that the initiation of the YD was more complex than initially thought – instead requiring multiple forcing mechanisms (Renssen et al., 2015) – and that a single catastrophic flood of freshwater from Lake Agassiz may not have been a prerequisite for initiating the cold reversal (Broecker et al., 2010). It is possible that a post-YD-initiation influx of Agassiz freshwater into the North Atlantic continued to supress the AMOC and prolonged the already-in-motion climate shift until the end of the Moorhead Phase, when freshwater discharge waned and lake levels transgressed (Leydet et al., 2018).

The possibility that the Moorhead Low occurred after the onset of the YD has led to an alternative hypothesis in which changes in climate and hydrology, instead of meltwater drainage, were responsible for the ~ 90 m drop in lake level (e.g. Lowell and Fisher, 2009; Lowell et al. 2009, 2013). Lowell et al. (2013) model a series of parameters necessary for regression in a closed Lake Agassiz basin and conclude that a reduction in meltwater, precipitation, and runoff, along with an increase in evaporation, would permit drawdown to Moorhead Low levels. Proponents of the negative hydrological forcing model argue that lake level would have needed to linearly regress starting some time before the onset of the YD in order to reach the Moorhead Low-water level (Lepper et al., 2013). However, the rate of evaporation required to overcome meltwater influx into the Agassiz basin in even the most modest runoff scenarios has been inferred to be untenable (Carlson et al., 2009; Teller, 2013). Similarly, paleoecological records from sites throughout the Agassiz basin do not support the notion that there was significant change in regional climate during the YD, and are thus inconsistent with increased evaporation rates and lake drawdown (Teller, 2013). Further, point elevation data for the strandlines bracketing the YD time interval indicate a rapid drawdown to the Moorhead Phase level, as opposed to a gradual, climatically-driven lake regression (Breckenridge, 2015).

The onset of the Emerson Phase was modelled as a transitional boundary between the low-stand Moorhead Phase and high-stand Campbell Beach ages. The

Bayesian model for initiation of the Emerson Phase gives a 2sigma age probability distribution of 11,600 – 11,280 cal yr BP (Fig. 2.4). This modelled age distribution is consistent with the longstanding hypothesis that Lake Agassiz transgressed to the Campbell Beach level around 10,000 $^{14}$C BP (11,500-11,340 cal yr BP) across the southern portion of the basin (Bjork and Keister, 1983; Clayton 1983; Fenton et al., 1983; Bajc et al., 2000; Teller et al., 2000; Yansa and Ashworth, 2005; Boyd, 2007). The rise in Lake Agassiz level to elevation of the Campbell Beaches during the Emerson Phase could be attributed to the closing of the (lower) northwestern outlet either by a glacial readvance (Yansa and Ashworth, 2005) or by isostatic rebound (Breckenridge, 2015). Freshwater discharge would have then likely reoccupied the southern outlet once lake level permits as it was available during this time (Fisher, 2003). As such, a reduction in oxygen isotope values from foraminifera in the Gulf of Mexico indicate meltwater drainage through the southern outlet after the Moorhead Phase, starting at ca. 10,000 $^{14}$C BP (Aharon, 2003; Wickert et al., 2013).

Radiocarbon dates within the Agassiz basin provide a better temporal constraint for the Emerson Phase than the Moorhead Phase. Out of 24 dates for the Emerson Phase, only one was identified as an outlier: TO-4285 (10,340 $^{14}$C BP ± 100) (Teller et al., 2000). The modelled rejection of this age supports the Teller et al. (2000) interpretation that this sample was likely reworked by littoral processes and redistribution of older, Moorhead Phase sediments as lake levels transgressed over the eastern portion of the Agassiz basin.

The termination of the Emerson Phase is generally attributed to glacial retreat uncovering lower outlets and routing meltwater to the east, progressively drawing down lake level from the Campbell shoreline elevation (Fenton et al., 1983; Thorleifson 1996; Teller, 2000). The modeled timing of this event is 10,710 – 10,320 cal yr BP (Fig 2.4), in agreement with earliest estimates of Campbell Beach sedimentation (Teller, 2000) and southern outlet abandonment ca. 9,400 $^{14}$C BP (Fisher, 2003) (10,570-10,430 cal yr BP).

The Bayesian model produced in this study provides filtered and refined age estimates for the Moorhead and Emerson Phase of glacial Lake Agassiz, and highlights the need for further work to improve chronological constraints on lake history. The current radiocarbon dataset in the Lake Agassiz basin is problematic for defining the onset of the Moorhead low-water Phase. At present, the few ages traditionally interpreted as defining the start of the Moorhead (e.g. W-723/TAM-1; Broecker et al., 1989) appear as temporal outliers with respect to all other Moorhead ages (Fig. 2.2). The OxCal model developed here assumes the radiocarbon ages to be normally distributed throughout their respective phases, but this assumption may not be valid in regard to the onset of the Moorhead Phase. It is possible that the scarcity of early ages (i.e. near the onset of the YD) may reflect a period in which, due to unfavourable climatic conditions, little organic material is available for incorporation in these deposits. Further, the Bayesian approach treats isolated ages as outliers and has no clear ability to discern between outliers and potentially accurate ages occurring in isolation.

The absence of suitable organic material situated in pre-Moorhead Phase strandlines (e.g. Lepper et al., 2013) suggests that the deglacial Agassiz basin and watershed lagged in re-vegetation for an unknown duration. The oldest ages in Moorhead Phase sediments are some of the oldest radiocarbon ages from the basin, and are likely a result of fluvial retransportion from older deglaciated surfaces west of Lake Agassiz as lake level dropped. However, if these "outlier" ages are, in fact, reliable chronological constrains for drawdown to the Moorhead Low, it is temporally possible to invoke catastrophic Lake Agassiz drainage – most likely through the Northwestern outlet (c.f. Breckenridge, 2015) – as being the causative mechanism for the Younger Dryas cold interval, as initially proposed by Broecker et al. (1989). Indeed, recent high-resolution AMS ages from low-$\delta^{18}$O planktonic foraminifera off the coast of the Mackenzie River delta indicating significant amounts of freshwater influx starting around 12.94 $^{14}$C yr BP (Keigwin et al., 2018), consistent with previous OSL ages on flood deposits on the Mackenzie Delta (Murton et al., 2010). If the age model for this near-shore marine record of Lake Agassiz drainage (Keigwin et al., 2018) is correct, it implies that the rejected outliers for the Moorhead initiation are actually valid, and that age modeling efforts need to better incorporate the potential for non-normal distribution of radiocarbon dates throughout a modeled phase. However, the Keigwin et al. (2018) age models are hampered by uncertain marine reservoir corrections, and details of the hydrological link between the Lake Agassiz basin and the Arctic Ocean remains unknown.

This study highlights the need for a systematic re-dating programme of Lake Agassiz radiocarbon samples, given current understanding of pre-treatment methods, potential biases associated with material choice, and increased precision from modern AMS techniques. A re-dating campaign would be particularly valuable in this contact because dates with large uncertainties (e.g. W-723) are still commonly used to define the Moorhead low water phase, and because plateaus on the calibration curve spanning the duration of Lake Agassiz tend to inflate the age ranges of samples with relatively large errors.

The chronology of the lake phases in question could also be better determined by acquiring multiple radiocarbon samples from a single stratigraphic locale. Ideally, many quality dates would be obtained from a site that spans multiple stages throughout lake development. A prime target, the Assiniboine Delta—the most extensive delta built into glacial Lake Agassiz—has thus far provided a wealth of information regarding lake dynamics and temporal constraints through lake evolution (e.g. Elson, 1967; Fenton et al., 1983; Teller, 1989). This delta complex is largely composed of subaqeous fan deposits associated with a pre-Moorhead high lake level during the late Lockhart Phase (Fig. 1B) (Fenton et al., 1983; Kehew and Teller, 1994; Thorleifson, 1996), with a subsequent Moorhead-drop initiating deep incision in these sediments (Fenton et al., 1983; Thorleifson, 1996), followed by valley-fill sedimentation and strandline development (i.e. Upper Campbell beach) during the ctransgressive Emerson Phase (Teller, 1989; Thorleifson, 1996; Boyd, 2007). Initial chronologies from the delta were largely hampered by the dating of unsuitable material, such as marl (e.g. GSC-383: 10,600 ± 150 $^{14}C$ yr BP, Elson, 1967), or from ambiguous stratigraphic contexts (e.g. wood sample Y-411: 10550 ± 200 $^{14}C$ yr BP, from a possible valley fill unit, Elson 1967). Teller (1989) refined the chronology of the Emerson Phase at a key site in the delta by justifiably rejecting some older dates on aquatic mosses and providing ages on wood macrofossils of 9510 ± 200 $^{14}C$ yr BP (GSC-4490) and 9600 ± 70 $^{14}C$ yr BP (TO 534). However, the stratigraphic information relating to these dates was still dependent on shallow backhoe pits and auger holes, making stratigraphic correlations problematic. In a more recent study, Boyd (2007) implemented a coring program that resulted in a high-resolution stratigraphic analysis of Emerson Phase sedimentation on the Assiniboine Delta. This data, coupled with radiocarbon dates of 9910 ± 90 $^{14}C$ yr BP (TO 11762) and 10,060 ± 60 $^{14}C$ yr BP (Beta-193587) permit more accurate regional connections, and therefore chronological improvement across larger areas.

The areal extent and temporal complexity of glacial Lake Agassiz requires additional quality radiocarbon ages from unambiguous stratigraphic settings throughout the southern basin. New ages spanning multiple stages of lake development across correlative sections would enable the development of a more robust chronological framework. The improved stratigraphically-constrained age data can be incorporated as priors in subsequent Bayesian models, allowing for more rigorous assessment of outliers and precise age ranges to be developed.

## 2.5 **Conclusion**

In this paper, we reassess a filtered radiocarbon dataset for the Moorhead and Emerson Phases of Lake Agassiz. The new vetted dataset excludes about one-third of existing dates from the Agassiz basin, including ages previously linking the start of the Moorhead Phase to the onset of the Younger Dryas cold reversal around ca. 12,900 cal yr BP. A revised chronology for prominent phases of Lake Agassiz, using a Bayesian framework, results in 2-sigma age probability distributions of: 12,470 – 12,120 cal yr

BP cal yr BP for the onset of the Moorhead Phase; 11,600 – 11,280 cal yr BP cal yr BP for the onset of the Emerson Phase; and 10,710 – 10,320 cal yr BP cal yr BP for the end of the Emerson Phase. The revised onset of the Moorhead Phase post-dates the onset of the YD cooling in the North Atlantic, suggesting either that drainage associated with Moorhead drawdown was not the immediate cause of the YD, or as we think more likely, the existing radiocarbon dataset is too incomplete to resolve events at centennial-scale temporal resolution.

## 2.6 References


Aharon, P., 2003. Meltwater flooding events in the Gulf of Mexico revisited: Implications for rapid climate changes during the last deglaciation. Paleoceanography 18, 1–14. https://doi.org/10.1029/2002PA000840

Ashworth, A., Clayton, L., Bickley, W., 1972. The Mosbeck Site: a Paleoenvironmental Interpretation of the Late Quaternary History of Lake Agassiz Based on Fossil and Mollusk Remains. Quat. Res. 188, 176–188.

Bajc, A.F., Schwert, D.P., Warner, B.G., Williams, N.E., 2000. A reconstruction of Moorhead and Emerson Phase environments along the eastern margin of glacial Lake Agassiz, Rainy River basin, northwestern Ontario. Can. J. Earth Sci. 37, 1335–1353. https://doi.org/10.1139/e00-051

Björck, S., Keister, C.M., 1983. The Emerson Phase of Lake Agassiz, independently registered in northwestern Minnesota and northwestern Ontario. Can. J. Earth Sci. 20, 1536–1542. https://doi.org/10.1139/e83-143

Blaauw, M., Christen, J.A., 2011. Flexible paleoclimate age-depth models using an autoregressive gamma process. Bayesian Anal. 6, 457–474. https://doi.org/10.1214/11-BA618

Blockley, S.P.E., Pinhasi, R., 2011. A revised chronology for the adoption of agriculture in the Southern Levant and the role of Lateglacial climatic change. Quat. Sci. Rev. 30, 98–108. https://doi.org/10.1016/j.quascirev.2010.09.021

Boyd, M., 2007. Early postglacial history of the southeastern Assiniboine Delta , glacial Lake Agassiz basin. J. Paleolimnol. 37, 313–329. https://doi.org/10.1007/s10933-006-9044-3

Breckenridge, A., 2015. The Tintah-Campbell gap and implications for glacial Lake Agassiz drainage during the Younger Dryas cold interval. Quat. Sci. Rev. 117, 124–134. https://doi.org/10.1016/j.quascirev.2015.04.009

Brock, F., Ramsey, C.B., Higham, T.G., 2007. Quality assurance of ultrafiltred bone dating. Radiocarbon 49, 187–192.

Broecker, W.S., Denton, G.H., Edwards, R.L., Cheng, H., Alley, R.B., Putnam, A.E., 2010. Putting the Younger Dryas cold event into context. Quat. Sci. Rev. 29, 1078–1081. https://doi.org/10.1016/j.quascirev.2010.02.019

Broecker, W.S., Kennett, J.P., Flower, B.P., Teller, J.T., Trumbore, S., Bonani, G., Wolfli, W., 1989. Routing of meltwater from the Laurentide Ice Sheet during the Younger Dryas cold episode. Nature 341, 318–321. https://doi.org/10.1038/341318a0

Bronk Ramsey, C., 2009a. Bayesian Analysis of Radiocarbon Dates. Radiocarbon 51, 337–360. https://doi.org/10.1017/S0033822200033865

Bronk Ramsey, C., 2009b. Dealing with outliers and offsets in radiocarbon dating. Radiocarbon 51, 1023–1045. https://doi.org/10.1017/S0033822200034093

Buck, C.E., Christen, J.A., James, G.N., 1999. BCal: an online Bayesian radiocarbon calibration tool. Internet Archaeol. 7.

Carlson, A.E., Clark, P.U., 2012. Ice Sheet Sources of Sea Level Rise and Freshwater Discharge During the Last Deglaciation. Rev. Geophys. 50, https://doi:10.1029/2011RG000371.

Carlson, A.E., Clark, P.U., Haley, B.A., Klinkhammer, G.P., Simmons, K., Brook, E.J., Meissner, K.J., 2007. Geochemical proxies of North American freshwater routing during the Younger Dryas cold event. Proc. Natl. Acad. Sci. 104, 6556–6561. https://doi.org/10.1073/pnas.0611313104

Carlson, A.E., Clark, P.U., Hostetler, S.W., 2009. Comment : Radiocarbon deglaciation chronology of the Thunder Bay , Ontario area and implications for ice sheet retreat patterns. Quat. Sci. Rev. 28, 2546–2547. https://doi.org/10.1016/j.quascirev.2009.05.005

Clark, P.U., Marshall, S.J., Clarke, G.K.C., Hostetler, S.W., Licciardi, J.M., Teller, J.T., 2001. Freshwater forcing of abrupt climate change during the last glaciation. Science. 293, 283–287. https://doi.org/10.1126/science.1062517

Clayton, L., 1983. Chronology of Lake Agassiz drainage to Lake Superior, In: Teller, J. T. and Clayton, L. Eds, Glacial Lake Agassiz. pp. 291–307.

Clayton, L., Moran, S.R., 1982. Chronology of late wisconsinan glaciation in middle North America. Quat. Sci. Rev. 1, 55–82. https://doi.org/10.1016/0277-3791(82)90019-1

Cronin, T.M., Rayburn, J.A., Guilbault, J.P., Thunell, R., Franzi, D.A., 2012. Stable isotope evidence for glacial lake drainage through the St. Lawrence Estuary, eastern Canada, ~13.1-12.9 ka. Quat. Int. 260, 55–65. https://doi.org/10.1016/j.quaint.2011.08.041

Davies, L.J., Appleby, P., Jensen, B.J.L., Magnan, G., Mullan-Boudreau, G., Noernberg, T., Shannon, B., Shotyk, W., van Bellen, S., Zaccone, C., Froese, D.G., 2018. High-resolution age modelling of peat bogs from northern Alberta, Canada, using pre- and post-bomb $^{14}C$, $^{210}Pb$ and historical cryptotephra. Quat. Geochronol. 47, 138–162. https://doi.org/10.1016/j.quageo.2018.04.008

Davies, L.J., Jensen, B.J.L., Froese, D.G., Wallace, K.L., 2016. Late Pleistocene and Holocene tephrostratigraphy of interior Alaska and Yukon: Key beds and chronologies over the past 30,000 years. Quat. Sci. Rev. 146, 28–53. https://doi.org/10.1016/j.quascirev.2016.05.026

Elson, J.A., 1967. Geology of glacial Lake Agassiz. In: Mayer-Oakes, W.J. (ed.), Life, Land, and Water. University of Manitoba Press, Winnipeg, pp. 37-95. 1967.

Fenton, M.M., Moran, S.R., Teller, J.T., Clayton, L., 1983. Quaternary stratigraphy and history in the southern part of the Lake Agassiz Basin, In: In J.T. Teller & L. Clayton (Eds.), Glacial Lake Agassiz. The Geological Association of Canada. pp. 49–74.

Fisher, T.G., 2003. Chronology of glacial Lake Agassiz meltwater routed to the Gulf of Mexico. Quat. Res. 59, 271–276. https://doi.org/10.1016/S0033-5894(03)00011-5

Fisher, T.G., Lowell, T. V, 2006. Questioning the age of the Moorhead Phase in the glacial Lake Agassiz basin. Quat. Sci. Rev. 25, 2688–2691. https://doi.org/10.1016/j.quascirev.2006.05.07

Fisher, T.G., Yansa, C.H., Lowell, T. V., Lepper, K., Hajdas, I., Ashworth, A., 2008. The chronology, climate, and confusion of the Moorhead Phase of glacial Lake Agassiz: new results from the Ojata Beach, North Dakota, USA. Quat. Sci. Rev. 27, 1124–1135. https://doi.org/10.1016/j.quascirev.2008.02.010

Grimm, E.C., Maher, L.J., Nelson, D.M., 2009. The magnitude of error in conventional bulk-sediment radiocarbon dates from central North America. Quat. Res. 72, 301–308. https://doi.org/10.1016/j.yqres.2009.05.006

Hamilton, W.D., Kenney, J., 2015. Multiple Bayesian modelling approaches to a suite of radiocarbon dates from ovens excavated at Ysgol yr Hendre, Caernarfon, North Wales. Quat. Geochronol. 25, 72–82. https://doi.org/10.1016/j.quageo.2014.10.001

Kehew, A.E., Teller, J.T., 1994. History of late glacial runoff along the southwestern margin of the Laurentide Ice Sheet. Quat. Sci. Rev. 13, 859–877. https://doi.org/10.1016/0277-3791(94)90006-X

Keigwin, L.D., Klotsko, S., Zhao, N., Reilly, B., Giosan, L., Driscoll, N.W., 2018. Deglacial floods in the Beaufort Sea preceded Younger Dryas cooling. Nat. Geosci., 11, 599-604. https://doi.org/10.1038/s41561-018-0169-6

Klassen, R.W., 1967. Stratigraphy and chronology of Quaternary deposits of Assiniboine River valley and its tributaries. Report of Activities Part B, November 1966 to April 1967; Geol. Surv. of Canada Pap. no. 67-1B, 55–60. https://doi.org/10.4095/106424.

Klassen, R.W., 1969. Quaternary Stratigraphy and Radicarbon Chronology in Southwestern Manitoba. Geol. Surv. Canada., Paper 69-27, 1-19.

Kuehn, S.C., Froese, D.G., Carrara, P.E., Foit, F.F., Pearce, N.J.G., Rotheisler, P., 2009. Major- and trace-element characterization, expanded distribution, and a new chronology for the latest Pleistocene Glacier Peak tephras in western North America. Quat. Res. 71, 201–216. https://doi.org/10.1016/j.yqres.2008.11.003

Lee, S., Ramsey, C.B., 2012. Development and Application of the Trapezoidal Model for Archaeological Chronologies. Radiocarbon 54, 107–122.

Lepper, K., Buell, A.W., Fisher, T.G., Lowell, T. V., 2013. A chronology for glacial Lake Agassiz shorelines along Upham's namesake transect. Quat. Res., 80, 88–98. https://doi.org/10.1016/j.yqres.2013.02.002

Lepper, K., Gorz, K.L., Fisher, T.G., Lowell, T.V., 2011. Age determinations for glacial Lake Agassiz shorelines west of Fargo, North Dakota, USA. Can. J. Earth Sci. 48, 1199–1207. https://doi.org/10.1139/E11-025

Leydet, D.J., Carlson, A.E., Teller, J.T., Breckenridge, A., Barth, A.M., Ullman, D.J., Sinclair, G., Milne, G.A., Cuzzone, J.K., Caffee, M.W., 2018. Opening of glacial Lake Agassiz's eastern outlets by the start of the Younger Dryas cold period. Geology 46, 155–158. https://doi.org/10.1130/G39501.1

Lowell, T. V, Applegate, P.J., Fisher, T.G., Lepper, K., 2013. What caused the low-water phase of glacial Lake Agassiz ? Quat. Res. 80, 370–382. https://doi.org/10.1016/j.yqres.2013.06.002

Lowell, T. V, Fisher, T.G., Hajdas, I., Glover, K., Loope, H., Henry, T., 2009. Radiocarbon deglaciation chronology of the Thunder Bay , Ontario area and implications for ice sheet retreat patterns. Quat. Sci. Rev. 28, 1597–1607. https://doi.org/10.1016/j.quascirev.2009.02.025

Moran, S., Clayton, L., Cvancara, A., 1971. New sedimentological and paleontological evidence for history of Lake Agassiz: Snake Curve Section, Red Lake County, Minnesota. Proceedings of the North Dakota Academy of Science 24, 61-73.

Moran, S.R., Clayton, L., Scott, M., Brophy, J., 1973. Catalog of North Dakota radiocarbon dates. North Dakota Geol. Surv. Misc. Ser. 53, 1–51.

Morlan, R.E., McNeely, R., Wolfe, S.A., Schreiner, B.T., 2000. Manitoba radiocarbon dates. Manitoba Ind. Trade, Mines. Manitoba Geol. Surv. Open File Rep. OF2000-1. 198.

Murton, J.B., Bateman, M.D., Dallimore, S.R., Teller, J.T., Yang, Z., 2010. Identification of Younger Dryas outburst flood path from Lake Agassiz to the Arctic Ocean. Nature 464, 740–743. https://doi.org/10.1038/nature08954

Nielsen, E., Gryba, E.M., Wilson, M.C., 1984. Bison Remains From a Lake Agassiz Spit Complex in the Swan River Valley, Manitoba - Depositional Environment and Paleoecological Implications. Can. J. Earth Sci. 21, 829–842. https://doi.org/10.1139/e84-089

Reimer, P.J., Bard, E., Bayliss, A., Beck, J.W., Blackwell, P.G., Ramsey, C.B., Buck, C.E., Cheng, H., Edwards, R.L., Friedrich, M., Grootes, P.M., Guilderson, T.P., Haflidason, H., Hajdas, I., Hatté, C., Heaton, T.J., Hoffmann, D.L., Hogg, A.G., Hughen, K.A., Kaiser, K.F., Kromer, B., Manning, S.W., Niu, M., Reimer, R.W., Richards, D.A., Scott, E.M., Southon, J.R., Staff, R.A., Turney, C.S.M., van der Plicht, J., 2013. IntCal13 and Marine13 Radiocarbon Age Calibration Curves 0–

50,000 Years cal BP. Radiocarbon 55, 1869–1887. https://doi.org/10.2458/azu_js_rc.55.16947

Renssen, H., Mairesse, A., Goosse, H., Mathiot, P., Heiri, O., Roche, D.M., Nisancioglu, K.H., Valdes, P.J., 2015. Multiple causes of the Younger Dryas cold period. Nat. Geosci. 8, 946–949. https://doi.org/10.1038/ngeo2557

Reyes, A. V, Cooke, C.A., 2011. Northern peatland initiation lagged abrupt increases in deglacial atmospheric $CH_4$. Proc. Natl. Acad. Sci. USA. 108, 4748-4753. https://doi.org/10.1073/pnas.1013270108.

Rubin, M., Alexander, C., 1960. U.S. Geological Survey Radiocarbon Dates V 2, 129–185.

Shotton, F.W., 1972. An example of hard-water error in radiocarbon dating of vegetable matter. Nature 240, 460–461. https://doi.org/10.1038/240460a0

Small, D., Clark, C.D., Chiverrell, R.C., Smedley, R.K., Bateman, M.D., Duller, G.A.T., Ely, J.C., Fabel, D., Medialdea, A., Moreton, S.G., 2017. Devising quality assurance procedures for assessment of legacy geochronological data relating to deglaciation of the last British-Irish Ice Sheet. Earth-Science Rev. 164, 232–250. https://doi.org/10.1016/j.earscirev.2016.11.007

Stipp, J.J., Davis, E.M., Noakes, J.E., Hoover, T.E., 1962. University of Texas Radiocarbon Dates 1. Radiocarbon 4, 43-50.

Teller, J.T., 2013. Lake Agassiz during the Younger Dryas. Quat. Res. 80, 361–369. https://doi.org/10.1016/j.yqres.2013.06.011

Teller, J.T., 2001. Formation of large beaches in an area of rapid differential isostatic rebound: The three-outlet control of Lake Agassiz. Quat. Sci. Rev. 20, 1649–1659. https://doi.org/10.1016/S0277-3791(01)00007-5

Teller, J.T., 1989. Importance of the Rossendale site in establishing a deglacial chronology along the southwestern margin of the Laurentide ice sheet. Quat. Res. 32, 12–23. https://doi.org/10.1016/0033-5894(89)90028-8

Teller, J.T., 1980. Radiocarbon dates in Manitoba. Manitoba Miner. Resour. Div. Geol. Rep. GR80-4. 1–61.

Teller, J.T., Boyd, M., Yang, Z., Kor, P.S.G., Fard, A.M., 2005. Alternative routing of Lake Agassiz overflow during the Younger Dryas: New dates, paleotopography, and a re-evaluation. Quat. Sci. Rev. 24, 1890–1905. https://doi.org/10.1016/j.quascirev.2005.01.008

Teller, J.T., Leverington, D.W., 2004. Glacial Lake Agassiz: A 5000 yr history of change and its relationship to the δ18O record of Greenland. Bull. Geol. Soc. Am. 116, 729–742. https://doi.org/10.1130/B25316.1

Teller, J.T., Riseberg, J., Gaywood, M., Zoltai, S., 2000. Postglacial history and paleoecology of Wampum , Manitoba , a former lagoon in the Lake Agassiz basin. GSA Bulletin 112, 943–958.

Thorleifson, L.H., 1996. Review of Lake Agassiz History. In: Teller, J.T., Thorleifson, L.H., Matile, G., and Brisbin, W.C., Eds, Sedimentology, geomorphology and histroy of the central Lake Agassiz basin: Winnipeg, Manitoba, Field Trip Guidebook B2, Geological Association of Canada/Mineralogical Association of Cannada Annual Meeting, May 27-29, 55-84.

Wickert, A.D., Mitrovica, J.X., Williams, C., Anderson, R.S., 2013. Gradual demise of a thin southern Laurentide ice sheet recorded by Mississippi drainage. Nature 502, 668–671. https://doi.org/10.1038/nature12609

Yansa, C.H., Ashworth, A.C., 2005. Late Pleistocene Palaeoenvironments of the Southern Lake Agassiz Basin. J. Quat. Sci, 20, 255–267. https://doi.org/10.1002/jqs.905

## 2.7 Figures and Tables

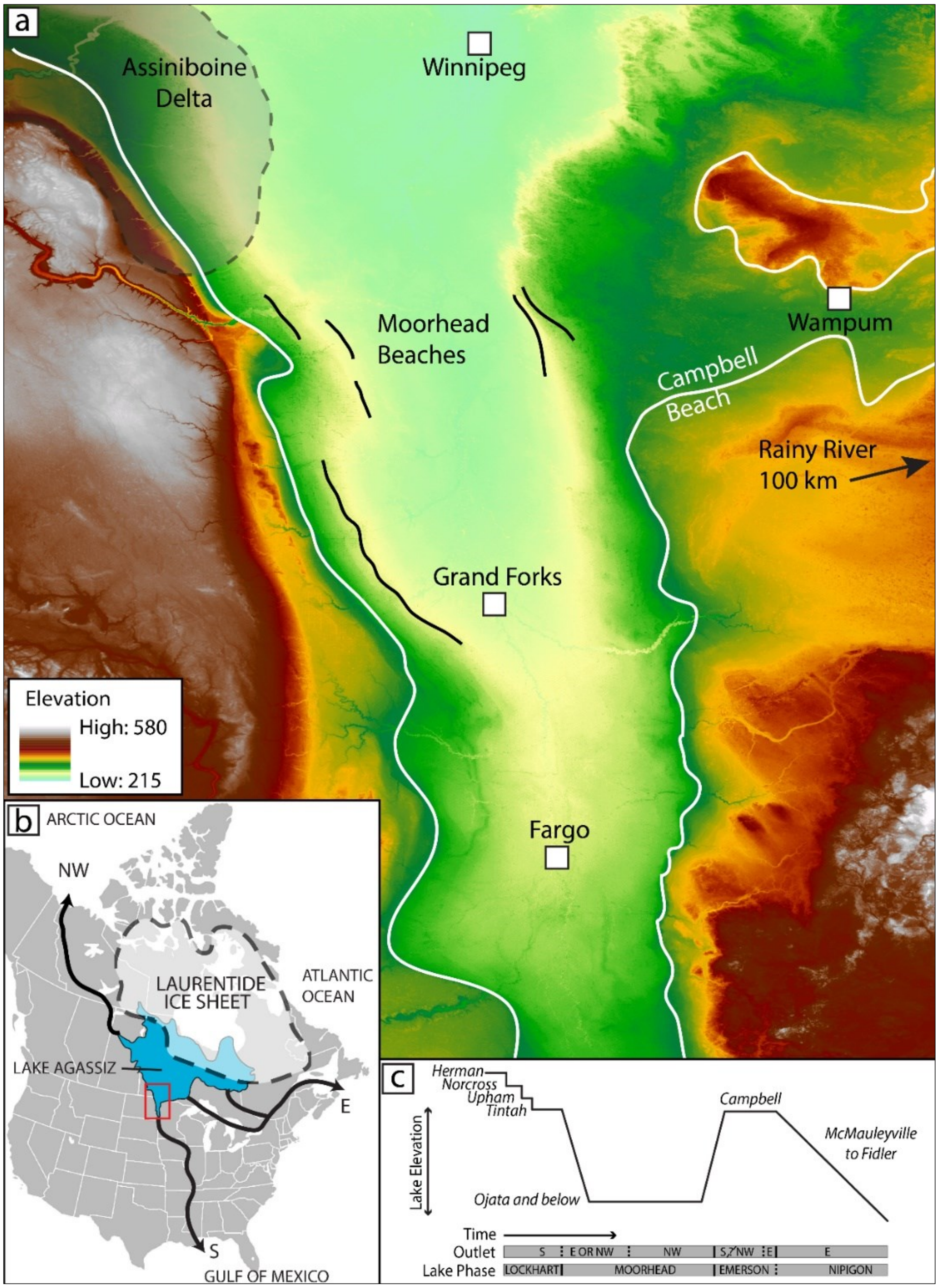


Figure 2.1. (a) Outline of the Campbell (white) and Moorhead (black) shorelines over a digital elevation model of the southern Agassiz basin. Locations of key sites discussed in text are labelled: Assiniboine Delta complex; Wampum, Manitoba; Rainy River, Ontario; Grand Forks, North Dakota; Fargo, North Dakota. (b) Maximum extent of glacial Lake Agassiz and the Laurentide Ice Sheet at 9.5 $^{14}$C ka (Dyke, 2004). Meltwater drainage routes: NW = northwest outlet; E = eastern outlet; S = southern outlet. (c) Schematic diagram of lake relative lake-level fluctuations, corresponding strandlines, and outlet activity from the Lockhart to Nipigon Phases.


Figure 2.2. Bayesian age model output from OxCal applied to vetted Moorhead and Emerson Phase radiocarbon ages of Lake Agassiz. The unmodelled (likelihood) probabilities are light colours, with modelled (posterior) probabilities in darker colours. Dates in red are outlying and do not influence the model. Agreement indices (A) show probability of individual dates agreeing with the model. Agreement indices (P) show the probability of individual outlying dates agreeing within the model. Thin and thick bars underlying the probability distributions are the 1 and 2 sigma confidence intervals from the modelled age ranges.

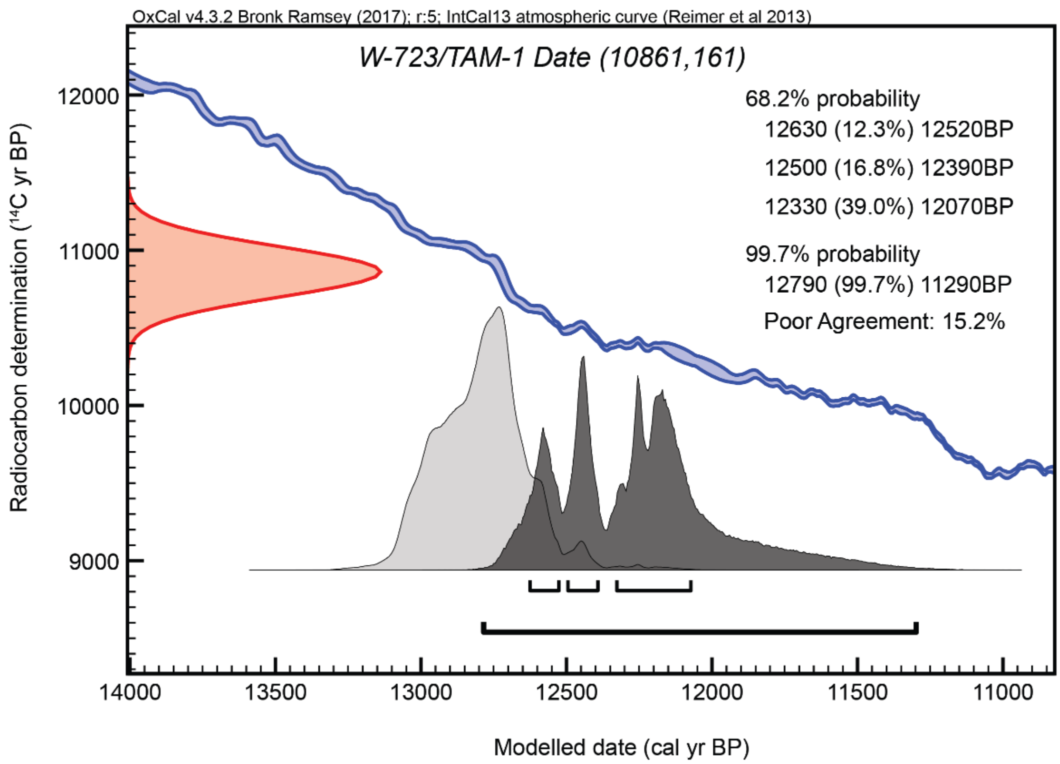


Figure 2.3. Initial modelling of the W-723/TAM-1 date showing unmodelled (light) and modelled (dark) age distributions from OxCal 4.3 (Bronk Ramsey, 2009a). Radiocarbon determination shown in red; IntCal13 calibration curve shown in blue (Reimer et al., 2013). Individual agreement of age distributions denoted by Poor Agreement.

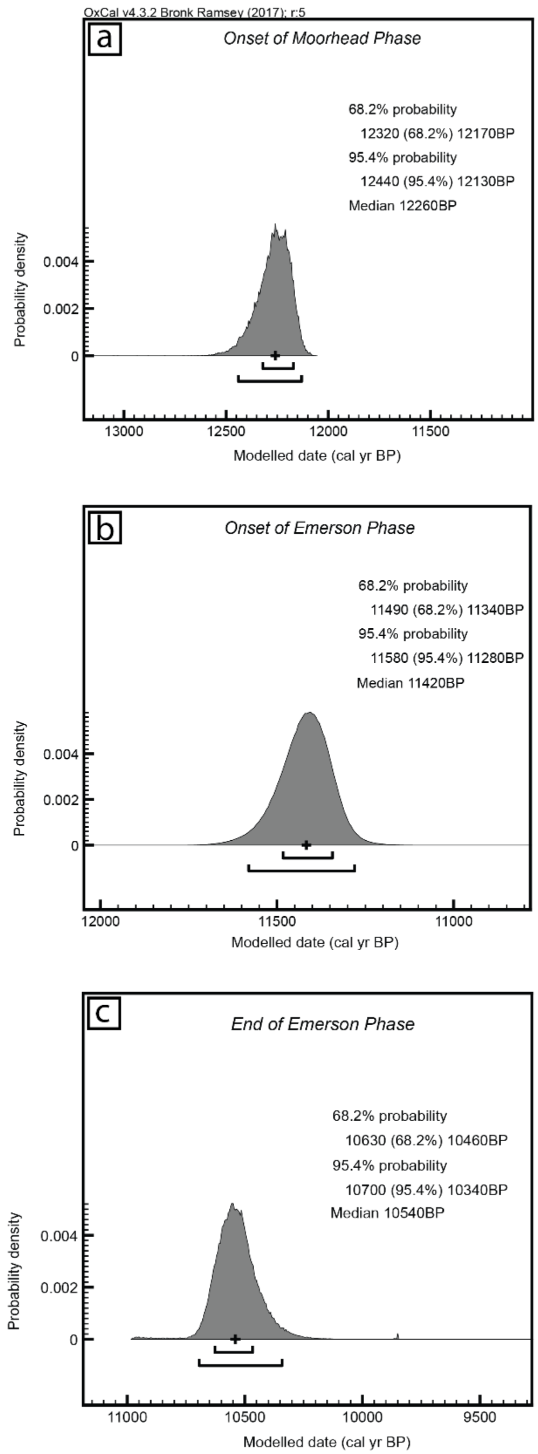


Figure 2.4. Modelled probability ages for a) onset of the Moorhead Phase; b) onset of the Emerson Phase; c) end of the Emerson Phase. Black bars represent 68.2% and 95.4% probability, with median and sigma ranges for each age distribution.

Table 2.1. Radiocarbon dates within the glacial Lake Agassiz basin relating to the Moorhead and Emerson Phases.

| Lab. Number | $^{14}C$ Age and error | Calibrated age BP at 2σ range[a] | Material | Location | Included in Model[b] | Comments | Counting Method[c] | Ref. |
|---|---|---|---|---|---|---|---|---|
| Moorhead Phase | | | | | | | | |
| AA-34343 | 9920±60 | 11610-11217 | Wood | Fargo, North Dakota | Y | Top of rhythmite deltaic sediments overlain by c. 1 m sand and c. 3.5 m of lacustrine sediments. | AMS | Yansa and Ashworth, (2005) |
| AA-34344 | 10040±120 | 12013-11239 | Wood | Fargo, North Dakota | Y | In rhythmite deltaic sediments overlain by c. 1 m sand and c. 3.5 m of lacustrine sediments | AMS | Yansa and Ashworth, (2005) |
| Beta-121851 | 10230±30 | 12107-11815 | Wood | Fargo, North Dakota | Y | At base of rhythmites deltaic sediments overlying Lockhart Phase sands | AMS | Yansa and Ashworth, (2005) |
| Beta-218508 | 10170±40 | 12043-11647 | Wood | Grand Forks, North Dakota | Y | Peat with laminated sands underlying littoral sands | AMS | Fisher et al. (2008) |
| BGS-1302 | 10080±160 | 12376-11213 | Wood | Rainy River Basin, Ontario | Y | Alluvial and (or) fluvial | Beta | Bajc et al., (2000) |
| BGS-1303 | 10020±120 | 11996-11231 | Wood | Rainy River Basin, Ontario | Y | Alluvial, deltaic. Re-date of WAT-1935 | Beta | Bajc et al., (2000) |
| BGS-1305 | 9920±110 | 11923-11163 | Fine plant detritus | Rainy River Basin, Ontario | N [1] | Offshore bar or spit; unsatisfactory material dated | Beta | Bajc et al., (2000) |
| ETH-32665 | 10150±75 | 12072-11404 | Carex cf C. rostrata seeds | Grand Forks, North Dakota | Y | Macrofossils from sandy peat underlying littoral sands | AMS | Fisher et al., (2008) |
| ETH-32666 | 10080±75 | 11983-11325 | Picea mariana needles | Grand Forks, North Dakota | Y | Macrofossils from sandy peat underlying littoral sands | AMS | Fisher et al., (2008) |
| ETH-32667 | 10520±70 | 12666-12146 | Populus sp. Abraded wood | Grand Forks, North Dakota | Y | Peat with laminated sands underlying littoral sands | AMS | Fisher et al., (2008) |
| ETH-32668 | 10260±80 | 12392-11715 | Carex seeds | Grand Forks, North Dakota | Y | Macrofossils from sandy peat underlying littoral sands | AMS | Fisher et al., (2008) |

| | | | | | | | | |
|---|---|---|---|---|---|---|---|---|
| ETH-32669 | 10440±80 | 12573-12047 | Picea mariana needles | Grand Forks, North Dakota | Y | Macrofossils from sandy peat underlying littoral sands | AMS | Fisher et al., (2008) |
| ETH-32670 | 10330±75 | 12516-11828 | Wood | Grand Forks, North Dakota | Y | Peat with laminated sands underlying littoral sands | AMS | Fisher et al., (2008) |
| ETH-32671 | 10470±75 | 12600-12085 | Root (Populus) | Grand Forks, North Dakota | Y | Roots from base of littoral sediments | AMS | Fisher et al., (2008) |
| ETH-32672 | 10390±75 | 12533-12009 | Root (Populus) | Grand Forks, North Dakota | Y | Roots from base of littoral sediments | AMS | Fisher et al., (2008) |
| ETH-32673 | 10370±45 | 12410-12035 | Root (Populus) | Grand Forks, North Dakota | Y | Roots from base of littoral sediments | AMS | Fisher et al., (2008) |
| ETH-32674 | 10710±75 | 12742-12544 | Root | Grand Forks, North Dakota | Y | Roots from base of littoral sediments | AMS | Fisher et al., (2008) |
| ETH-32675 | 10160±70 | 12096-11406 | Populus sp. Trunk | Grand Forks, North Dakota | Y | Stump at base of littoral sediments | AMS | Fisher et al., (2008) |
| ETH-32676 | 10010±70 | 11799-11250 | Populus sp. Trunk | Grand Forks, North Dakota | Y | Stump at base of littoral sediments | AMS | Fisher et al., (2008) |
| ETH-32677 | 10260±75 | 12389-11725 | Partially abraded Wood | Grand Forks, North Dakota | Y | Partially abraded wood from base of littoral sands | AMS | Fisher et al., (2008) |
| ETH-32678 | 10030±70 | 11921-11261 | Wood | Grand Forks, North Dakota | Y | Wood from base of littoral sands | AMS | Fisher et al., (2008) |
| ETH-32679 | 10000±70 | 11766-11247 | Highly abraded wood | Grand Forks, North Dakota | Y | Highly abraded wood from base of littoral sands | AMS | Fisher et al., (2008) |
| ETH-32680 | 10340±75 | 12520-11835 | Highly abraded wood | Grand Forks, North Dakota | Y | Highly abraded wood from base of littoral sands | AMS | Fisher et al., (2008) |
| ETH-32681 | 10210±70 | 12372-11506 | Wood | Grand Forks, North Dakota | Y | Wood from base of littoral sands | AMS | Fisher et al., (2008) |
| ETH-32682 | 10210±70 | 12372-11506 | Partially abraded wood | Grand Forks, North Dakota | Y | Partially abraded wood from base of littoral sands | AMS | Fisher et al., (2008) |
| ETH-32683 | 39440±750 | 44649-42239 | Wood fragment | Grand Forks, North Dakota | N [5] | Log at base of littoral sands | AMS | Fisher et al., (2008) |
| GSC-4732 | 9940±80 | 11716-11213 | Wood | Rainy River Basin, Manitoba | Y | Sandy organic layer below possible Moorhead beach berm | Beta | Morlan et al., (2000) |
| GSC-5296 | 10000±90 | 11932-11235 | Wood | Rainy River Basin, Manitoba | Y | Enclosed in terrestrial plant remains in silt | Beta | Morlan et al., (2000) |

| | | | | | | | | |
|---|---|---|---|---|---|---|---|---|
| GSC-5330 | 9940±90 | 11755-11205 | Wood | Rainy River Basin, Manitoba | Y | Sandy organic layer below possible Moorhead beach berm | Beta | Morlan et al., (2000) |
| GSC-5357 | 10100±90 | 12036-11316 | Wood | Rainy River Basin, Manitoba | Y | Interpreted as flotsam in littoral sands | Beta | Morlan et al., (2000) |
| GSC-5363 | 10900±100 | 13025-12675 | Bivalve Shells | Rainy River Basin, Manitoba | N [1] | From a sand-clay rhythmite in a Moorhead channel | Beta | Morlan et al., (2000) |
| GSC-5430 | 10200±110 | 12382-11401 | Abraded Wood | Rainy River Basin, Manitoba | Y | Interpreted as Moorhead wood in littoral sands | Beta | Morlan et al., (2000) |
| GSC-5697 | 9950±100 | 11817-11198 | Wood | Rainy River Basin, Manitoba | Y | Wood from backhoe test pit containing silts and sands of a possible Moorhead beach berm | Beta | Morlan et al., (2000) |
| GSC-5710 | 10100±140 | 12370-11236 | Wood fragment | Rainy River Basin, Manitoba | Y | Enclosed in organic muds within a drowned river channel | Beta | Morlan et al., (2000) |
| GSC-5731 | 9960±190 | 12369-10792 | Wood | Rainy River Basin, Manitoba | Y | Wood from backhoe test pit containing silts and sands of a possible Moorhead channel | Beta | Morlan et al., (2000) |
| GSC-667 | 10690±190 | 13010-12065 | Wood | Assiniboine Valley, Manitoba | N [2] | Wood at contact between organic silt alluvium and an overlying till slump block on the bank of the Assiniboine River | Beta | (Klassen, n.d.) |
| I-4853 | 9890±150 | 11987-10799 | Wood | Snake Curve, Minnesota | Y | Within sandy gravel unit within a buried stream valley | Beta | Moran et al. (1971) |
| I-5213 | 10340±170 | 12661-11410 | Forest litter | Northeast North Dakota | N [1] | From beds within c. 6 m sand unit | Beta | Moran et al., (1973) |
| TAM-1 | 10820±190 | 13116-12188 | Wood | Northeast North Dakota | Y | Re-date of W-723. | Beta | Stipp et al., (1962) |
| TO-1504 | 10810±240 | 13187-12074 | Wood | Rainy River Basin, Ontario | Y | Alluvial and (or) fluvial | AMS | Bajc et al., (2000) |
| TO-4286 | 10000±110 | 11963-11225 | Wood | Wampum, Manitoba | Y | In silty sands below c. 10 m of Upper Campbell beach sands | AMS | Teller et al., (2000) |
| TO-4871 | 10040±70 | 11932-11268 | Gyttja | Wampum, Manitoba | N [1] | From within unit consisting of gyttja, marl, peat, and mollusc shells | AMS | Teller et al., (2000) |
| TO-4872 | 10140±80 | 12079-11395 | Fine organic detritus | Wampum, Manitoba | N [1] | Unspecified organic material in marl unit overlying gyttja and peat | AMS | Teller et al., (2000) |

| | | | | | | | | |
|---|---|---|---|---|---|---|---|---|
| TO-4874 | 9950±50 | 11613-11241 | Wood | Wampum, Manitoba | Y | At base of peat layer underlyinh gytjja, silty sands and peat | AMS | Teller et al., (2000) |
| W-1005 | 10050±300 | 125669-10775 | Wood | Grand Forks, North Dakota | Y | Wood in Moorhead Ojata beach sediment | Beta | Moran et al. (1973) |
| W-1360 | 9810±300 | 12384-10433 | Branches, twigs, | Trail, North Dakota | N [1] | Wood fragments in sandy gravels containing waterworn wood fragments and fine-grained carbonaceous material. | Beta | Moran et al. (1973) |
| W-1361 | 9820±300 | 12388-10440 | Wood fragments | Trail, North Dakota | N [1] | Wood fragments in sandy gravels containing waterworn wood fragments and organic material. | Beta | Moran et al. (1973) |
| W-388 | 9930±280 | 12421-10608 | Wood | Moorhead, Minnesota | Y | Wood in same peat as W-993 | Beta | Clayton and Moran, (1982) |
| W-723 | 10960±300 | 13454-12127 | Wood | Grand Forks, North Dakota | Y | Within sands overlying till, overlain by clayey silts and sands. Traditionally used to establish onset of the Moorhead Phase. | Beta | Rubin and Alexander , (1960) |
| W-900 | 10080±280 | 12605-10796 | Wood | Grand Forks, North Dakota | Y | From base of c. 3 m cross-bedded sand unit | Beta | Moran et al. (1973) |
| W-993 | 9900±400 | 12639-10405 | Wood | Fargo, North Dakota | Y | In peat unit overlain by laminated silts | Beta | (Fenton et al., 1983) |
| WAT-1689 | 10100±200 | 12513-11195 | Wood | Rainy River Basin, Ontario | Y | Alluvial and (or) fluvial | Beta | Bajc et al. (2000) |
| WAT-1749 | 10400±160 | 12693-11712 | Wood | Rainy River Basin, Ontario | Y | Alluvial and (or) fluvial | Beta | Bajc et al. (2000) |
| WAT-1910 | 10700±140 | 12897-12153 | Fine organic detritus | Rainy River Basin, Ontario | N [1] | From a restricted pond | Beta | Bajc et al. (2000) |
| WAT-1935 | 10050±180 | 12381-11183 | Wood | Rainy River Basin, Ontario | Y | Alluvial, deltaic. Re-dated as BGS-1303 | Beta | Bajc et al. (2000) |
| WAT-1936 | 10100±180 | 12387-11220 | Charcoal fragments | Rainy River Basin, Ontario | Y | From a small pond or lake | Beta | Bajc et al. (2000) |
| Emerson Phase | | | | | | | | |

| | | | | | | | | |
|---|---|---|---|---|---|---|---|---|
| AA-50801 | 9530±70 | 11133-10601 | Wood fragment | Snake Curve, Minnesota | Y | In silty, sandy, clayey, and organically laminated sediment | AMS | Fisher et al. (2008) |
| AA-50803 | 9490±70 | 11090-10575 | Wood fragment | Snake Curve, Minnesota | Y | In silty, sandy, clayey, and organically laminated sediment | AMS | Fisher et al. (2008) |
| Beta-188953 | >48500 | Out of Range | Particulate Carbon | Assiniboine Delta, near Rossendale Manitoba | N [1] | At base of c. 7 m sand unit underlying c. 7 m silt to clayey silt unit. Rejected by Boyd (2007) | AMS | Boyd, (2007) |
| Beta-192660 | 8270±40 | 9415-9127 | Wood (root) | Assiniboine Delta, near Rossendale Manitoba | N [2] | Root in humified sand layer underlying peat; clear evidence of root peneration; rejected by Boyd (2007) | AMS | Boyd, (2007) |
| Beta-193587 | 10060±60 | 11947-11316 | Picea needles | Assinibione Delta, Manitoba | Y | Wood from peaty unit underlying TO-11763. In same unit as TO-11762 | AMS | Boyd, (2007) |
| BGS-617 | 10300±200 | 12639-11359 | Bone | Swan River Valley, Manitoba | N [3] | Water worn bison bone underlying the Upper Campbell beach | Beta | Nielsen et al., (1984) |
| BGS-840 | 9500±150 | 11215-10400 | Swan River Valley, Manitoba | Swan River Valley, Manitoba | N [3] | Water worn bison bone in Campbell level beach spit | Beta | Nielsen et al., (1984) |
| BGS-887 | 9400±125 | 11090-10280 | Swan River Valley, Manitoba | Swan River Valley, Manitoba | N [3] | Water worn bison bone in Campbell level beach spit | Beta | Nielsen et al., (1984) |
| BGS-1304 | 9750±170 | 11755-10601 | Wood | Rainy River Basin, Ontario | N [4] | Beach and (or) foreshore; re-date of WAT-1760. Combining dates BGS-1304 and WAT-1760 resulted in a failed chi squared test; both dates were excluded | Beta | Bajc et al., (2000) |
| BGS-1408 | 9770±110 | 11601-10751 | Wood | Rainy River Basin, Manitoba | Y | Alluvial silts and sands that may be contemporaneous with the Lower Campbell beach | Beta | McNeely and Neilson, (2000) |
| GSC-1219 | 12100±160 | 12702-11618 | Moss | Rossendale, Manitoba | N [1] | Organic rich unit in a lagoon behind the Upper Campbell beach | Beta | Teller, (1989) |
| GSC-1428 | 10000±280 | 12526-10752 | Wood | Assinibione Delta, Manitoba | N [2] | Wood fragment in alluvium from borehole c. 9 m below surface | Beta | Teller, (1980) |
| GSC-1909 | 10300±200 | 12639-11355 | Organic detritus | Swan River Valley, Manitoba | N [1] | 8 m below surface of Campbell strandline | Beta | Teller, (1980) |

| | | | | | | | | |
|---|---|---|---|---|---|---|---|---|
| GSC-383 | 10600±150 | 12751-12054 | Marl | Assinibione Delta, Manitoba | N [1] | Marl from valley fill | Beta | Elson, (1967) |
| GSC-384 | 9580±220 | 11602-10595 | Marl | Assinibione Delta, Manitoba | N [1] | Marl from valley fill under beach gravel | Berta | Elson, (1967) |
| GSC-391 | 9990±160 | 12133-11123 | Wood | Assinibione Delta, Manitoba | Y | c. 2 m below Campbell terrace surface | Beta | Teller, (1980) |
| GSC-492 | 10670±160 | 12890-12080 | Shells | Holland, Manitoba | N [1] | Shells in silt 1-3 m above modern river level in the Assinibione Valley. | Beta | (Klassen, 1967) |
| GSC-4490 | 9510±90 | 11144-10573 | Wood | Rossendale, Manitoba | Y | Organic rich peat unit in a lagoon behind the Campbell beach. From same unit as TO-534 | Beta | Teller, (1989) |
| GSC-797 | 9700±140 | 11596-10590 | Wood | Assiniboine Valley, Manitoba | Y | Clayey silt unit c. 4 m below surface of upper Campbell terrace | Beta | Klassen, (1969) |
| GSC-870 | 10000±150 | 12091-11176 | Wood | Assiniboine Valley, Manitoba | Y | From base of same clayey silt unit at GSC-797 c. 8 m below surface of upper Campbell terrace | Beta | Klassen, (1969) |
| GSC-902 | 10600±150 | 12751-12054 | Plant detritus | Assiniboine Valley, Manitoba | N [1] | Fluvial-lacustrine sediment c. 18 m below upper Campbell terrace | Beta | Klassen, (1969) |
| I-3880 | 9940±160 | 12073-10874 | Wood | Northeast North Dakota | Y | Base of fine sands overlying peat c. 5 m below Upper Campbell beach | Beta | Ashworth et al., (1972) |
| I-5123 | 9650±150 | 11393-10561 | Wood | Northeast North Dakota | Y | Driftwood in laminated clays | Beta | Moran et al., (1973) |
| I-5123c | 9730±160 | 11700-10594 | Wood | Northeast North Dakota | Y | Re-date of I-5123 | Beta | Moran et al., (1973) |
| TO-4284 | 9460±90 | 11106-10497 | Peat | Wampum, Manitoba | Y | To of 7 cm thick humified peat unit (same unit as TO 4285) below silty clays with scattered wood fragments and root fibers | AMS | Teller et al., (2000) |

| | | | | | | | | |
|---|---|---|---|---|---|---|---|---|
| TO-4285 | 10340±100 | 12536-11814 | Peat | Wampum, Manitoba | Y | Base of 7 cm thick humified peat unit (same unit as TO 4284) below silty clays with scattered wood fragments and root fibers. Interpreted to be reworked by Teller et al., (2000). | AMS | Teller et al., (2000) |
| TO-4854 | 9760±80 | 11348-10789 | Wood Fragment | Wampum, Manitoba | Y | In Upper Campbell Beach sands below TO 4855 | AMS | Teller et al., (2000) |
| TO-4855 | 9340±90 | 10776-10251 | Wood Fragment | Wampum, Manitoba | Y | In Upper Campbell Beach sands above TO 4854 | AMS | Teller et al., (2000) |
| TO-4856 | 9330±80 | 10727-10276 | Charcoal fragment | Wampum, Manitoba | Y | In peat layer underlying c. 7 m of peat, gyttja and marl units in lagoon behind Upper Campbell Beach | AMS | Teller et al., (2000) |
| TO-4857 | 10930±100 | 13031-12693 | Silty gyttja | Wampum, Manitoba | N [1] | Silty gytjja with mollusks overlain by gyttja, marl, organic-rich marl and peat. Interpreted to be reworked by Teller et al., (2000) | AMS | Teller et al., (2000) |
| TO-4869 | 9690±70 | 11235-10785 | Wood Fragment | Wampum, Manitoba | Y | Lower boundary of sand unit overlying laminated silty clay | AMS | Teller et al., (2000) |
| TO-4870 | 12240±80 | 14636-13868 | Fine organic detritus | Wampum, Manitoba | N [1] | At contact of gyttja and silt. Interpreted to be reworked by Teller et al., (2000) | AMS | Teller et al., (2000) |
| TO-4873 | 9380±90 | 11068-10287 | Wood | Wampum, Manitoba | Y | In laminated silty clays under 7 m of Upper Campbell Beach Sands | AMS | Teller et al., (2000) |
| TO-11762 | 9910±40 | 11593-11223 | Wood | Assiniboine Delta, Manitoba | Y | Wood from peaty unit underlying TO-11763 | AMS | Boyd, (2007) |
| TO-11763 | 5300±70 | 6271-5929 | Wood (root) | Assiniboine Delta, Manitoba | N [2] | Root c. 1 m below surface in humified organic sand layer; date rejected by Boyd (2007) | AMS | Boyd, (2007) |
| TO-534 | 9600±70 | 11177-10732 | Wood Fragments | Rossendale, Manitoba | Y | Lowermost organic rich unit at Rossendale site. From same unit as GSC-4490. | AMS | Teller, (1989) |
| WAT-1760 | 10500±200 | 12765-11647 | Wood | Rainy River Basin, Ontario | N [4] | Beach and (or) foreshore; re-dated as BGS-1304. Combining dates BGS-1304 and WAT-1760 resulted in a failed chi squared test; both dates were excluded | Beta | Bajc et al. (2000) |

| | | | | | | | | |
|---|---|---|---|---|---|---|---|---|
| WAT-1934 | 9530±140 | 11219-10443 | Wood | Rainy River Basin, Ontario | Y | Alluvial, deltaic | Beta | Bajc et al. (2000) |
| WIS-1324 | 9350±100 | 11065-10250 | Peat | Swift, Minnesota | Y | At top of thick peat above gyttja and organic silts | Beta | Bjorck and Keister, (1983) |
| WIS-1325 | 10050±100 | 11979-11259 | Peat | Swift, Minnesota | Y | At base of thick peat above gyttja and organic silts | Beta | Bjorck and Keister, (1983) |
| Y-411 | 10550±200 | 12819-11761 | Wood fragments | Assiniboine Delta, Manitoba | N [2] | Valley fill | Beta | Elson, (1957) |
| Y-415 | 9110±110 | 10575-9920 | Wood | Assiniboine Delta, Manitoba | N [2] | Valley fill | Beta | Elson, (1957) |
| Y-416 | 8020±100 | 9240-8595 | Wood fragments | Assiniboine Delta, Manitoba | N [2] | Valley fill | Beta | Elson, (1957) |

[a] Calibrated in OxCal V. 4.3 (Bronk Ramsey, 2009a) using IntCAL13 calibration curve (Reimer et al., 2013).

[b] Y - dates are dates used in the initial Bayesian model. N - dates did not pass manual quality checks due to: [1] unsuitable material dated; [2] unclear stratigraphic context; [3] unsuitable pre-treatment employed; [4] combined dates failed chi squared test; [5] non-finite determination.

[c] AMS = accelerator mass spectrometry. Beta = beta-counting by liquid scintillation or gas proportional methods.

# Chapter 3: Northwestern Outlet of glacial Lake Agassiz in the Fort McMurray area, Alberta, Canada


## Abstract

The northwestern outlet of glacial Lake Agassiz was a conduit for meltwater drainage into the Arctic Ocean via the lower Athabasca River valley. Current models suggest one (or possibly two) floods deposited proximal sheets of flood gravels and a distal braid delta into glacial Lake McConnell during the last deglaciation of the Laurentide Ice Sheet (LIS). However, timing of these drainage events and their possible association to the onset of the Younger Dryas (YD) cold reversal remains contentious. We revisit the late Pleistocene stratigraphy within the lower Athabasca River valley from mining and river-cut exposures and identify eleven principal lithofacies from three distinct reaches in the valley relating to 1) pre-LIS paleo-Athabasca River sedimentations; 2) ice-contact sedimentation along the fluctuating margin of the deglacial LIS; 3) post-glacial sedimentation of the Athabasca River; 4) catastrophic drainage from Lake Agassiz; and 5) post-flood fluvial-deltaic sedimentation into glacial Lake McConnell. Flood deposits exposed in mining operations south of the Firebag moraine are approximately 6 times more steeply graded than the modern Athabasca River, projecting below the modern river within 20 km north of the Firebag moraine. The absence of clear flood sedimentation north of the Firebag moraine suggests flood sedimentation is graded below the modern Athabasca River with the corollary that the distal braid delta was built into glacial Lake McConnell sometime following catastrophic drainage. After correcting for bitumen contamination from regional oil sands deposits, radiocarbon dates on terrestrial macrofossils from the braid delta indicate that meltwater drainage occupied the northwestern outlet of glacial Lake Agassiz prior to 12,200 cal years BP, consistent with the Moorhead phase drop of glacial lake Agassiz. This new conceptual model better explains the evolution of the northwestern outlet and its temporal relation to the YD.

### 3.1 Introduction

Melting of the Laurentide Ice Sheet in central North America during the last deglacial period resulted in the formation of large proglacial lakes on its receding southern and western margins (Dyke, 2004). Glacial Lake Agassiz was the largest of these lakes, encompassing an area of over 1.5 million square kilometres over the course of its history (Teller and Leverington, 2004). Freshwater derived from Lake Agassiz periodically discharged into surrounding oceans through three main outlets: 1) southward into the Gulf of Mexico via the Mississippi River system; 2) eastward into the Atlantic Ocean through the Great Lakes region and St. Lawrence valley; and 3) to the northwest, through the Clearwater and Athabasca River system into Glacial Lake McConnell en route to the Arctic Ocean (Fig. 3.1). Changes in meltwater routing from the southern outlet has been hypothesized as the mechanism for oceanic thermohaline disruption (THC) (e.g. Rooth, 1982; Clark et al., 2001; Teller et al., 2002; Tarasov and Peltier, 2005; Wickert et al., 2013, causing abrupt climatic reversals such as the Younger Dryas (YD) cold reversal and the Preboreal oscillation (PBO) (e.g. Broecker et al., 1989; Fisher et al., 2002; Teller et al., 2002; Murton et al., 2010; Keigwin et al., 2018). Initial work by Smith and Fisher, (1993) documented extensive sedimentological and geomorphic evidence indicating Lake Agassiz drained catastrophically through the Clearwater and lower Athabasca River valleys in northeastern Alberta and built an extensive braid delta complex (Smith and Fisher, 1993) into Lake McConnell.

Initial northwestern outlet chronologies linked catastrophic discharge with the highstand Emerson Phase of Lake Agassiz at ca. 9.9 $^{14}$C ka BP based on averaged radiocarbon ages from flood and deltaic sediments in the lower Athabasca River valley (Smith and Fisher, 1993) and later attributed to triggering the PBO (Fisher et al., 2002). Further dating by Fisher et al., (2009) on moraine lake cores led to the proposition that an ice dam blocked northward drainage until ca 9.6 $^{14}$C ka BP, well later than the deglacial chronology of Dyke et al. (2004). Conversely, several researchers contend that the northwestern outlet was a viable drainage route for the Moorhead low-water phase at the start of the Younger Dryas ca. 10.9 $^{14}C$ ka (Teller et al., 2005; Murton et al., 2010). The connection between northwestward routing and the onset of the Younger Dryas is largely based on luminescence ages on flood deposits in the Mackenzie River Delta with >10 $^{14}C$ ka BP ages and apparent corresponding flood terraces in the lower Athabasca River valley (Murton et al., 2010).

In this paper, we report on the stratigraphy in the lower Athabasca River valley and present a detailed analysis of 11 sedimentological units to establish their age, origin, distribution, and relations to Lake Agassiz drainage. A conceptual depositional model is proposed to explain the evolution of Lake Agassiz's northwestern outlet.

## 3.2 Regional Setting

The study area is located in the lower Athabasca River valley north of Fort McMurray, Alberta, an extensive lowland rarely exceeding 230 m asl, topographically bounded by the Birch Mountain Uplands (ca. 830 m asl) to the west, and to the east by the Muskeg Hills (ca. 650 m asl) (Pettapiece, 1986). Within the valley, physiographic remnants of the Laurentide Ice Sheet retreat provide the only substantial topographic relief, expressed as the Richardson and Firebag moraine complexes (Fig. 3.1). A broad sand plain blankets the northern section of the lower valley, consisting of both active and stabilized parabolic dune systems (Rhine and Smith, 1988). Further south, lacustrine and outwash sediments dominate the surficial deposits, whereas the uplands are largely blanketed by till deposits (Andriashek and Atkinson, 2007).

### *3.2.1 The Lower Athabasca Valley*

The first investigation in the lower Athabasca valley was conducted by Taylor (1960) on a single river-cut section immediately below the confluence of the Athabasca and Firebag Rivers (Fig. 3.1). He interpreted the complex sediment package as being dominantly lacustrine in origin, with a lower deltaic sequence recording changes in water level from a fluctuating ice dam. Later, Rhine and Smith (1988) investigated exposures in the distal reaches of the valley, identifying an expansive (>4000 km$^2$) fan-shaped sandplain which they interpreted as an anomalously large Late Pleistocene braid delta complex, built into glacial Lake McConnell, that was fed primarily from eolian sediment from the erosion of sand-rich till. Subsequently, the connection between the northwestern outlet of glacial Lake Agassiz and the Athabasca River valley was established by Smith and Fisher (1993), when they attributed sheets of boulder gravels coupled with a prominent spillway complex to catastrophic drainage via the Clearwater Athabasca Spillway (CLAS). The evolutionary model proposed by Smith and Fisher (1993) argues that an outburst from Lake Agassiz eroded the CLAS, with deposition of sheets and bars of boulder gravels starting north of Fort McMurray with deposition of a braid delta complex into glacial Lake McConnell at ~ 300 m a.s.l.

### *3.2.2 Clearwater-Lower Athabasca Spillway*

The most prominent geomorphic feature in the area is the CLAS—a steep-walled, straight-trending meltwater channel presumably formed as catastrophic drainage from glacial Lake Agassiz flowed through the region en route to the Arctic Ocean via glacial Lake McConnell (Smith and Fisher, 1993). The head of the spillway, originating 30 km southwest of the Cree Lake Moraine, is defined by a series of anastomosing channels deeply incised into sedimentary rocks and Canadian Shield bedrock in northwestern Saskatchewan. Above the head of the CLAS, in the Churchill Valley of northwestern Saskatchewan, two principal water plane elevations constrain westward meltwater flow through the area: a highstand lake phase demarcated by strandlines abutting the Cree Lake Moraine at 484 m, and a well-defined wave-cut scarp indicative of sustained flow at 438 m (Fisher and Smith, 1994). Meltwater was routed along the CLAS 150 km to the west where it converged with the Athabasca River valley, diverting flow northward another 60 km before bifurcating around the Firebag moraine (also referred to as the Fort Hills). The western reach mirrors the modern Athabasca River valley through to the Bitumount Gap, whereas the eastern reach progresses up the Muskeg River valley (Smith and Fisher, 1993; Woywitka et al.,

2017) (Fig. 3.1). Distal portions of the CLAS around Fort McMurray are incised into the underlying the Lower Cretaceous McMurray Formation, resulting in large bituminous clasts reworked into flood-derived sediments within the spillway (Smith and Fisher, 1993).

### 3.3 Methods

A 190 km transect along the lower Athabasca River from Fort McMurray through the modern delta provided opportunity to observe and describe the regional stratigraphy. Lithostratigraphic logs at river-cut and mining exposures were compiled at a bed-by-bed scale, using standard sedimentological field techniques. Facies were defined by documenting primary sedimentological characteristics at a centimeter scale, including lithology, grain size and shape, sorting and texture, bed geometry, and paleocurrent indicators (Table 3.1). Secondary structures, including folding, faulting, drop stones, clastic dykes and bitumen abundance were also documented. Multiple logs were taken at large exposures to document lateral variation in sedimentary units. Bulk sediment samples were collected to identify sand and silt lithologies under magnification. Locations for each section and elevations of mining pit exposures were recorded with a handheld GPS unit. Elevations of samples and sections along river sections were measured with respect to the Athabasca River level during August 2016 using a Lasertech 200XL laser range finder with a vertical accuracy of 0.2 m.

The slope profiles of the boulder gravel deposits and modern Athabasca River trajectories were derived using ArcGIS 10.2 with a 5 m resolution Light Detection and Ranging (LiDAR) elevation model. Surface elevations of gravel-cored, streamlined flood bedforms (c.f. Woywitka et al., 2017) were compiled over a ~ 23 km continuous transect south of the Firebag moraine (Fig. 3.1) and compared against the northward-trending surface of the modern river.

Radiocarbon determinations by accelerator mass spectrometry (AMS) from terrestrial plant macrofossils provided the basis of chronology for this study. The presence of bitumen in the lower Athabasca valley has the potential to contaminate radiocarbon samples, resulting in potential bias of radiocarbon ages because of the incorporation of old carbon (e.g. Vance, 1986). To mitigate this, a two-step pre-treatment protocol was employed at the University of Alberta. Samples were first subjected to an organic solvent mixture consisting of 2:1 toluene:ethanol or 2:1 chloroform:ethanol and left to reflux in a soxhlet apparatus for 48 hours to extract α-cellulose. Samples were then air dried within a fume hood before undergoing standard acid-base-acid pre-treatment protocol to remove humic acids and inorganic carbon (e.g. Reyes et al., 2010). Pre-treated samples and standards were submitted to the Keck-Carbon Cycle AMS facility (University of California, Irvine) for $^{14}C$ measurement. This protocol was also concurrently applied to five $^{14}C$ standard samples: Queets A wood shavings (non-finite), AVR07-PAL-37 wood cellulose (non-finite), IAEA C5 wood cellulose (11.8 $^{14}C$ ka BP), FIRI-D wood shavings (4.51 $^{14}C$ ka BP) and FIRI F wood cellulose (4.53 $^{14}C$ ka BP).

## 3.4 Results

### *3.2.1 Stratigraphy*

The stratigraphic architecture through the lower Athabasca River valley can be subdivided into three main geographical reaches, each with a distinctive sedimentological character. From south to north, we divide these reaches as: 1) proximal, 2) middle, and 3) distal (Fig. 3.1). Within these reaches, we recognize eleven distinct units based on sedimentological characteristics and inferred depositional environments. Composite stratigraphic logs for the middle and distal reaches are shown in Figure 3.2 with a composite cross section for the proximal reach shown in Figure 3.3.

#### Proximal Reach (Unit 1- Unit 4)

For more than a decade we have visited pits in the mineable oilsands region and developed an overall stratigraphic framework for the proximal lower Athabasca fluvial deposits (Froese et al., 2013). This framework is based on strath terraces, road cuts and open pit mine sites on both sides of the Athabasca River (CNRL-Horizon, Susan Lake, Suncor-Fort Hills and Shell Albian Sands). We recognize 4 units across these exposures that have been developed into a sedimentological framework for the proximal lower Athabasca valley, from the southern limit of mining operations, to just south of the Firebag moraine. A schematic cross-section of the stratigraphy is shown in Figure 3.3.

*Unit 1*

Mostly toward the south end of the Susan Lake Gravel Pit, a grey quartzite-rich, well-rounded gravel is present at thicknesses of 2-4 m over bedrock. Unit 1 is commonly overlain by a dark grey diamict according to the mine operators, that likely represents the late Wisconsinan till in the area.

*Unit 2*

Unit 2 is 2-3 m of grey, quartzite-rich gravel, variably, though documented on both the east (Susan Lake) and west (CNRL-Horizon) sites in 2006. It consists low-angle planar-tabular cross bed sets that normally grade from cobble gravel near the base to stratified sands with down-valley paleocurrent directions. These units are variably interbedded with imbricate planar gravel beds. Average clast size is about 5 cm diameter. Distinctively, this unit is largely lacking in bitumen in comparison to the overlying Unit 3.

*Unit 3*

Unit 3 consists of approximately 5 m of massive-to-poorly sorted cross-bedded boulder gravel overlying Unit 2. Commonly, this unit coarsens upward before fining toward the surface with weak to moderately developed planar cross beds (Fig 3.4c). Clasts are typically rounded, disk-shaped, and regularly display imbrication indicative of north-trending flow matching the present course of the Athabasca River. Clast composition is dominated by bituminous rich sands, carbonates, ironstones and quartzites while granites and gniesses are less frequently present (Fig. 3.3a). Characteristic of this lithofacies is the prevalence of orange to yellow oxide staining of the gravels with an abundance of carbonate clasts. Bituminous sand ripups of the McMurray Formation and carbonates of the Waterways Formation, up to several meters across are commonly present within this unit. Larger rafts up to 15 m have been recorded in gravel bars by Fisher and Lowell (2017). Unit 3 sharply overlies unit 2 in the mining pit exposures on both sides of the Athabasca River, and in some cases, scours into the underlying McMurray or Waterways formations. Elevations of unit 3 deposition on strath terraces range from 14-35 m above river level (247-268 m a.s.l.), sloping to the north before terminating near the Firebag moraine.

*Unit 4*

Lateral to unit 3, and at similar elevation, is a planar-to-sub-horizontal well-stratified pebbly sand (Fig. 3.4b). The surface of unit 4 is at the same level as the boulder gravel, but it lacks the coarse material that characterizes the earlier unit. Thin planar-tabular cross-bed sets and pebble-rich planar to sub-horizontal sands (15-50 cm thick) are common in the unit. Near the surface of the unit, wedge features are present extending to depths of ~80 cm with an upper width of ~40 cm (Fig. 3.4d). Infill largely consists of overlying brown silt to fine sand with sub-vertical orientated clasts.

### Middle Reach (Unit 5 – Unit 8)

The lateral transition with the lower valley into lithofacies 5-8 occurs just north of the Firebag moraine complex and is demarcated by an abrupt change from boulder gravel sedimentation (Unit 3) to an assemblage of sands and silts of Unit 5. Middle reach sedimentation extends for approximately 30 km along the lower Athabasca River before grading over a ~20 km distance north of the mouth of the Firebag River (Fig. 3.1). The ~35 m exposure at the confluence of the Firebag and Athabasca Rivers provides the most complete exposure of the sedimentological and deformational characteristics that define this lithofacies package (Fig. 3.5). Exposures in this reach are shown in the composite stratigraphic log in Figure 3.2a.

*Unit 5*

The lowest unit in the middle reach consists of alternating well-stratified beds of sand (up to 60 cm thick) and silt (1-15 cm thick). These beds are graded from medium sand to fine sand and silts, with bitumen-rich matrix cemented sands common in the finer fractions. A section ~ 15 km south of the Firebag River exposure contains a ca. 50 cm thick laminated to massive silt bed with soft-sediment deformation in the form of flame structures into the overlying sands (Figure 3.6). The orientation of these silt diapirs projects to the north with laminated pink clay rip-up clasts (< 5 cm diameter) associated with loading structures.

*Unit 6*

Unit 6 consists of tilted, heavily deformed diamicts and stratified sands and silts of variable thickness capped by a flat lying, ~1 m thick pink diamict. The basal contact is sharp. The upper ~1.5 m of unit 5 exhibits a brittle deformation to compressional forces, frequently in the form of reverse faulting (Fig. 3.7). Large scale deformational structures are present in the northern portions of the Firebag River exposure, where two large open folds with northward-plunging axes occupy the lower ~14 m of the section. These high-amplitude features of Unit 6 (Fig. 3.8) consist of inverted and deformed stratified beds of silts and sands with outsized clasts of pink sandstone and diamict blocks, interbedded with an intensely folded sandy pink diamict with laminated shearing planes. Clasts of deformed pink clays are also present throughout this unit.

Several vertical to semi-vertical clastic dikes intrude the folded sediments of Unit 6, ranging in thickness from 2-10 cm (Fig. 3.8). They are comprised of vertically laminated fine sands and silts and frequently cut through the entirety of the deformation structures. Overlying the deformed sediment package, also confined to the Firebag River exposure, is a ca. 1 m thick (at ca. 16 m a.r.l.) crudely-stratified pebble-gravel supported diamict with pink silty-clay clasts. Associated clasts are predominantly sub-rounded to angular pink to white sandstone with ranging from 2-60 cm in size (Fig. 3.9).

*Unit 7*

Unit 7 is characterized by a thick (up to ~16 m at the Firebag River section) package of silt to coarse sand interbedded by 1.4 m of brown diamict overlain by 70 cm of pink to grey laminated silt and clay. The bed geometry within Unit 7 is largely comprised of rhythmic planar beds of silt (4-25 cm thick) and sand (15-60 cm thick), with less occurrences of trough cross-sets, massive sand, and ripple cross-laminated interbeds of fine sand. Local scouring structures, less than 50 cm deep and 2 m wide, that fine upward from pebble to cobble lags, are rare in Unit 7.

A well sorted pink medium sand, 1.5 to 3 m thick, is present ca. 16 m a.r.l. at the base of unit 7. These distinctively coloured pink sands contrast with the adjacent white to yellow sand present that is typically present in much of the Firebag exposure and in the area south of the Fort Hills. Planar bedding is the dominant bedding architecture within the pink sands aside from a section ~30 km south of the Firebag River exposure, where ripple cross-laminations and planar cross-beds indicate an up-valley (southward) paleocurrent.

Sharply overlying the pink sands is a 5 m thick unit of tan medium sand grading to silt. These sand beds are massive or horizontally stratified and range in thickness from 2 – 15 cm. Coarser sands display a sharp basal contact and are infrequently found in the upper third of unit 7 where they are situated in trough cross-stratified sets <1 m thick with occasional isolated clasts. Where present, the uppermost ~1 m (~30 m a.r.l.) of unit 7 grades into 2-4 cm thick sets of ripple cross-laminated fine sands. Bedding planes in all sands overlying the distinctive pink sand unit of unit 7 indicate a northward paleocurrent direction.

Laminated clay and silt overlying a brown diamict interrupts the sandy sequence from 24 to 25.5 m a.r.l. (Fig. 3.10). The lower diamict, with a silty-sand matrix has rare sub-rounded to sub-angular clasts of varying lithologies including sandstone, granite, gneiss, and mudstone, typically <10 cm in diameter. Thin lenses of fine to medium sand are present in the lower portions of this diamict. The laminated pink clay to grey silt (~ 70 cm thick) is present for tens of kilometers in the middle reaches and often contains outsized clasts of Athabasca Group sandstone up to 30 cm in diameter.

*Unit 8*

Unit 8, up to 2 m thick, commonly caps sections in the middle reaches and consists of rhythmically bedded silt and fine sand grading from ripple cross-laminated sand of unit 7. Individual beds range in thickness from 1-6 cm with laminations prevalent in both the dark brown silts and white-to-yellow fine sand layers. Fine sand layers are present in some beds, and display ripple-cross laminated bedding with paleocurrent directions to the north. An absence of bitumen rip-ups or matrix in these sediments is anomalous, considering all exposures lie within the inferred flood spillway of Smith and Fisher (1993) and are within ~30 km of McMurray Formation outcrops along the Athabasca River.

### Distal Reach (Unit 9 – Unit 11)

The lowermost Athabasca River valley, from north of the Firebag River confluence to the modern Athabasca River delta, includes the Big Bend cutbank section, exposing up to 21 m of sediment for approximately 4 km (Fig. 3.12). Three principal units (9-11) are present in the composite stratigraphy (Figure 3.2).

*Unit 9*

Unit 9 is present in the lowermost ~ 5 m of sediment exposed at river level at the Big Bend section (ca. 225 m a.s.l.) and extends below the modern Athabasca River to an unknown depth. It consists of laterally continuous fine-laminated-to-wavy clay and silt beds up to 8 cm thick. Dropstones are rare and deform underlying beds (Fig. 3.13a). Interbeds of ripple cross laminated silts are also present up to 2 cm thick. Soft sediment deformation features are common through the unit, including ball and pillow structures, load clasts, rip-up clasts, and flame structures (Fig. 3.13a).

*Unit 10*

Grading up from Unit 9, and also confined to the Big Bend exposure, is 3-5 m of variably preserved well-stratified beds of mud and silt to fine sand. These wavy to sub-horizontal beds of *unit 10* range from 2-15 cm thick with sharp basal contacts. The grey mud layers are massive to thinly laminated. Sand layers consist of climbing ripple sequences indicating predominantly northward paleoflow with lee-side slopes frequently draped in bitumen (Fig. 3.13d).

*Unit 11*

The uppermost sand-dominated unit is documented at all exposures in the distal reaches and ranges in thickness from 10-15 m (225-240 m a.s.l.). Trough and planar cross-beds (up to 50 cm thick) of fine-to-coarse quartz sands are the main component of this facies, with interbeds of ripple cross laminated sands up to 15 cm thick present at varying elevations (Fig. 3.13d). Bedding planes on cross-stratified sands indicate a range of paleocurrent directions from 230°-120°, but dip predominantly to the north and northeast. Reworked bitumen from the McMurray Formation is prevalent in the trough cross-stratified beds of Unit 11, forming bituminous clasts 3-7 cm diameter that can locally amalgamate to form thicker bituminous-rich clast concentrations. Weathering of these bitumen clasts and matrix from the sand-supported units results in continued oil seepage into the modern Athabasca River.

Terrestrial organics are dispersed sporadically in Unit 11 aside from 10-50 cm thick peaty interbeds at the Big Bend exposure. Where present, approximately 50 cm of massive brown silt caps Unit 11.

*3.2.2. Chronology*

Chronology through the lower Athabasca valley is derived primarily from $^{14}C$ measurements of terrestrial macrofossils (Table 3.2). Many of the radiocarbon samples were recovered from the trough and planar cross-stratified sands, or peaty interbeds of Unit 11 at the Big Bend section, ranging in age from ~ 10.2 to 9.6 $^{14}C$ ka yr BP, situated approximately 225-235 m a.s.l. Spruce (*Picea)* needles and a large wood fragment were taken from Unit 10.

A single wood sample (UCIAMS 187140) was collected from within the boulder gravels of unit 3 at the Susan Lake Gravel Pit. This sample was encased in a reworked bitumen clast and thoroughly stained dark black from bitumen. A date on alpha cellulose of 19.0 ± 60 $^{14}$C ka yr BP is problematic as the Laurentide Ice Sheet was near its maximum extent during that time (*e.g.* Dyke, 2004). The sample was re-dated (UCIAMS 197746) using the same pre-treatment methods and returned a non-finite date.

## 3.5 Interpretations

### *3.5.1 Stratigraphy*

#### Proximal Deposits (Units 1 – 4)

We interpret the quartz rich gravels of Unit 1 at the lowest 2-4 m in mining operations as channel deposition in a paleo-Athabasca River wandering gravel bed system (Desloges and Church, 1987). We correlate Unit 1 to gravels from the Suncor gravel pit east of the Athabasca River that yielded a shoulder girdle bone of a mammoth. High precision radiocarbon ages on ultrafiltered collagen from this fossil yielded an age of 32,140 ± 230 $^{14}$C yr BP (OxA-16322) (Burns and Young, 2017; Froese, unpub.)

Unconformably overlying Unit 1 in the gravel pit exposures are the clean (i.e. lacking oilsand ripups) pebbly sands and fine gravels of Unit 2. Planar tabular crossbed sets and horizontal sheets of fine gravels suggest Unit 2 was a product of bar migration in a competent braided river system (Miall, 1977). We interpret this as deglacial Athabasca River gravel following retreat of the Laurentide Ice Sheet in the Athabasca Valley. Unit 2 is sharply overlain by oilsand-rich boulder gravels of unit 3. The cross-bedded to massive proximal boulder gravels of Unit 3 corresponds to the flood sediments associated with catastrophic flow (e.g. Lord and Kehew, 1987) as first inferred by Fisher and Smith (1993). These deposits represent the peak discharge from outburst floods in the CLAS, and by inference glacial Lake Agassiz as it drained through its northwestern outlet. Unit 3 is the only facies in the study area that frequently scours into and incorporates rip-up clasts of the McMurray Formation and Waterways Formation, suggesting that Unit 3 records the most erosive event in the region associated with the formation of the CLAS.

Unit 4 is present at the same elevation as Unit 3 but lacks the coarse material that characterizes the previous unit. The thin planar-tabular cross-bed sets of Unit 4 are commonly draped in bitumen and are characteristic of braided river deposits, specifically foreset development during a relative high-water stage (Miall, 1977). It is likely that Unit 4 represents the continued flow through the CLAS from Lake Agassiz after the catastrophic discharge recorded in Unit 3. The wedge-features at the surface of Unit 4 are interpreted as ice-wedge casts and are indicative of periglacial conditions following deposition (Murton and French, 1993).

### Middle Reach Sedimentation (Units 5 – 8)

Middle-reach sedimentation records the fluctuation of a retreating ice margin associated with a local ice-contact lake. The lithofacies observed in this reach reflect an interplay of sedimentation between the paleo-Athabasca River system and sediment-rich discharge from a receding Laurentide Ice Sheet dominated by subaqueous debris flows. Ice proximity can be further inferred from the variety of deformation of sediments in the reach, including complex assemblages of soft sediment and brittle deformation and the presence of dewatering structures.

The graded thin stacks of planar-bedded sand to silt rhythmites of unit 5 are interpreted as the product of consecutive surge type turbidity flows into an ice-distal glaciolacustrine environment. The finer grain textures of Unit 5 with an absence of current ripples indicate deposition was dominated by suspension settling of sediment plumes into a relatively low-energy system (e.g. Ó Cofaigh and Dowdeswell, 2001; Russell and Arnott, 2003). However, the anomalously thick silt beds observed with southward plunging soft sediment deformation structures suggest large amounts of sediment were periodically delivered to the lake basin from the ice margin with sufficient energy to enable sediment liquefaction. Further, laminated pink clay rip-up clasts associated with these loaded silt beds (unit 5) indicate subaqueous flows scoured and transported pre-existing glaciolacustrine sediments to distal reaches of the lake basin.

The transition from an ice-distal to ice-proximal glaciolacuistrine environment is suggested by the presence of deformational structures associated with ice-overriding pre-existing sediments and the deposition of the flat-lying diamict of unit 6. The large scale folding and shearing structures at the Firebag section (Fig. 3.8) is interpreted as subglacial deformation from an overriding ice mass. The presence of abundant clastic dikes injected through the glaciotectonized sediments of Unit 6 record the hydraulic over pressurization and rapid dewatering of the underlying sediments in a subglacial system (van der Meer et al., 2009). We interpret these large-scale hydrofracturing structures as being contemporaneous with local glaciotectonism near the ice margin (e.g. Piotrowski, 2007). In contrast, brittle deformation displayed by the upper rhythmites of unit 5 suggest that these sediments were de-watered and competent before shearing occurred. A consistent southward direction of subglacial shearing is indicated in the orientation of the thrust planes and fold axes in this sequence.

The clast-supported pink diamict capping the glaciotectonized sediments is interpreted as direct ice-marginal sedimentation either as a subglacial traction till (Evans et al., 2006), or a gravel-rich debris flow from an oscillating ice front. The association with significant deformation and truncation of the underlying sediments is consistent with the diamict forming under significant shearing conditions, as expected in subglacial traction tills formed after glacial deformation (e.g. Evans et al., 2013). However, the absence of a discernable fissile matrix, coupled with incomplete homogenization of clay and silt clasts is not consistent with typical characteristics of a subglacial traction till (Evans et al., 2006). The coarse nature and faint stratification displayed in this diamict may better be interpreted as the product of an ice-proximal subaqueous debris flow. Indeed, similar clast-supported diamicts in glaciolacuistrine settings have been interpreted to record concentrated sediment-rich plumes into a lake basin from a stagnant ice margin (e.g. Eyles et al., 1987).

The up-valley thinning pink sand overlying the pink diamict at the Firebag River section indicates a sediment source from the north. The distinctive pink colouration of these sands is similar to the pink diamicts (till) in the area, suggesting a similar glacially-influenced sediment origin. The laterally extensive graded rhythmic sand to silt beds of unit 7 are attributed to a re-activation of density currents into a proximal ice-dammed lake. The wider variation, increased thickness of beds, and larger range in grain size compared to the thin rhythmites of unit 5 indicates a higher-energy depositional environment coupled with an increase in sediment input from both the retreating LIS and the paleo-Athabasca River. Scouring of planar beds by pebble to cobble clasts indicates local influxes of debris-rich traction currents (Cheel, 1982; Bennett et al., 2002; Talling et al., 2012). Similar infilled scour features are commonly observed in subaqueous outwash deposition in proximal ice-margin settings (e.g. Livingstone et al., 2015; Winsemann et al., 2018). Further, the presence of trough cross-stratified sands with isolated pebbles in Unit 7 indicates the transport of traction currents that enable dune formation and migration along the lake floor after large mass-flow events (Eyles et al., 1987; Russell and Arnott, 2003). Waning stages of such turbid flows are characterized by ripple cross-laminated fine sands (Ashley et al., 1982) similar to the uppermost portions of Unit 7.

The diamicts and laminated silt to clay package that interrupt the sand-dominated sedimentation of Unit 7 further evidence the sedimentological influence of the retreating ice margin in the middle-reaches of the study area. The lower silt-supported diamict is interpreted to record a sediment flow event into the lake basin, likely initiated by a fluctuating ice margin. A relative scarcity of clasts along with the incorporation of stratified sand and silt interclasts without significant deformation to the underlying sediments is consistent with a subaqueous mass flow origin (Eyles, 1987). The stratified pink to grey clay Unit with dispersed, often striated clasts is a typical example of deep-water proglacial sedimentation from rain-out of ice-rafted debris (e.g. Ó Cofaigh and Dowdeswell, 2001; Howard, 2010).

The highest surfaces in the area of the Firebag moraine are capped by distinctive tan brown to light grey laminated silts and fine sands of Unit 8. These beds represent lacustrine sedimentation associated with the final stage of ice-damming of the lower Athabasca valley, fed primarily from the paleo-Athabasca River system; the pink diamicts or similarly coloured fine beds are absent. These observations are consistent with the northward trending beds of ripple cross-bedded sands. Similar rhythmic sequences have been interpreted as forming through pulses of sediment-laden underflows (e.g. Smith and Ashley, 1985; Ó Cofaigh and Dowdeswell, 2001; Johnsen and Brennand, 2006) rather than rainout debris as typified in 'classic' proglacial lake sequences (c.f. Smith, 1978; Livingstone et al., 2015). These upper rhythmites of Unit 8 likely represent seasonal variations in stream discharge and sediment supply and suggest that the final ponding of water in the middle reaches may have existed for years to a few decades.

Most of the gravels and boulders in the diamicts of the middle reaches are sourced from the predominantly pink, hematite stained Paleoroterozoic Athabasca Group (Post, 2003). The very well sorted, southerly (up-valley) flowing pink quartz sand beds within Unit 7 and pink clay rip-up clasts of unit 5 and unit 6 indicate a sediment source from this group.

### Distal Deposits (Units 9 – 11)

Interpretations on the stratigraphy observed in the most distal portions of the study area are largely consistent with those described by Rhine and Smith (1988), particularly as their inferences are primarily derived from the Big Bend cutbank section (see Fig. 7 in Rhine and Smith, 1988). Our lithostratigraphic investigations agree with the tripartite architecture initially proposed by Rhine and Smith (1988) in the distal reaches of the study area. The well-organized stratigraphy in this area is characteristic of a braid delta sequence where lacustrine muds (Unit 9) are overlain by prodelta sediments (Unit 10) and a thick assemblage of trough, planar, and ripple cross-bedded sands (Unit 11) indicative of braided river deposition (Miall, 1977; McPherson, 1987; Rhine and Smith, 1988).

The well-stratified basal clay to sand couplets of Unit 9 are interpreted to represent suspension settling and sediment plume sedimentation into the basin of glacial Lake McConnell. Rare dropstones were likely ice-rafted into the basin. The clay layers are derived from the settling of fine material in a low-energy system, whereas occasional ripple cross-laminated sand indicate sedimentation influenced from turbidity currents migrating across the lake floor (Ashley et al., 1982). The most probable trigger mechanism for liquefaction in these significantly deformed lacustrine units is overloading from rapid sedimentation from river-fed plumes that originate from the delta to the south (Owen and Moretti, 2011). In some cases, rapid loading from the overlying Unit 10 resulted in the incorporation of a coarser sediment load, including large sandy rip-ups.

The alternating silty sand to clay beds of Unit 10 are interpreted to be the product of periodic pulses of underflow sedimentation across the lake basin. Silt and sand sequences displaying ripple-cross lamination is consistent with waning sedimentation from a traction flow (Eyles et al., 1987) in a prodelta setting. Beds of grey clays are interpreted to represent sedimentation from suspension settling in a quiescent water column before sediment was delivered to the prodelta from underflows.

The primary component of distal sedimentation in the lower Athabasca valley – beginning ~35 km north of the Firebag Section – consists of stacked sets of pebbly-sand trough and planar cross-beds (Unit 11), interpreted as channel bar and dune deposition in a braided river system (e.g. Cant and Walker, 1978; Miall, 1985). The concentrated distribution of sporadic bitumen-rich clasts on the troughs and lee sides of cross-bedded pebble-sands suggest they were transported as typical bedload in a braided Athabasca River system (Ashmore, 1991), and may record periods of increased erosion from the upstream McMurray Formation. The massive silts situated atop Unit 11 at the Big Bend section are interpreted to record aeolian reworking of deltaic deposits following deposition.

*3.5.2 Chronology*

Results from the standardized radiocarbon material (Table 3.2) show that the additional pretreatment using organic solvents (i.e. ethanol, toluene, chloroform) did not change the radiocarbon measurement of the standardized material. This shows that variances in radiocarbon measurements between unknown samples (i.e. standard ABA only vs. standard ABA plus organic solvent pretreatment) is from the removal of a solable fraction within the material, rather than contamination by the solvent. In contrast, solvent-pretreated wood and needles (*Picea)* that were recovered from the distal braided delta sands generally yielded younger $^{14}$C ages than corresponding samples that were pretreated by ABA only (Table 3.2). Samples from one log (DF06-14) returned solvent-pretreated ages that were indistinguishable from the ABA-only ages. A simialr solvent-pretreated sample from another log was ~50 $^{14}$C years younger than the corresponding ABA-only samples (DF06-WP21) from the same log, although within standard error. Samples of *Picea* needles had the largest variance between only ABA and ABA plus organic solvent pretreated radiocarbon ages, with one solvent-pretreated subsample (DF06-005D) yielding an age that was ca. 800 $^{14}$C yr younger than an ABA-only alliquot.

Most of the radiocarbon ages from the lower Athabasca valley are sourced from the sandy fluvial-deltaic facies of Unit 11 in the distal reaches from 230-235 m a.s.l. The ages range from ca. 10.2 to 9.6 $^{14}$C ka yr BP (Table 3.2) and represent maximum ages for the formation and duration of the distal braid delta complex. The temporal associations between individual samples is tightly-constrained, suggesting that re-working of older material from the Athabasca River watershed was insignificant and contamination from bituminous ‘old carbon’ was effectively mitigated in the α-cellulose fraction.

The absence of dateable material from the middle reach sections is not surprising considering an early deglacial environment in an ice-contact setting. A single sample (SLGP-16-01) was found in the proximal reaches however, dated to an age of 19,000 ± 60 $^{14}$C yr BP. This sample was subsequently re-dated (SLGP-16-02), as the Laurentide Ice Sheet was near its maximum extent during this time (Dyke et al., 2004), resulting in a non-finite age of >45900 $^{14}$C yr BP. It is possible that this sample is a fossilized wood fragment (e.g. Roy, 1972) within the lower Cretaceous McMurray Formation, and that the initial date was contaminated by a younger carbon source.

## 3.6 Discussion

### *3.6.1 Lower Athabasca River valley stratigraphy*

Previous reconstructions of the stratigraphy in the study area have suggested than a large (>4000 km$^2$) braid delta was built in glacial Lake McConnell immediately north of the Fort Hills at ~300 m a.s.l. (Rhine and Smith, 1988). Later it was thought these sediments were derived from catastrophic flooding and erosion of the CLAS spillway (Smith and Fisher, 1993; Fisher et al., 2002). Results from this study indicate the braid delta to be smaller, and the overall lower Athabasca valley stratigraphy to be more complex than previously considered. Here, we present the analysis of 11 principal sedimentological units that are separated into three distinct depositional phases bracketing catastrophic drainage from glacial Lake Agassiz.

#### Pre-flood Phase (Deglacial Athabasca River)

Deposition of the well-rounded quartzite gravels of unit 1 occurred as channel deposits in a shallow wandering gravel bed river system (e.g. Desloges and Church, 1987) at a similar base level (~210 m a.s.l.) as the modern Athabasca River system. It is likely that this lithofacies corresponds to the 'lithologically different gravel' below the catastrophic flood gravels (unit 3) identified by Teller et al. (2005), which yielded a radiocarbon age on wood of >45 810 $^{14}$C yr BP (Beta-193988). However, clear observations or documentation of these 'lithologically different gravels' have yet to be reported. Teller et al., (2005) and Teller and Boyd, (2006) interpret the non-finite wood age as being the product of incomplete scouring within the Athabasca Valley, and that gravels underlying Unit 3 record an earlier Lake Agassiz flooding event, possibly contemporaneous with the Younger Dryas interval. Although we agree with Teller et al. (2005) and Teller and Boyd's (2006) interpretation that the entirety of gravel in the valley is not a product of a single flooding event and that fluvial scouring was incomplete, we find no evidence of multiple catastrophic flows from Lake Agassiz in the stratigraphy of the lower Athabasca Valley. In 1974 a mostly articulated pelvis of a woolly mammoth was recovered from the Suncor mine site at a depth of ~ 15 m below the surface (Burns and Young, 2017). The mammoth was dated to 32,140 ±325 $^{14}$C years BP (OxA-16322) consistent with a mid-Wisconsinan (MIS 3) age for the associated gravel. We think it is most likely that the quartzitic homogeneity and the absence of abundant McMurray Formation rip-ups within these lowermost gravels coupled with the non-finite wood and finite mammoth collagen age suggest Unit 1 is a mid-Wisconsin or earlier low-energy fluvial system. Therefore, the proximal valley stratigraphy in the Fort McMurray region is likely not directly correlative with the multiple flooding episodes (Murton et al., 2010) or sediment grain increases from deep-water cores (Keigwin et al., 2018) in the Mackenzie Delta region. It is possible that discharge from a glacial or subglacial lake(s) situated in the Mackenzie Valley was responsible for one or possibly two of these flooding surfaces observed.

The pebble sands and fine gravel of Unit 2 record deposition of a deglacial Athabasca River system following the northward retreat of the Laurentide Ice Sheet from the Survive Moraine. At the same time, the topographically-confined LIS retreated downslope, blocking northward drainage and resulted in a series of fluctuating proto-glacial Lake McMurray waterbodies occupying the proximal to middle reaches of the lower valley. The depositional influence of ice in the lower Athabasca valley is comparable to that in the westward Peace and Wabasca Valleys, where reverse-gradient proglacial lakes produced a series of characteristic ice-marginal to glaciolacuistrine lithofacies evidencing the sedimentological influence and relative position of the ice margin (c.f. Slomka and Utting, 2018).

Critical to the explanation of the pre-flood, ice-marginal process sedimentology is the complex stratigraphy at the Firebag River section (Fig. 3.5). Previous investigations have yielded conflicting interpretations. Taylor (1960) suggested that intermittent fluctuations in lake levels were controlled by fluctuations in the thickness of an ice dam to the north, ultimately resulting in deposition of the interbedded pink clay diamict (of Unit 7) in a lacustrine setting. Subsequently, Rhine, (1984) documented multiple 'sedimentological anomalies' that were inconsistent with the stratigraphy observed in more northerly sections along the Athabasca River. The interbedded pink clay-rich diamict of Unit 7 was interpreted as a till derived from iceberg dumping interrupting fluvial sedimentation. Additionally, Rhine (1984) documented laminated deposits capping middle-reach sections (Unit 8 in this study), interpreting the rhythmites as poorly-developed varves in either a local shallow lake, or by a rapid lake transgression. Lastly, vegetation and colluvium cover limited Rhine and Smith (1988) to documenting only the lowermost turbidities (Unit 5) at the Firebag Section – suggesting they record prodelta deposition into glacial Lake McConnell – and inferred all sediments overlying Unit 5 as high angle foreset beds, consistent with their braid delta depositional model largely derived from sections at the Big Bend section ~60 km down river. In short, the enigmatic Firebag Section records the complex sedimentological influence of the LIS in the Athabasca valley.

We interpret the rhythmites of Unit 5 as recording the earliest stages of ice influence in the lower Athabasca valley. During this time, the ice margin was to the north, at or near the Richardson Moraine where it fed a proto-Lake McMurray basin with laterally migrating sediment plumes, resulting in occasional pink clay rip-ups and up-valley trending flame structures. The rarity of dropstones within these deposits is consistent with an IRD starved ice-distal subaqeous system (e.g. Slomka and Utting, 2018) from the suppression of iceberg rafting possibly by anticyclonic winds from the southeast (Wolfe et al., 2004). It is also possible that silt and sand sedimentation rates within this unit outpaced the influx of ice-rafted debris, effectively masking the ice-derived contribution (Domack, 1984). A readvance over these earlier deglacial sediments is recorded in the suite of glaciotectonic deformational and water escape structures of unit 6, coupled with the overlying diamict. Indeed, similar large-scale compressional deformation overriding and incorporating ice-contact deposits have been used to infer the oscillatory behaviour of ice-margins (e.g. Lønne, 1995; Benn and Evans, 1996; Evans et al., 2013). This moderate readvance was likely responsible for the widespread glaciotectonism associated with the Firebag moraine complex, extending at least 40 km to the south of the Firebag River exposure (Andriashek and Atkinson, 2007).

Further retreat of the LIS resulted in a series of multi-stage lakes where the pink and white to yellow sandy beds near the base of Unit 7 were deposited. Subaqueous sedimentation rates increased during this time from a rapidly retreating ice sheet depositing pink sands, and the relative proximity of the mouth of the paleo-Athabasca River depositing white to yellow sands. The pink colours observed in glacially-influenced sediments is a product of erosion from hematite-stained quartz grains from the Paleoproterozoic Athabasca Group. This predominantly-sandstone group dominates the bedrock to the northeast of the lower Athabasca valley and does not occur within, or to the south of the lower Athabasca valley (including along or near the head of the CLAS) (Post, 2003). A north to south glacially-transported origin of material derived from this formation is the simplest explanation for its prevalence in the middle reaches.

A period of lake transgression in the Athabasca valley interrupted proximal ice-margin sedimentation as evidenced in the silty clay-supported pink to grey unit of unit 7. Similar laminated deep-water deposits have been mapped at exposures from up the Firebag River, to south of the Clearwater-Athabasca confluence near Fort McMurray (Bayrock, 1971; Bayrock and Reimchen, 1973; Fisher and Smith, 1993b; Andriashek and Atkinson, 2007; Fisher and Lowell, 2017), and attributed to sedimentation into the late Wisconsinan glacial Lake McMurray at 460 m a.s.l. (Rhine and Smith, 1988).

The paleo-Athabasca River built a delta in the southwestern arm of Lake McMurray during this highstand (Fisher and Smith 1993b) and has been assigned a minimum luminescence age of 14.0 ± 1.0 ka from post-depositional dune formation by Munyikwa et al. (2017). The timing and nature of drainage from glacial Lake McMurray are poorly constrained, but viable routes include to the west, around the southern margin of the Birch Mountains, and to the east, north of the Grizzly Bear Hills (Fisher et al., 2009; Fisher and Lowell, 2017). Once the levels of Lake McMurray dropped, the mouth of the paleo-Athabasca River migrated northward concurrently with the ice margin and continued to deposit silts and sands into a regional multi-phase lake occupying the lower valley, as indicated by the upper cross-stratified sands of Unit 7. A final ponding the valley before full ice retreat is recorded in the rhythmic beds of Unit 8 which represents the final sedimentological influence of Laurentide Ice. Importantly, there is no evidence of McMurray Formation rip-ups, or indications of catastrophic influxes displayed in the ice-marginal sequences, indicating these sediments were deposited prior to, and remained above maximum flood sedimentation.

A flood capable of eroding the CLAS and depositing high-energy boulder gravels (unit 3) less than 50 km to the south would be expected to leave a discrete sedimentological signature in depositional environments situated along the flood spillway. For example, modern and paleofloods of relatively small magnitudes can be evidenced in lake sediment records by abrupt increases in grain size (Arnaud et al., 2002), anomalously thick structureless beds (Lewis et al., 2009), and mineralogically-distinct layers (Schillereff et al., 2014), all of which are absent in the ice-marginal successions.

### Flood Phase (Catastrophic drainage from glacial Lake Agassiz)

A transgression of glacial Lake Agassiz to at least its lowest Tintah level would have enabled drainage through the northwest outlet (Breckenridge, 2015), incising the Clearwater lower-Athabasca Spillway and depositing sheets of boulder gravel in the lower Athabasca Valley (Smith and Fisher, 1993; Fisher and Smith, 1994). The catastrophic flood deposits documented in Smith and Fisher (1993) are equivalent to the proximal boulder gravel of Unit 3. LiDAR profiles of Unit 3 along a discrete flooding surface south of the Firebag moraine (at 280 m a.s.l.) indicates a gradient of 1.6 m/km. This slope is five times steeper than the modern Athabasca River slope below Fort McMurray (at 230 m a.s.l.) of 0.27 m/km (Fig. 3.14). Given these differences in slope, the flood profile would project under the modern river approximately 30 km down stream from the measured flood profile, approximately 10 km north of the Firebag moraine. Indeed, this inference mirrors the observed stratigraphy at sections that indicate Unit 3 terminates in that area.

Previous authors have suggested that the Laurentide Ice Sheet was situated at the Firebag moraine immediately prior to catastrophic flooding, and that northward drainage through the Athabasca valley was permitted only when the ice margin decoupled from the eastern flank of the Birch Mountains (Fisher et al., 2009; Fisher and Lowell, 2012; Fisher and Lowell, 2017). However, as previously mentioned, sections north of the Firebag moraine show no evidence of a catastrophic flood sedimentation. Further, flood waters routed along (or under) an ice margin across the lower valley would result in a series of meltwater landforms along the valley slope, most notably lateral and/or subglacial meltwater channels formed by the erosion of sediment and/or bedrock from the confined drainage (Benn and Evans, 2010). The absence of discernible erosional benches or abandoned meltwater channels on the eastern slope of the Birch Mountains from the LiDAR data (Fig. 3.15) indicates that the ice did not act as blockade for catastrophic drainage instead the LIS was absent from the lower Athabasca Valley and did not influence the flooding locally.

### Post Flood Phase (sustained Lake Agassiz flow)

The post-flooding phase in this study refers to the period of sustained flow from glacial Lake Agassiz following catastrophic drainage, as demarcated by prominent strandlines at 438 m a.s.l. near the head of the spillway (Fig. 3.1) (Smith and Fisher, 1993). Continued discharge resulted in the deposition of the braided river pebbly sands of unit 4 in the proximal reaches. The presence of vertical ice wedge casts dissecting the well-stratified sands of unit 4 indicate that permafrost conditions persisted for some period of time after deposition, and thus likely during the late Pleistocene. Comparable ice wedge features have been documented in flood and post-flood sediments throughout the mineable oilsands region (e.g. Saxberg and Robertson, 2017; Woywitka et al., in prep.) and near the head of the Clearwater Spillway, where their formation is constrained between 11 and 9.9 ka BP (Fisher, 1996).

Initial stratigraphic interpretations on the formation of the distal delta (unit 9 – unit 11) suggested that a massive influx of eolian sand from anticyclonic winds off the Laurentide Ice Sheet into the Athabasca River watershed was the primary sediment source for a meso-energy, braided river-dominated complex (Rhine, 1984; Rhine and Smith, 1988). Smith and Fisher (1993) later suggested that the delta was derived from sediment eroded from the CLAS during a flood phase. This inference is based on an apparent temporal connection around 9.9 $^{14}$C ka BP between 3 averaged radiocarbon dates from the braid delta and 3 dates from the flood sediments respectively (Table 3.3). However, as Teller et al., (2005) and Teller and Boyd (2006) note, the age attributed to flood by Smith and Fisher (1993) is instead from a peat unit overlying the boulder gravels (Unit 3), indicating the flood must pre-date the oldest organics deposited in the depression at 10.3 $^{14}$C ka (BP GX-5301-II).

We thus interpret the formation of the distal braid delta (Unit 9 – Unit 11) records sustained flow from continued – but significantly decreased – discharge from glacial Lake Agassiz after the initial outburst. Indeed, the sediments observed in Unit 11 closely resemble the sand-dominated South Saskatchewan River model (c.f. Cant and Walker, 1978; Miall, 1978), where planar and trough cross stratified beds recording channel and compound bar formation comprise the majority of the architecture with frequent low-energy, small-scale bedforms.

Like the middle-reach ice-marginal deposits, a distinct downstream sedimentological fingerprint would be expected in the distal fluvial-deltaic complex from hyperconcentrated flood flows (Smith and Fisher, 1993) depositing decameter rip up clasts within a spillway channel (Fisher and Lowell, 2017). For example, upper-flow discharge in distal braided river systems are typically recorded in 1-3 m thick, laterally continuous fining-upwards successions of horizontally-bedded sands with scoured erosional surfaces (Miall, 1985). Similarly, Hjellbakk, (1997) interprets sequences of massive sand beds as the product of hyperconcentrated flows into a high-energy braided river system. No such architecture is recorded in the lower Athabasca valley. Further, other structures commonly attributed to high-energy fluvial deposition, for example rip up clasts, inversely graded and/or anomalously thick units, strongly uniform paleoflow indication, chutes, grain size breaks, outsized imbricated clasts, or coarse cut-and-fill structures are also absent within the organized fluvial sands of Unit 11.

The braid delta complex was previously inferred to cover an anomalously large area of over 4,200 $km^2$ from just north of the Firebag moraine at ~300 m a.r.l. to the modern Athabasca River delta (Rhine, 1984; Rhine and Smith, 1988). This extent was likely derived from initial interpretations that the middle reach sections, including the Firebag River site, represented deltaic sedimentation into glacial Lake McConnell. As such, a revised stratigraphy of the ice-marginal sections permits the revision on the extent of the Lake McConnell deltaic complex. From this study, the distribution of fluvial-deltaic sediments (Unit 9 – Unit 11) span only the distalmost ~ 25 km of the lower Athabasca valley, approximately 75 percent less than previously inferred. This suggests that extreme influxes of sediment were not a requirement for the formation of the delta into Lake McConnell.

In summary, there are no unequivocal sedimentological features displayed in the distal fluvial-deltaic facies that can be attributed to high-magnitude flooding. The organized tripartite stratigraphy is instead characteristic of a traditional meso-energy glaciofluvial braided outwash system (c.f. McPherson et al., 1987), more aligned with the initial sedimentological interpretations of Rhine (1984) and Rhine and Smith

(1988). This model is consistent with formation following catastrophic drainage from glacial Lake Agassiz and deposition of the proximal flood gravels of Unit 3.

*3.6.2 Chronology*

The radiocarbon calibration curve is highly non-linear during the time period relating to the samples from the fluvial-deltaic sediments (Units 9 - 11) in the distal reach of the lower Athabasca valley. Thus even small shifts in measured $^{14}C$ age due to bitumen contamination can produce meaningful differences in their respective calibrated age ranges. Given the importance of precise and accurate dating of sediments related to northwest drainage of glacial Lake Agassiz with respect to potential climate forcing, it is important to include pretreament methods that mitigate bitumen contamination of radiocarbon samples in the Fort McMurray region.

Fisher et al. (2009) cored small lakes along Don's moraine, the Firebag moraine and Richardson moraine in the lower Athabascsa valley. They propose a chronology for deglaciation and outlet availability based on radiocarbon ages mainly on plant macrofossils and charcoal from the basal lake sediments (Table 3.3).

These basal ages on the lakes suggested Don's moraine ranged from about 10.21 to 10.46 $^{14}C$ ka BP, and Fisher et al., (2009) use these dates to suggest it was formed about 10.46 $^{14}C$ ka BP. Basal ages from lakes proximal to the Firebag moraine ranged from ca. 9.09 to 9.85 ka $^{14}C$. They assigned a minimum age of 9.66 $^{14}C$ ka BP and a maximum age of 9.85 $^{14}C$ ka BP to the Firebag moraine based on their oldest ages from the cores. Ages from basal lake cores for the Richardson moraine ranged from about 8.33 to 9.51 $^{14}C$, prompting Fisher et al. (2009) to assign a mimum age of 9.51 $^{14}C$ ka BP and maximum age of 9.66 $^{14}C$ ka BP. On the basis of these ages, they argue that the lower Athabasca valley was only ice-free after ca. 9.66 $^{14}C$ ka BP. Collectively these data, according to Fisher et al., (2009) and Fisher and Lowell (2012; 2017) are used to indicate that the Laurentide Ice Sheet occupied the lower Athabasca River valley from about 10.5 ka $^{14}C$ yr BP until after ca. 9.6 ka $^{14}C$ ka BP. Any catastrophic flooding down the lower Athabasca River valley must have therefore taken place after that time.

Our peat, wood, and log dates however, are more aligned with previous ages from distal fluvial-deltaic sands of 9,910 ± 190 $^{14}$C BP from (Rhine and Smith, 1988) and 9,710 ± 130 $^{14}$C BP from (Smith and Fisher, 1993), suggesting that 'basal' radiocarbon ages from small morainal lakes poorly constrain ice margin retreat and outlet availability. The oldest high-quality wood age in this study (UCIAMS 187136) indicates that the lower Athabasca valley was a fully-operational outlet for glacial Lake Agassiz well within the Younger Dryas chronozone by at least ca. 10,200 $^{14}$C BP, possibly decades to a hundreds of years earlier considering ecesis. Indeed, Lake Agassiz flow through the Fort McMurray region during this time is permitted by the radiocarbon and luminesence deglacial chronologies of Dyke et al. (2004) and Mukinaywa et al. (2017) respectively. Persistance of the northwestern outet into glacial Lake McConnell continued for at least ~ 800 radiocarbon years up to 9.60 $^{14}$C BP – consistent with abandonment estimates near the head of the outlet at 9.45 $^{14}$C BP (Fisher, 2007). This chronology is consistent with diversion of flow to the southern outlet (Teller et al., 2000; Fisher, 2003; Lepper et al., 2015) as a result of differential post-glacial uplift (Teller, 2001).

The timing of initial Lake Agassiz drainage through the CLAS, and deposition of the flood sediments (Unit 3), is less well constrained. Sedimentological observations from this study suggests that the catastrophic flooding occurred well before development of the braid delta complex at ca. 10,200 $^{14}$C yrs BP. This interpretation is consistant with IRSL dates on the catastrophic flood deposits of 12.8 ± 1.0 ka yr BP (Woywitka et al., in prep.) and would allow for Lake Agassiz discharge to the Arctic Ocean at the onset of the YD around 12.9 ka yr BP (e.g. Teller et al., 2005; Murton et al., 2010; Condron and Winsor, 2012). Alternatively, it is possible that the eastern outlet facilitated Lake Agassiz overflow at the onset of the YD (e.g. Carlson et al., 2007; Levac et al., 2015; Leydet et al., 2018), and that catastrophic northwestward drainage acted as a THC supression mechanism only after abandonment of the eastern outlet (Leydet et al., 2018). Refined dates directly relating to the flood deposits of Unit 3 are required to determine the timing of initial Lake Agassiz flooding in the Fort McMurray region.

*3.6.3 McConnell Lowstand Hypothesis*

Previous reconstructions on the depositional model regarding catastrophic Lake Agassiz drainage through the lower Athabasca River valley infer a simultaneous sequence that eroded the CLAS, depositing sheets of boulder gravels (Unit 3) while building a braid delta (Unit 9 – Unit 11) into Lake McConnell at ~ 300 m a.s.l. starting just north of the Firebag moraine (e.g. Rhine and Smith, 1988; Smith and Fisher, 1993).

We suggest an alternative hypothesis is warranted given: i) the flooding profile slopes five time steeper than the modern Athabasca River south of the Firebag Moraine ii) there is no clear flood sedimentation or influence in the lower Athabasca River valley stratigraphy north of the Firebag moraine, and iii) Lake McConnell is confined to a maximum of ~240 m a.s.l. in the distal reaches. A possible evolutionary model that explains these sedimentological discrepancies is that initial catastrophic flooding graded into a lowstand of Lake McConnell, depositing Unit 3 in the proximal reaches while incising the ice-marginal sediments in the middle reaches. A subsequent transgression of Lake McConnell up to a maximum of 240 m a.s.l. – facilitated by a combination of rapid isostatic rebounding (Smith, 1994) and/or increased meltwater influx – fed by continued discharge from Lake Agassiz would then have built the braid delta observed in the distal reaches (Unit 9 – Unit 11) from ~ 10.2 to 9.6 $^{14}$C ka yr BP. Of course, this model would situate the hypothetical Lake McConnell flood delta below the basal muds of Unit 9 and the modern Athabasca Delta (~ 210 m a.s.l.), which has yet to be identified.

At present, relatively few studies have been conducted in relation to the evolution of glacial Lake McConnell, specifically on the effect of glacial Lake Agassiz outbursts on route to the Arctic Ocean during the Younger Dryas. Future work constraining the extent, timing and dynamics of comparable Lake McConnell deltas – in the Peace, Hay, and Liard Rivers for example – are required to test the lowstand hypothesis and further improve the understanding between deglacial meltwater routing and abrupt climate change.

### 3.7 Conclusion

Revisiting the northwestern outlet of glacial Lake Agassiz within the lower Athabsaca River valley resulted in the identification of 11 principal sedimentological units. Radiocarbon dates from mammoth bone suggest a mid-Wisconsin Athabasca River operated at a similar baselevel as the modern river. A fluctuating late-Wisconsin Laurentide Ice Sheet periodically blocked northward drainage of the valley before vacating it completely and enabling catastrophic drainage from Lake Agassiz. Sustained Lake Agassiz flow from then built a braid delta complex in the distal valley into glacial Lake McConnell at ~ 240 m a.s.l. from 10.2 to 9.6 $^{14}C$ ka during the later portion of the Younger Dryas.

An absence of clear flood sedimentation north of the Firebag moraine coupled with a six-fold difference in flood vs modern river slope prompts the development of a conceptual depositional model in which catastrophic flooding inflows into a low stand of glacial Lake McConnell. Additional work documenting the influence of catastrophic glacial Lake Agassiz drainage in the Mackenzie River valley is required to temporally and genetically link meltwater routing to climatic perturbations at the end of the last Ice Age.

**References**


Andriashek, L.D., Atkinson, N., 2007. Buried channels and glacial-drift aquifers in the Fort McMurray Region, northeast Alberta, Alberta Geological Survey, Earth Sciences Report 2007-01.

Arnaud, F., Lignier, V., Revel, M., Desmet, M., Beck, C., Pourchet, M., Charlet, F., Trentesaux, A., Tribovillard, N., 2002. Flood and earthquake disturbance of Pb geochronology. Terra Nov. 14, 225–232. https://doi.org/10.1046/j.1365-3121.2002.00413.x

Ashley, G.M., Southard, J.B., Boothroyd, J.C., 1982. Deposition of climbing-ripple beds: a flume simulation. Sedimentology 29, 67–79. https://doi.org/10.1111/j.1365-3091.1982.tb01709.x

Ashmore, P., 1991. How do gravel-bed rivers braid? Can. J. Earth Sci. 28, 326–341. https://doi.org/10.1139/e91-030

Bayrock, L.A., 1971. Surficial geology Bitumount, NTS 74E. Alberta Res. Counc. Alberta Geol. Surv. Map 34, scale 1:250 000.

Bayrock, L.A., Reimchen, T.H.F., 1973. Surficial geology, Waterways, NTS 74D. Alberta Res. Counc. Alberta Geol. Surv. Map 34, scale 1:250 000.

Benn, D.I., Evans, D.J.A., 2010. Glaciers and Glaciation, 2nd ed. Hopper Education, London.

Benn, D.I., Evans, D.J.A., 1996. The Interpretation and Classification of Subglacially-deformed Materials 15, 23–52.

Bennett, M.R., Huddart, D., Thomas, G.S.P., 2002. Facies architecture within a regional glaciolacustrine basin: Copper River, Alaska. Quat. Sci. Rev. 21, 2237–2279. https://doi.org/10.1016/S0277-3791(02)00027-6

Breckenridge, A., 2015. The Tintah-Campbell gap and implications for glacial Lake Agassiz drainage during the Younger Dryas cold interval. Quat. Sci. Rev. 117, 124–134. https://doi.org/10.1016/j.quascirev.2015.04.009

Broecker, W.S., Kennett, J.P., Flower, B.P., Teller, J.T., Trumbore, S., Bonani, G., Wolfli, W., 1989. Routing of meltwater from the Laurentide Ice Sheet during the Younger Dryas cold episode. Nature 341, 318–321. https://doi.org/10.1038/341318a0

Bronk Ramsey, C., 2009. Bayesian Analysis of Radiocarbon Dates. Radiocarbon 51, 337–360. https://doi.org/10.1017/S0033822200033865

Burns, J.A., Young, R.R., 2017. A Tale of Two Floods. How the End of the Ice Age Enhanced Oil Sands Recovery-and Decimated the Fossil Record. In: Alberta's Lower Athabasca Basin: archaeology and palaeoenvironments. Edited by B.M. Rogaghan. AU Press, Edmonton. 25–43.

https://doi.org/10.15215/aupress/9781926836904.01 43

Cant, D.J., Walker, R.G., 1978. Fluvial processes and facies sequences in the sandy braided South Saskatchewan River, Canada. Sedimentology 25, 625–648. https://doi.org/10.1111/j.1365-3091.1978.tb00323.x

Carlson, A.E., Clark, P.U., Haley, B.A., Klinkhammer, G.P., Simmons, K., Brook, E.J., Meissner, K.J., 2007. Geochemical proxies of North American freshwater routing during the Younger Dryas cold event. Proc. Natl. Acad. Sci. 104, 6556-6561. https://doi.org/10.1073/pnas.0611313104

Cheel, R.J., 1982. The depositional history of an esker near Ottawa, Canada. Can. J. Earth Sci. 19, 1417–1427.

Clark, P.U., Dyke, A.S., Shakun, J.D., Carlson, A.E., Clark, J., Wohlfarth, B., Mitrovica, J.X., Hostetler, S.W., and McCabe, A.M., 2006. the Last Glacial Maximum. Science 325, 710–714. https://doi.org/10.1029/2005GC001226

Clark, P.U., Marshall, S.J., Clarke, G.K.C., Hostetler, S.W., Licciardi, J.M., Teller, J.T., 2001. Freshwater forcing of abrupt climate change during the last glaciation. Science. 293, 283–287. https://doi.org/10.1126/science.1062517

Condron, A., Winsor, P., 2012. Meltwater routing and the Younger Dryas. Proc. Natl. Acad. Sci. 109, 1–6. https://doi.org/10.1073/pnas.1207381109

Desloges, J.R., Church, M., 1987. Channel and floodplain facies in a wandering gravel-bed river. Recent Dev. Fluv. Sedimentol. - Contrib. from Third Int. Fluv. Sedimentol. Conf. Special P, 99–109.

Domack, E.W., 1984. Rhythmically bedded glaciomarine sediments on Whidbey Island, Washington. J. Sediment. Res. 54, 589–602. https://doi.org/10.1306/212F847C-2B24-11D7-8648000102C1865D

Dyke, A.S., 2004. An outline of North American deglaciation with emphasis on central and northern Canada. Dev. Quat. Sci. 2, 373–424. https://doi.org/10.1016/S1571-0866(04)80209-4

Evans, D.J.A., Phillips, E.R., Hiemstra, J.F., Auton, C.A., 2006. Subglacial till: Formation, sedimentary characteristics and classification. Earth-Science Rev. 78, 115–176. https://doi.org/10.1016/j.earscirev.2006.04.001

Evans, D.J.A., Rother, H., Hyatt, O.M., Shulmeister, J., 2013. The glacial sedimentology and geomorphological evolution of an outwash. Sediment. Geol. 284–285, 45–75. https://doi.org/10.1016/j.sedgeo.2012.11.005

Eyles, N., Clark, B.M., Clague, J.J., 1987. Coarse-grained sediment gravity flow facies in a large supraglacial lake. Sedimentology 34, 193–216. https://doi.org/10.1111/j.1365-3091.1987.tb00771.x

Fisher, T.G., 1996. Sand-wedge and Ventifact Palaeoenvironmental Indicators in

Northwest Saskatchewan, Canada, 11 ka to 9.9 ka BP. Permafrost and Periglacial Processes 7, 391–408. https://doi.org/10.1002/(SICI)1099-1530(199610)7:4<391::AID-PPP229>3.0.CO;2-W

Fisher, T.G., Lowell, T. V., 2017. Glacial Geology and land-forming events in the Fort McMurray region. Alberta's Low. In: Alberta's Lower Athabasca Basin: archaeology and palaeoenvironments. Edited by B.M. Rogaghan. AU Press, Edmonton, 45–68. https://doi.org/10.15215/aupress/9781926836904.01

Fisher, T.G., Lowell, T. V., 2012. Testing northwest drainage from Lake Agassiz using extant ice margin and strandline data. Quat. Int. 260, 106–114. https://doi.org/10.1016/j.quaint.2011.09.018

Fisher, T.G., Smith, D.G., 1994. Glacial Lake Agassiz: Its northwest maximum extent and outlet in Saskatchewan (Emerson Phase). Quat. Sci. Rev. 13, 845–858. https://doi.org/10.1016/0277-3791(94)90005-1

Fisher, T.G., Smith, D.G., 1993. Exploration for Pleistocene aggregate resources using process-depositional models in the Fort Mcmurray region, NE Alberta, Canada. Quat. Int. 20, 71–80. https://doi.org/10.1016/1040-6182(93)90037-G

Fisher, T.G., Smith, D.G., Andrews, J.T., 2002. Preboreal oscillation caused by a glacial Lake Agassiz flood. Quat. Sci. Rev. 21, 873–878. https://doi.org/10.1016/S0277-3791(01)00148-2

Fisher, T.G., Waterson, N., Lowell, T. V., Hajdas, I., 2009. Deglaciation ages and meltwater routing in the Fort McMurray region, northeastern Alberta and northwestern Saskatchewan, Canada. Quat. Sci. Rev. 28, 1608–1624. https://doi.org/10.1016/j.quascirev.2009.02.003

Froese, D., Smith, D., Woywitka, R., 2013. Susan Lake Gravel Pit Catastrophic Flood Deposits and stratigraphy of the lower Athabasca valley, In: Froese, D., Woywitka, R., Andriashek, L. Smith, D. and Atkinson, N. (Eds.) Field Trip Guide to the Quaternary Geology and Geoarchaeology of the Oil Sands Region , NE Alberta. CANQUA Field Trip Guidebook. pp. 23–27.

Hjellbakk, A., 1997. Facies and Fluvial Architecture Of a High-Energy Braided River - the Upper Proterozoic Seglodden Member, Varanger Peninsula, Northern Norway. Sediment. Geol. 114, 131-. https://doi.org/10.1016/S0037-0738(97)00075-4

Howard, J.L., 2010. Late Pleistocene glaciolacustrine sedimentation and paleogeography of southeastern Michigan, USA. Sediment. Geol. 223, 126–142. https://doi.org/10.1016/j.sedgeo.2009.10.006

Keigwin, L.D., Klotsko, S., Zhao, N., Reilly, B., Giosan, L., Driscoll, N.W., 2018. Deglacial floods in the Beaufort Sea preceded Younger Dryas cooling. Nat. Geosci. https://doi.org/10.1038/s41561-018-0169-6

Levac, E., Lewis, M., Stretch, V., Duchesne, K., Neulieb, T., 2015. Evidence for meltwater drainage via the St. Lawrence River Valley in marine cores from the Laurentian Channel at the time of the Younger Dryas. Glob. Planet. Change 130, 47–65. https://doi.org/10.1016/j.gloplacha.2015.04.002

Lewis, T., Francus, P., Bradley, R.S., 2009. Recent occurrence of large jökulhlaups at Lake Tuborg, Ellesmere Island, Nunavut. J. Paleolimnol. 41, 491–506. https://doi.org/10.1007/s10933-008-9240-4

Leydet, D.J., Carlson, A.E., Teller, J.T., Breckenridge, A., Barth, A.M., Ullman, D.J., Sinclair, G., Milne, G.A., Cuzzone, J.K., Caffee, M.W., 2018. Opening of glacial Lake Agassiz's eastern outlets by the start of the Younger Dryas cold period. Geology 46, 155–158. https://doi.org/10.1130/G39501.1

Livingstone, S.J., Piotrowski, J.A., Bateman, M.D., Ely, J.C., Clark, C.D., 2015. Discriminating between subglacial and proglacial lake sediments: An example from the Dänischer Wohld Peninsula, northern Germany. Quat. Sci. Rev. 112, 86–108. https://doi.org/10.1016/j.quascirev.2015.01.030

Lønne, I., 1995. Sedimentary facies and depositional architecture of ice-contact glaciomarine systems. Sediment. Geol. 98, 13–43. https://doi.org/10.1016/0037-0738(95)00025-4

Lord, M.L., Kehew, A.E., 1987. Sedimentology and paleohydrology of glacial-lake outburst deposits in southeastern Saskatchewan and northwestern North Dakota. Geol. Soc. Am. Bull., 99, 663–673.

McPherson, J.G., 1987. Fan-deltas and braid deltas: Varieties of coarse-grained deltas. Geol. Soc. Am. Bull. 7606, 331–340. https://doi.org/10.1130/0016-7606(1987)99<331

Miall, A.D., 1985. Architectural-Element Analysis: A New Method of Facies Analysis Applied to Fluvial Deposits. Earth-Science Rev. 22, 261–308. https://doi.org/10.1016/0012-8252(85)90001-7

Miall, A.D., 1978. Lithofacies types and vertical profile models in braided river deposits: a summary. Fluv. Sedimentol. 5, 597–600.

Miall, A.D., 1977. A review of the braided river depositional environment. Earth-Sciences Rev. 13, 1–62.

Munyikwa, K., Rittenour, T.M., Feathers, J.K., 2017. Temporal constraints for the Late Wisconsinan deglaciation of western Canada using eolian dune luminescence chronologies from Alberta. Palaeogeogr. Palaeoclimatol. Palaeoecol. 470, 147–165. https://doi.org/10.1016/j.palaeo.2016.12.034

Murton, J.B., Bateman, M.D., Dallimore, S.R., Teller, J.T., Yang, Z., 2010. Identification of Younger Dryas outburst flood path from Lake Agassiz to the Arctic Ocean. Nature 464, 740–743. https://doi.org/10.1038/nature08954

Murton, J.B., French, H.M., 1993. Thaw modification of frost-fissure wedges, Richards Island, Pleistocene Mackenzie Delta, Western Arctic Canada. J. Quat. Sci. 8, 185–196. https://doi.org/10.1002/jqs.3390080302

Ó Cofaigh, C., Dowdeswell, J.A., 2001. Laminated sediments in glacimarine environments: Diagnostic criteria for their interpretation. Quat. Sci. Rev. 20, 1411–1436. https://doi.org/10.1016/S0277-3791(00)00177-3

Owen, G., Moretti, M., 2011. Identifying triggers for liquefaction-induced soft-sediment deformation in sands. Sediment. Geol. 235, 141–147. https://doi.org/10.1016/j.sedgeo.2010.10.003

Pettapiece, W.W., 1986. Physiographic subdivision of Alberta; Agriculture Canada, physiographic map, scale 1:500 000.

Piotrowski, J.A., 2007. Groundwater Under Ice Sheets and Glaciers. Glacier Sci. Environ. Chang. 50–60. https://doi.org/10.1002/9780470750636.ch9

Post, R.., 2003. Stratigraphy and Sedimentology of the Athabasca Group in the Net Lake-Maybelle River Area , Northeastern Alberta. EUB/AGS Earth Sciences Report 2003-01, 1-96.

Reimer, P.J., Bard, E., Bayliss, A., Beck, J.W., Blackwell, P.G., Ramsey, C.B., Buck, C.E., Cheng, H., Edwards, R.L., Friedrich, M., Grootes, P.M., Guilderson, T.P., Haflidason, H., Hajdas, I., Hatté, C., Heaton, T.J., Hoffmann, D.L., Hogg, A.G., Hughen, K.A., Kaiser, K.F., Kromer, B., Manning, S.W., Niu, M., Reimer, R.W., Richards, D.A., Scott, E.M., Southon, J.R., Staff, R.A., Turney, C.S.M., van der Plicht, J., 2013. IntCal13 and Marine13 Radiocarbon Age Calibration Curves 0–50,000 Years cal BP. Radiocarbon 55, 1869–1887. https://doi.org/10.2458/azu_js_rc.55.16947

Reyes, A. V., Froese, D.G., Jensen, B.J.L., 2010. Permafrost response to last interglacial warming: Field evidence from non-glaciated Yukon and Alaska. Quat. Sci. Rev. 29, 3256–3274. https://doi.org/10.1016/j.quascirev.2010.07.013

Rhine, J.L., 1984. Sedimentological and Geomorphilogical Reconstruction of the Late Pleistocene Athaasca Fan-Delta, Northwast Alberta. Msc. Thesis, University of Calgary, Canada.

Rooth, C., 1982. Hydrology and ocean circulation. Prog. Oceanogr. 11, 131–149. https://doi.org/10.1016/0079-6611(82)90006-4

Roy, S.K., 1972. Fossil wood of Taxaceae from the Mc Murray formation (Lower Cretaceous) of Alberta, Canada. Can. J. Bot. 50, 349–352.

Russell, H. a J., Arnott, R.W.C., 2003. Hydraulic-Jump and Hyperconcentrated-Flow Deposits of a Glacigenic Subaqueous Fan: Oak Ridges Moraine, Southern Ontario, Canada. J. Sediment. Res. 73, 887–905. https://doi.org/10.1306/041103730887

Schillereff, D.N., Chiverrell, R.C., Macdonald, N., Hooke, J.M., 2014. Flood stratigraphies in lake sediments: A review. Earth-Science Rev. 135, 17–37. https://doi.org/10.1016/j.earscirev.2014.03.011

Smith, D.G., 1994. Glacial lake McConnell: Paleogeography, age, duration, and associated river deltas, mackenzie river basin, western Canada. Quat. Sci. Rev. 13, 829–843. https://doi.org/10.1016/0277-3791(94)90004-3

Smith, D.G., Fisher, T.G., 1993. Glacial Lake Agassiz: The northwest outlet and paleoflood. Geol. 21. 9–12.

Smith, N.D., 1978. Sedimentation processes and patterns in a glacier-fed lake with low sediment input. Can. J. Earth Sci. 15, 741–756. https://doi.org/10.1139/e78-081

Talling, P.J., Masson, D.G., Sumner, E.J., Malgesini, G., 2012. Subaqueous sediment density flows: Depositional processes and deposit types. Sedimentology 59, 1937–2003. https://doi.org/10.1111/j.1365-3091.2012.01353.x

Tarasov, L., Peltier, W.R., 2005. Arctic freshwater forcing of the Younger Dryas cold reversal. Nature, 435, 662–665. https://doi.org/10.1038/nature03617

Taylor, R.S., 1690. Some Pleistocene Lakes of Northern Alberta and Adjacent Areas. J. Alberta Soc. Pet. Geol. 8, 167–178.

Teller, J.T., 2001. Formation of large beaches in an area of rapid differential isostatic rebound: The three-outlet control of Lake Agassiz. Quat. Sci. Rev. 20, 1649–1659. https://doi.org/10.1016/S0277-3791(01)00007-5

Teller, J.T., Boyd, M., 2006. Two possible routings for overflow from Lake Agassiz during the Younger Dryas. A Reply to Comment by T. Fisher, T. Lowell, H. Loope on "Alternative routing of Lake Agassiz overflow during the Younger Dryas: new dates, paleotopography, a re-evaluation." Quat. Sci. Rev. 25, 1142–1145. https://doi.org/10.1016/j.quascirev.2006.01.011

Teller, J.T., Boyd, M., Yang, Z., Kor, P.S.G., Fard, A.M., 2005. Alternative routing of Lake Agassiz overflow during the Younger Dryas: New dates, paleotopography, and a re-evaluation. Quat. Sci. Rev. 24, 1890–1905. https://doi.org/10.1016/j.quascirev.2005.01.008

Teller, J.T., Leverington, D.W., 2004. Glacial Lake Agassiz: A 5000 yr history of change and its relationship to the δ18O record of Greenland. Bull. Geol. Soc. Am. 116, 729–742. https://doi.org/10.1130/B25316.1

Teller, J.T., Leverington, D.W., Mann, J.D., 2002. Freshwater outbursts to the oceans from glacial Lake Agassiz and their role in climate change during the last deglaciation. Quat. Sci. Rev. 21, 879–887. https://doi.org/10.1016/S0277-3791(01)00145-7

van der Meer, J.J.M., Kjær, K.H., Krüger, J., Rabassa, J., Kilfeather, A.A., 2009. Under pressure: clastic dykes in glacial settings. Quat. Sci. Rev. 28, 708–720. https://doi.org/10.1016/j.quascirev.2008.07.017

Vance, R.E., 1986. Pollen stratigraphy of Eaglenest Lake , northeastern Alberta. Can. J. Earth Sci. 23, 11–20. https://doi.org/10.1139/e86-002

Wickert, A.D., Mitrovica, J.X., Williams, C., Anderson, R.S., 2013. Gradual demise of a thin southern Laurentide ice sheet recorded by Mississippi drainage. Nature 502, 668–671. https://doi.org/10.1038/nature12609

Winsemann, J., Lang, J., Polom, U., Loewer, M., Ingel, J., Pollok, L., Brandes, C., 2018. Ice-marginal forced regressive deltas in glacial lake basins: geomorphology, facies variability and large-scale depositional architecture. Boreas.

Wolfe, S. a., Huntley, D.J., Ollerhead, J., 2004. Relict Late Wisconsinan Dune Fields of the Northern Great Plains, Canada. Géographie Phys. Quat. 58, 323. https://doi.org/10.7202/013146ar

Woywitka, R.J., Froese, D.G., Wolfe, S.A., 2017. Raised Landforms in the East-Central Oil Sands Region: Origin, Age, and Archaeological Implications. In: Alberta's Lower Athabasca Basin: archaeology and palaeoenvironments. Edited by B.M. Rogaghan. AU Press, Edmonton. 69–82. doi: 10.15215/aupress/9781926836904.01

## Figures and Tables

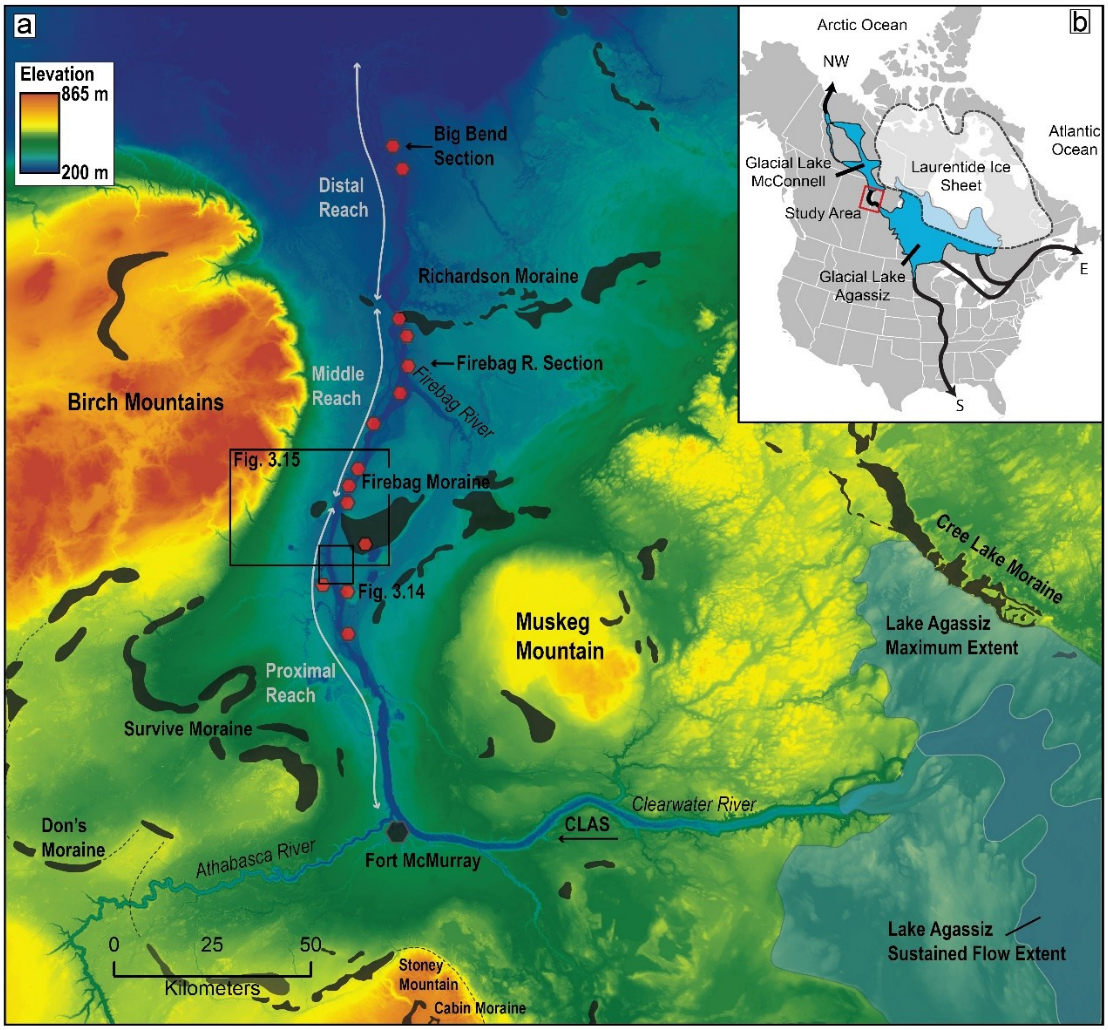


Figure 3.1. a) Digital elevation map of study area within the lower Clearwater and Athabasca River valleys with moraines (Fisher et al.,2009) and glacial Lake Agassiz stages at its northwestern outlet (Smith and Fisher, 1993). Red polygons indicate logged stratigraphic sections. b) Maximum extents of glacial Lakes Agassiz and McConnell along the margin of the Laurentide Ice Sheet. Red box delineates extent of Fig. 3.1a.

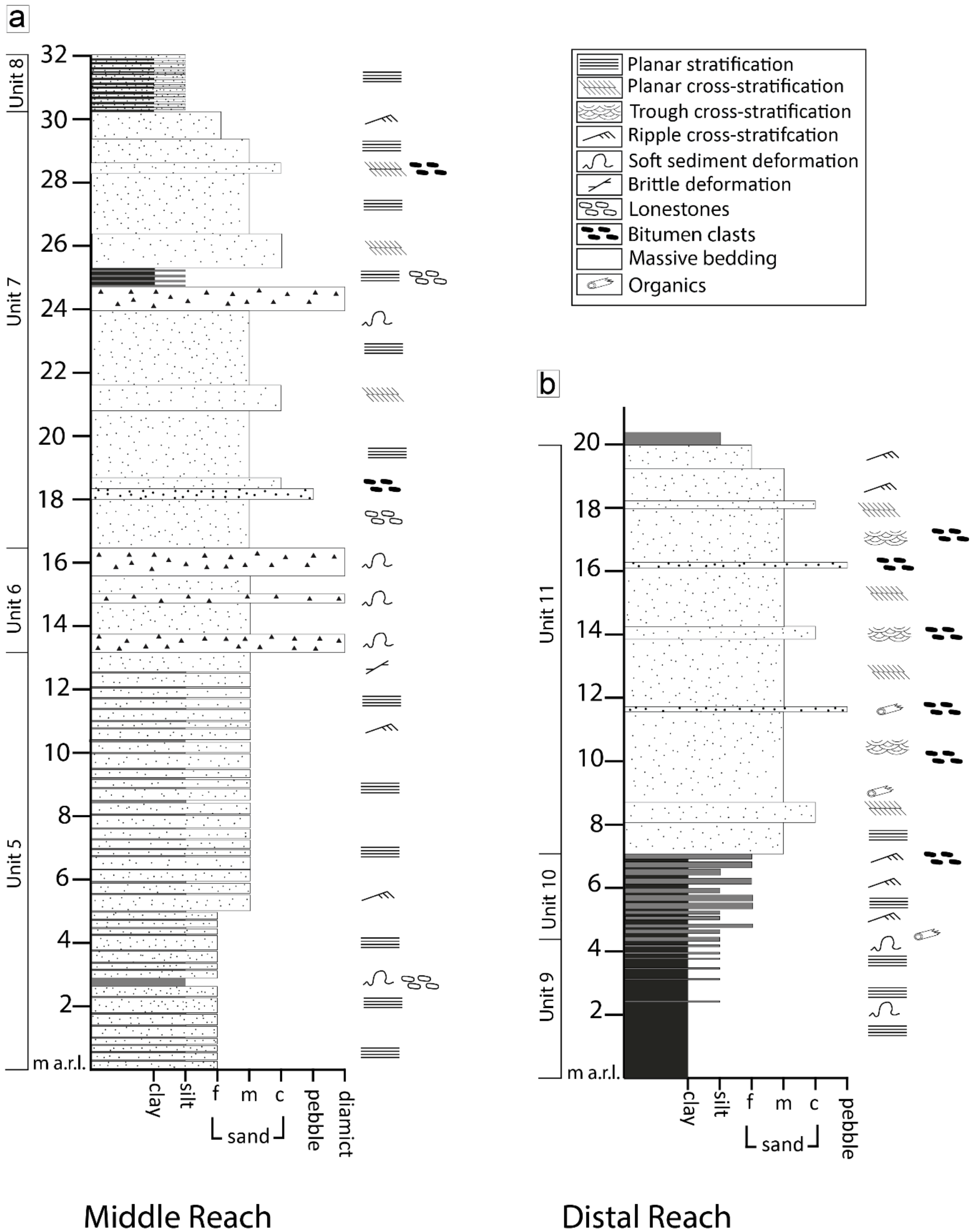


Figure 3.2. Composite stratigraphic logs of sediments observed a) in the middle reach and b) distal reach of the lower Athabasca valley.

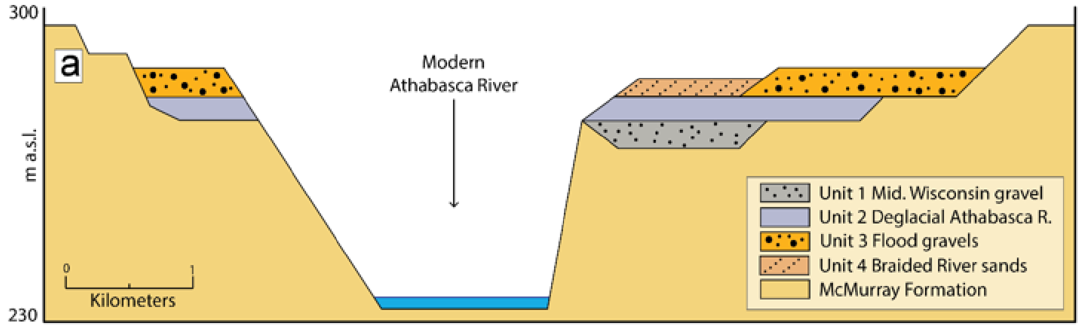


Figure 3.3. a) Schematic cross-section of the proximal reach evidencing Units 1-4 mapped from mining and river-cut exposures.

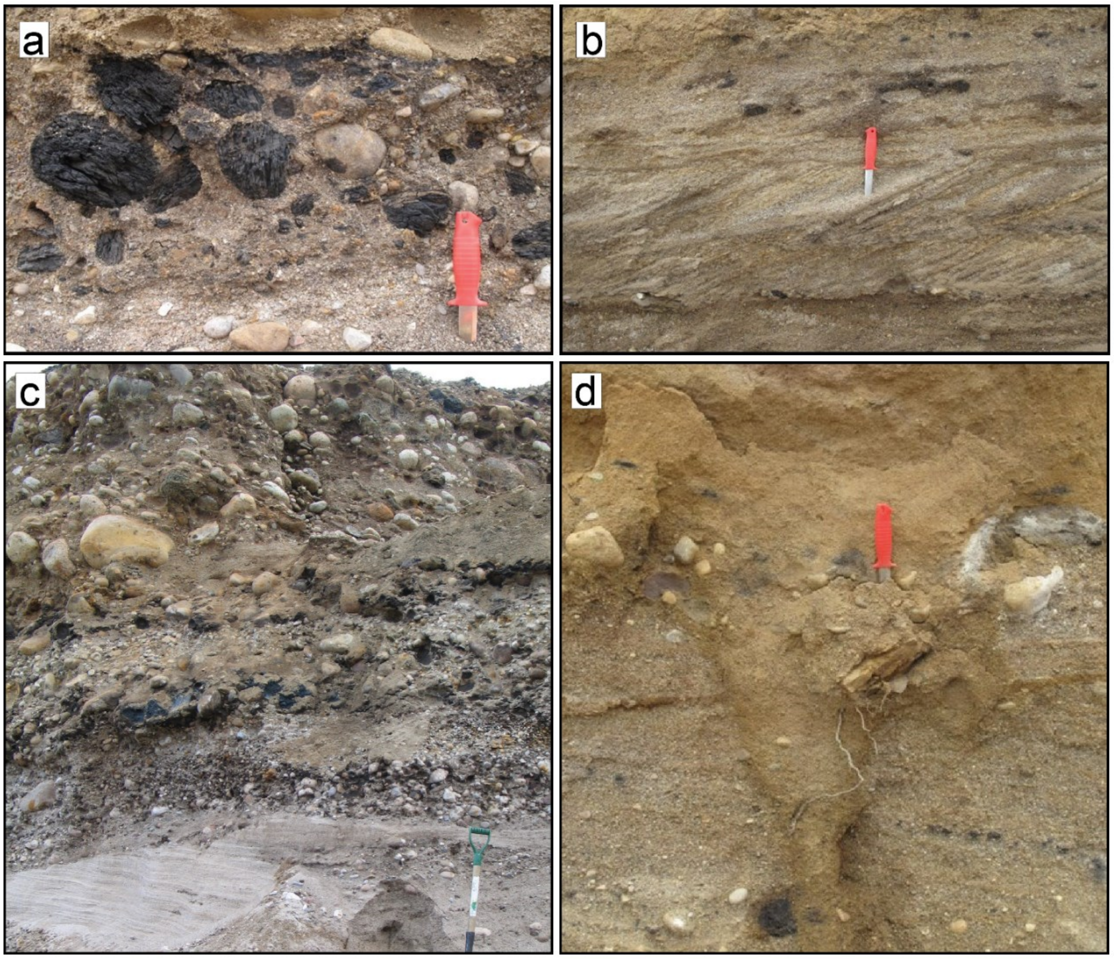


Figure 3.4. a) Rip-up clasts of McMurray Formation oil sands within sands and gravels of Unit 3. b) Northward dipping cross-bedding in sands of Unit 4. c) Basal contact of Unit 3 scouring into unit 2. Note contrast in abundance of oil sand rip-ups and upward-coarsening of Unit 3. d) Ice-wedge cast dissecting pebbly sands of Unit 4.

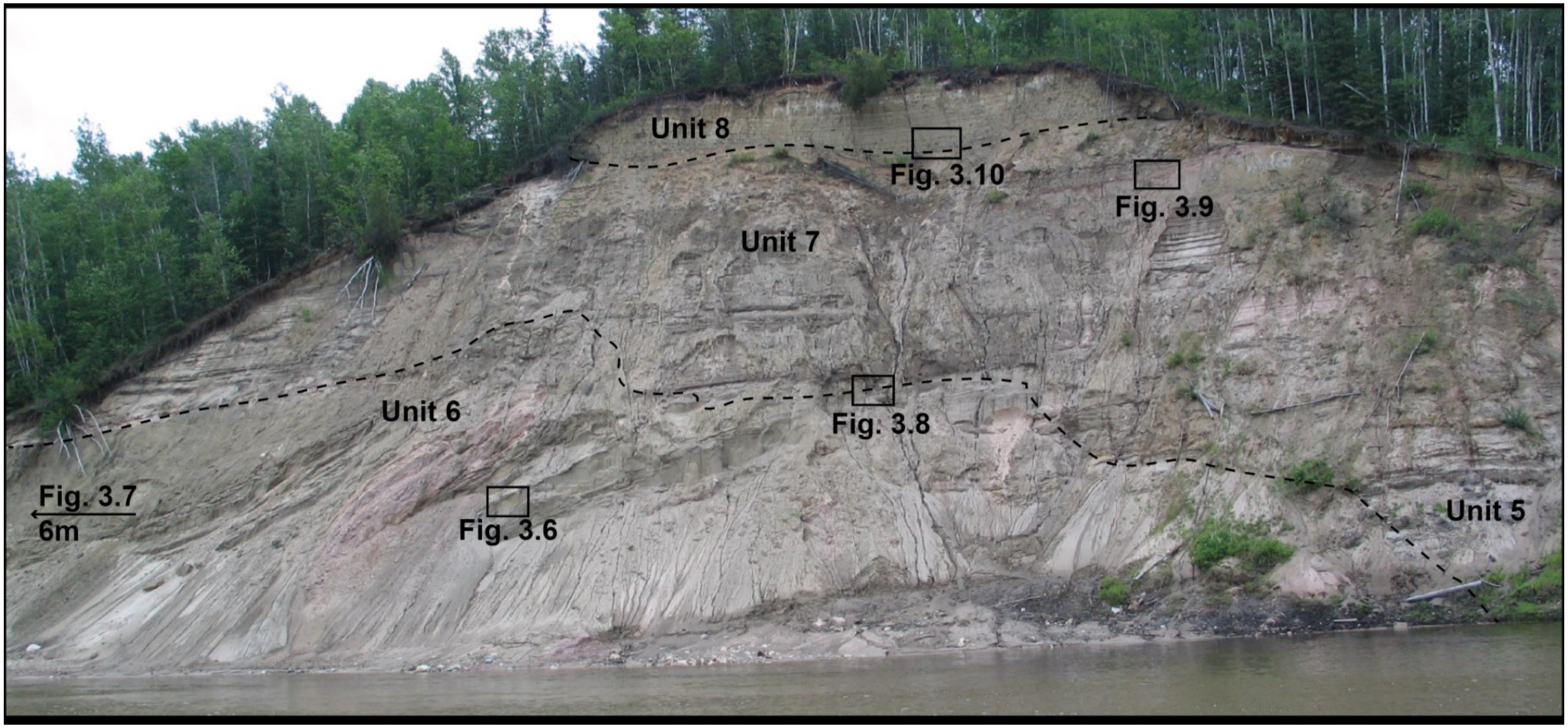


Figure 3.5. Annotated Firebag River exposure showing Units 5-8. Approximate locations of select figures noted and outlined in black box. Height of the exposure is ~35m.

Figure 3.6. Deformed silt bed in Unit 5.  South is to the left.

Figure 3.7. Brittle deformation in thrusted sand and silt rhythmites.

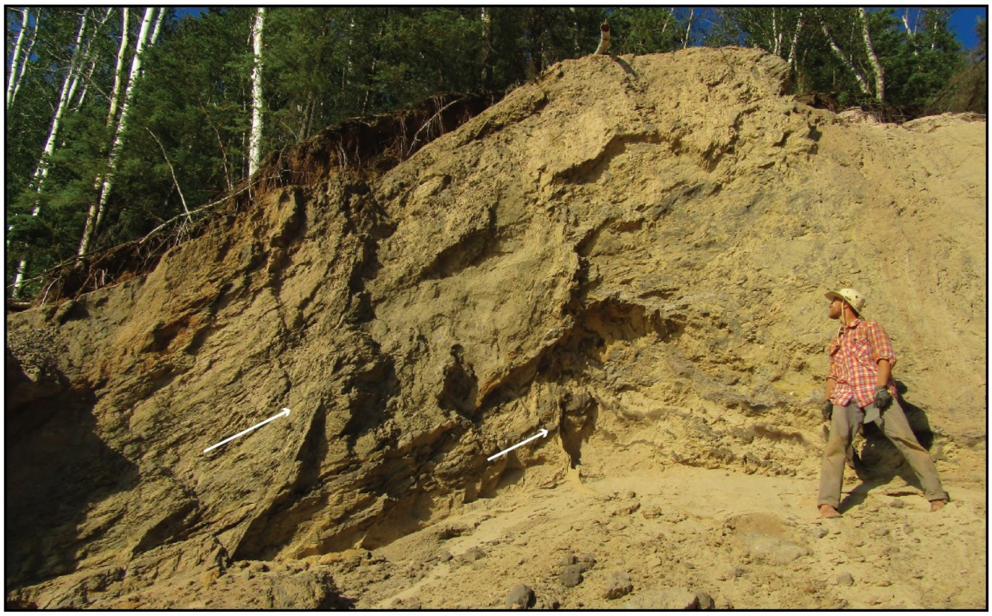

Figure 3.8. Large-scale thrust folds with clastic dyke injections (white arrows) in Unit 6.

Figure 3.9. Diamict overlying deformed sediment package of Unit 6.

Figure 3.10. Laminated pink clays with an Athabasca Group sandstone clast overlying brown diamict in Unit 7.

Figure 3.11. Uppermost rhythmites of Unit 8 showing no evidence of bitumen or catastrophic sedimentation.

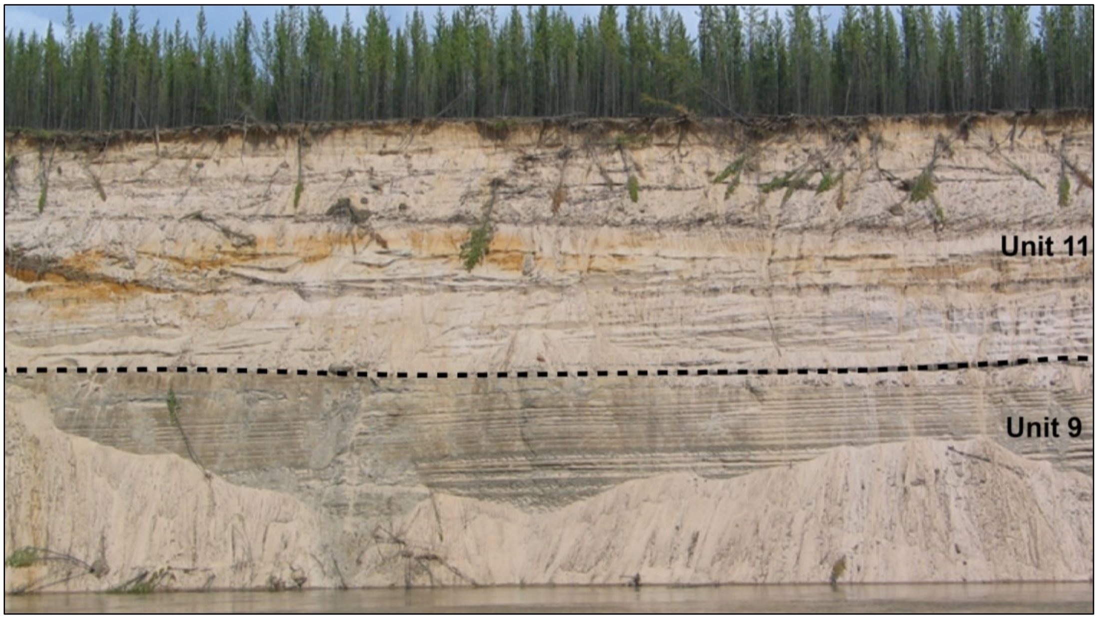


Figure 3.12. Architecture of distal braid delta complex at the Big Bend section with Units 9 and 11 present.

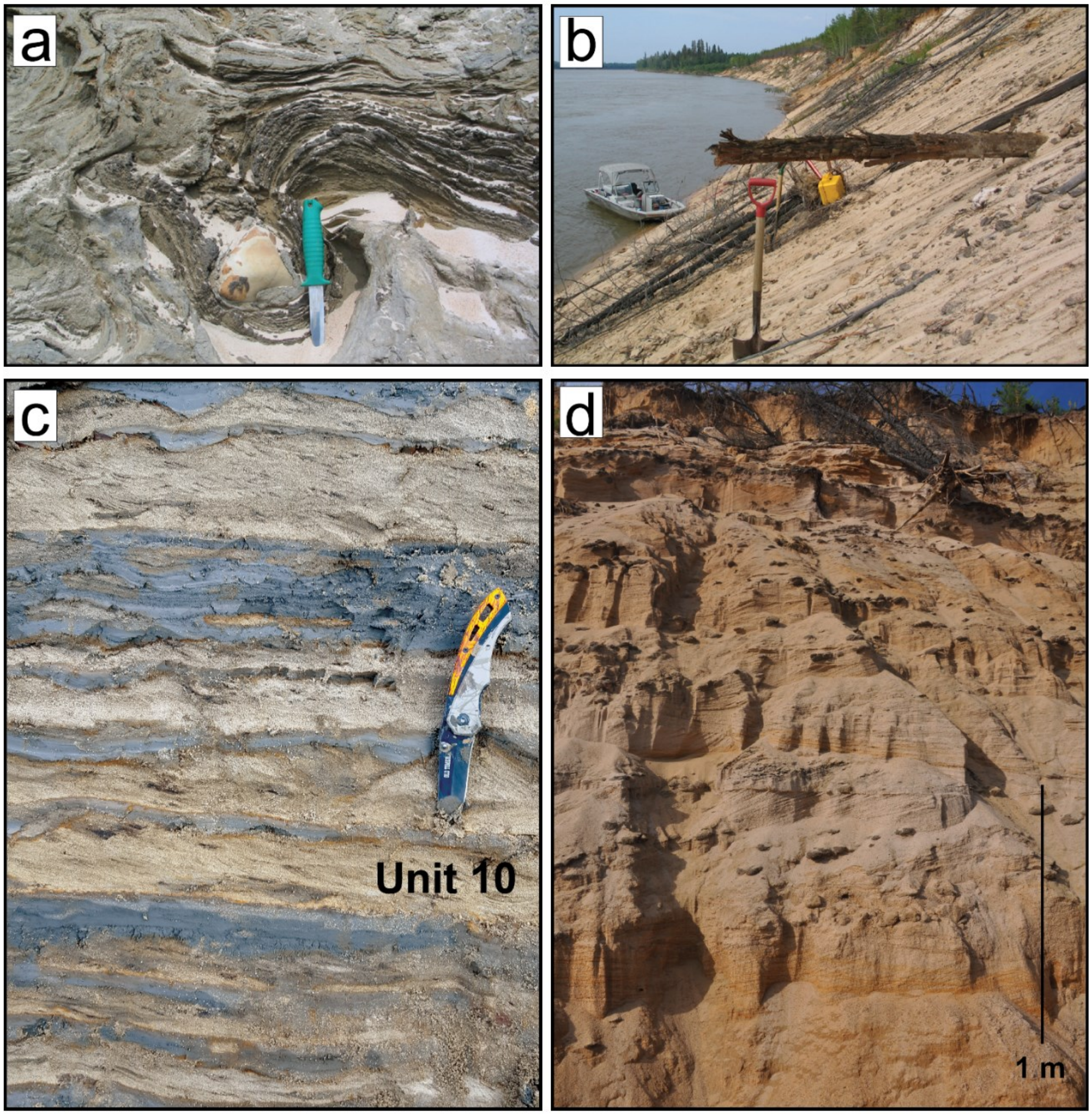


Figure 3.13. a) Soft-sediment deformation from ice-rafted clast in Unit 9. b) *In situ* log in braided sands of Unit 11. c) Alternating beds of clay and ripple cross-bedded silty sands of Unit 10. d) Stacked sets of planar and trough cross beds of Unit 11.

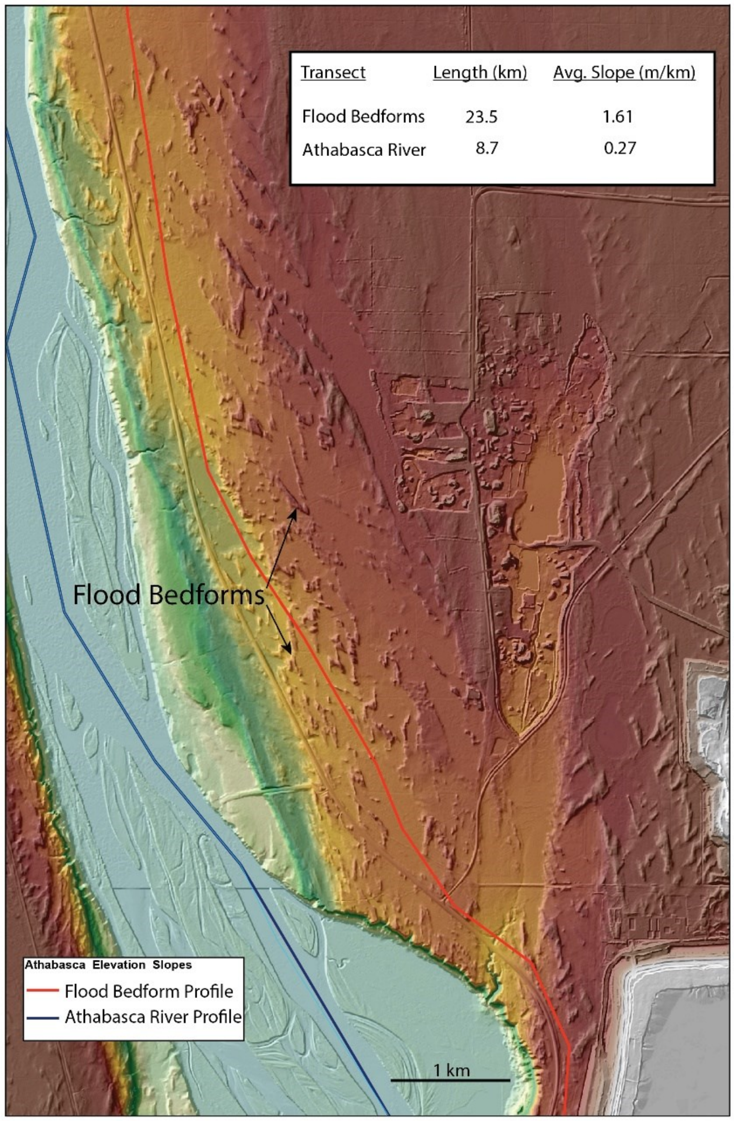


Figure 3.14. Digital elevation model below the Firebag moraine evidencing flood deposited bedforms. Flooding gradient calculated from the red line transect against the modern river gradient from the blue line transect.

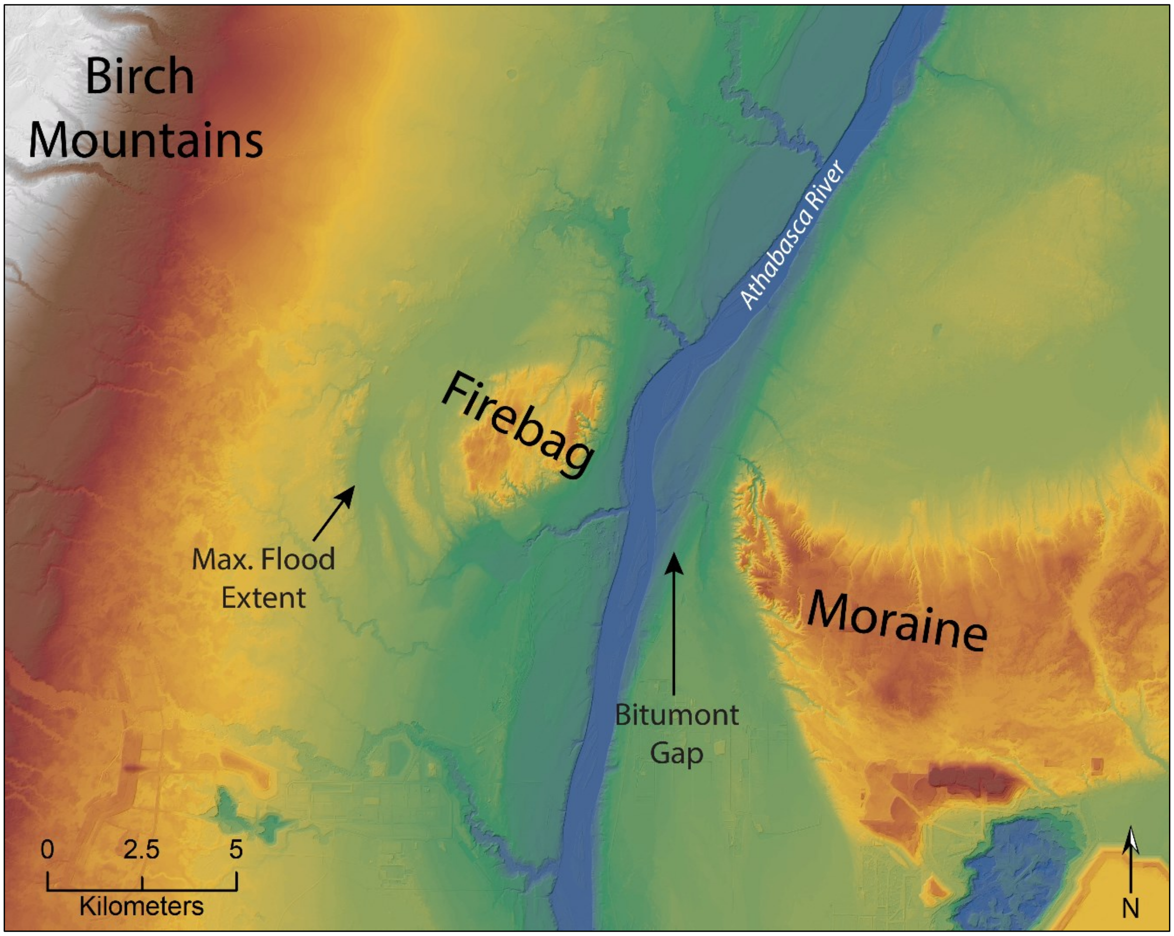


Figure 3.15. LiDAR imagery of the eastern flank of the Birch Mountains near the Firebag moraine with the Maximum flood-flow extent indicated.

Table 3.1. Summary of sedimentary units recognized in the study area.

| Unit | Description | Interpretation |
|---|---|---|
| Proximal Reach | | |
| 1 | Well rounded gravels dominated by quartzite clasts. Maximum thickness of 4 m at base of gravel pits. Commonly overlain by brown diamict. | Channel deposits from Paleo-Athabasca River (mid-Wisconsin) at similar baselevel to the modern river |
| 2 | Variably preserved quartzite rich gravel, lacking rip-ups | Bedload deposition from wandering gravel bed river following |
| 3 | Massive to cross-boulder gravels with common large rafts of bituminous sandstone and carbonates. | Catastrophic flood sedimentation associated with increased erosion of the McMurray and Waterways Formations |
| 4 | Planar to sub-horizontal well-stratified pebbly sand | Bedload deposition of a braided river system following catastrophic drainage |
| Middle Reach | | |
| 5 | Planar to sub-horizontal well-stratified silts and sands with occasional soft sediment deformation structures and pink clay rip ups | Thin stacked turbidite deposition into an ice-contact lake with occasional sediment plumes originating from the ice sheet |
| 6 | Stratified sediments displaying brittle and ductile deformation structures. Overlain by a flat-lying pinkish diamict | Glaciotectonized sediments recording a re-advance of the glacier margin |
| 7 | Package of stratified silts and sands with interbedded diamicts. Pink sand packages displaying reversed paleoflow indication. | Interplay of sedimentation between the paleo-Athabasca river and ice sheet derived material into a proglacial lake with a fluctuating ice margin.<br><br>Stratified pink diamict represents period of deep-water lacustrine sedimentation. |
| 8 | Rhythmically bedded silts and sands | Lake sedimentation associated with the last influence of ice in the valley |
| Distal Reach | | |

| | | |
|---|---|---|
| 9 | Stratified muds | Basal sediments of glacial Lake McConnell |
| 10 | Interbedded, well-stratified muds and sands | Wave-influenced prodelta deposits recording rapid sedimentation |
| 11 | Trough and planar cross-stratified fine to pebbly sands | Channel and bar deposition of a braided river system |

Table 3.2. Radiocarbon dates from the lower Athabasca River valley with various bitumen mitigation pre-treatment techniques applied. *Converted to calendar years with the IntCal 13 calibration curve (Reimer et al., 2013) using OxCal V 4.3 (Bronk Ramsey, 2009a). ** Pre-treatment nomenclature: 2T:1A + ABA = 2:1 solution of toluene:ethanol in soxhlet + acid-base-acid wash. 2C:1A + ABA = 2:1 solution of chloroform:ethanol in soxhlet + acid-base-acid wash.

| Sample ID | Lab ID | 14C age and error | Calendar Age (2-sigma)* | Material | Pre-Treatment** | Location (m a.r.l.) |
|---|---|---|---|---|---|---|
| | | | | | | |
| DF16-LAR2 | UCIAMS 187136 | **10210 ± 25** | 12060-11774 | Wood | 2T:1E + ABA | Unit 11 (6.5) |
| LAR4-16 | UCIAMS 187137 | **9575 ± 25** | 11089-10755 | Wood | 2T:1E + ABA | Unit 11 (6) |
| AVR-15-3 | UCIAMS 187138 | **9965 ± 20** | 11599-11267 | Wood | 2T:1E + ABA | Unit 11 (N/A) |
| DF15-09 | UCIAMS 187139 | **9630 ± 25** | 11170-10793 | Wood | 2T:1E + ABA | Unit 11 (N/A |
| SLGP-16-01 | UCIAMS 187140 | **19000 ± 60** | 23103-22619 | Wood | 2T:1E + ABA | Unit 3 (N/A) |
| SLGP-16-01 (2) | UCIAMS 197746 | **>45900** | N/A | Wood | 2T:1E + ABA | Unit 3 (N/A) |
| BB-16-11 | UCIAMS 187141 | **9655 ± 20** | 11177-10875 | Wood | 2T:1E + ABA | Unit 11 (10) |
| AK-BB-17-01 | UCIAMS 205522 | **10100 ± 25** | 11970-11411 | Wood | 2T:1E + ABA | Unit 10 (4.5) |
| AK-BB-17-02 | UCIAMS 205523 | **9605 ± 25** | 11133-10780 | Wood | 2T:1E + ABA | Unit 11 (9.5) |
| FIRCP-001 | UCIAMS 187142 | **3320 ± 15** | 3592-3480 | Wood | 2T:1E + ABA | Standard |
| FIRI-F-Sox. | UCIAMS 187143 | **4535 ± 15** | 5309-5065 | Wood | 2T:1E + ABA | Standard |
| AVR07-PAL-37-Sox. | UCIAMS 187144 | **48900 ± 210** | N/A | Wood | 2T:1E + ABA | Standard |
| AVR-07-PAL-37 SX | UCIAMS 197737 | **46580 ± 220** | N/A | Wood | 2T:1E + ABA | Standard |
| FIRI-F-SX | UCIAMS 197748 | **4545 ± 20** | 5314-5063 | Wood | 2T:1E + ABA | Standard |
| FIRI F-SX | UCIAMS 205524 | **4515 ± 15** | 5299-5053 | Wood | 2T:1E + ABA | Standard |
| AVR-07-PAL-37-SX | UCIAMS 205525 | **51010 ± 240** | N/A | Wood | 2T:1E + ABA | Standard |
| | | | | | | |
| DF06-14 | UCIAMS 56395 | **9620 ± 20** | 11156-10791 | Wood | 2C:1E + ABA | Unit 11 |
| DF06-14 | UCIAMS 56400 | **9635 ± 25** | 11173-10796 | Wood | ABA | Unit 11 |
| DF06-14 | UCIAMS 26771 | **9645 ± 20** | 11175-10813 | Wood | ABA | Unit 11 |
| DF06-WP21 | UCIAMS 56396 | **9945 ± 20** | 11398-11262 | Wood | 2C:1E + ABA | Unit 11 |
| DF06-WP21 | UCIAMS 56401 | **9995 ± 20** | 11610-11316 | Wood | ABA | Unit 11 |
| DF06-WP21 | UCIAMS 26772 | **10055 ± 20** | 11745-11404 | Wood | ABA | Unit 11 |
| DF06-005D | UCIAMS 36656 | **10450 ± 30** | 12533-12127 | Picea needles | 2T:1E + ABA | Unit 11 |
| DF06-005D | UCIAMS 36657 | **10090 ± 25** | 11924-11406 | Picea needles | 2T:1E + ABA | Unit 11 |
| DF06-005D | UCIAMS 36651 | **10905 ± 30** | 12816-12706 | Picea needles | ABA | Unit 11 |
| Queets-A | UCIAMS 36658 | **49370 ± 270** | N/A | Wood | 2T:1E + ABA | Standard |
| Queets-A | UCIAMS 36659 | **48980 ± 240** | N/A | Wood | 2T:1E + ABA | Standard |
| Queets-A | UCIAMS 36652 | **50730 ± 330** | N/A | Wood | ABA | Standard |
| FIRI-D | UCIAMS 36660 | **4560 ± 20** | 5319-5071 | Wood | 2T:1E + ABA | Standard |
| FIRI-D | UCIAMS 36661 | **4560 ± 20** | 5319-5071 | Wood | 2T:1E + ABA | Standard |
| FIRI-D | UCIAMS 36655 | **4510 ± 20** | 5296-5053 | Wood | ABA | Standard |
| Queets-A | UCIAMS 56385 | **51050 ± 200** | N/A | Wood | 2T:1E + ABA | Standard |
| Queets-A | UCIAMS 56402 | **49310 ± 260** | N/A | Wood | ABA | Standard |
| Queets-A | UCIAMS 56404 | **50340 ± 250** | N/A | Wood | ABA | Standard |
| FIRI-D | UCIAMS 56397 | **4510 ± 15** | 5295-5053 | Wood | 2C:1E + ABA | Standard |
| FIRI-D | UCIAMS 56394 | **4545 ± 15** | 5313-5071 | Wood | ABA | Standard |
| FIRI-D | UCIAMS 56405 | **4500 ± 15** | 5288-5050 | Wood | ABA | Standard |
| FIRI-D | UCIAMS 56410 | **4505 ± 15** | 5290-5052 | Wood | ABA | Standard |
| IAEA C5 | UCIAMS 56398 | **11725 ± 25** | 13586-13463 | Wood | 2C:1E + ABA | Standard |
| IAEA C5 | UCIAMS 56407 | **11690 ± 50** | 13610-13410 | Wood | ABA | Standard |
| IAEA C5 | UCIAMS 56406 | **11720 ± 25** | 13583-13462 | Wood | ABA | Standard |

Table 3.3. Previously published radiocarbon ages in the Fort McMurray region. * Converted to calendar years with the IntCal 13 calibration curve (Reimer et al., 2013) using OxCal V 4.3 (Bronk Ramsey, 2009). ** Published as GX-5301-II by Smith and Fisher (1993) with material noted as wood.

| Lab ID | 14C age | Calendar Age (2-sigma)* | Material Dated | Location | Reference |
|---|---|---|---|---|---|
| GSC-4302 | **9910 ± 190** | 12075-10770 | Wood | Athabasca Delta | Smith (1994) |
| AECV-1183C | **9710 ± 130** | 11593-10658 | Wood | Athabasca Delta | Smith (1994) |
| Wat-2661 | **9850 ± 80** | 11610-11130 | Wood | Peace Delta | Smith (1994) |
| GSC-4821 | **10600 ± 120** | 12727-12146 | Gyttja | Nipawin Bay | Anderson and Lewis (1992) |
| UCIAMS 34698 | **10000 ± 35** | 11697-11285 | Wood fragments | Nipawin Bay | Teller, 2007, unpublished |
| GSC-4807 | **11100 ± 150** | 13230-12714 | Plant detritus | Long Lake | Anderson and Lewis (1992) |
| GX-5031 | **10310 ± 290** | 12716-11238 | Shells | Syncrude Mine | Syncrude (1977), unpublished; Smith and Fisher (1993) |
| GX-5036-I | **10015 ± 320** | 12581-10703 | Wood fragments | Syncrude Mine | Syncrude (1977), unpublished |
| GX-5036-II** | **11405 ± 245** | 13740-12780 | Shells | Syncrude Mine | Syncrude (1977), unpublished |
| GX-5030-II | **13075 ± 340** | 16706-14398 | Shells | Syncrude Mine | Syncrude (1977), unpublished |
| Unknown | **10040 ± 60** | 11817-11274 | Twigs | Fort Hills, Syncrude | Syncrude (1977), unpublished |
| Unknown | **10400 ± 180** | 12705-11617 | Wood | Fort Hills, Syncrude | Syncrude (1977), unpublished |
| GX8910 | **11280 ± 275** | 13711-12699 | Bulk sediment | Eaglesnest Lake | Vance (1986) |
| GSC-2038 | **11300 ± 110** | 13420-12940 | Gyttja | Mariana Lake | Hutton and MacDonald (1994) |
| ETH-28524 | **9635 ± 75** | 11200-10750 | Charcoal | Hanging Stone Lake | Fisher et al., 2009 |
| Beta-200071 | **10030 ± 50** | 11763-11306 | Wood | Cabin Lake | Fisher et al., 2009 |
| Beta-200072 | **10040 ± 50** | 11800-11311 | Wood | Cabin Lake | Fisher et al., 2009 |
| ETH-28525 | **9795 ± 75** | 11403-10815 | Wood | Cabin Lake | Fisher et al., 2009 |
| ETH-28526 | **9730 ± 65** | 11256-10794 | Wood | Cabin Lake | Fisher et al., 2009 |
| ETH-29206 | **9710 ± 70** | 11247-10787 | Wood | Cabin Lake | Fisher et al., 2009 |
| ETH-29207 | **9705 ± 75** | 11245-10784 | Wood | Cabin Lake | Fisher et al., 2009 |
| ETH-30172 | **9835 ± 75** | 11602-11105 | Wood | Cabin Lake | Fisher et al., 2009 |
| ETH-30173 | **9940 ± 70** | 11704-11220 | Plant | Cabin Lake | Fisher et al., 2009 |
| ETH-30185 | **9985 ± 110** | 11955-11213 | Wood | Cabin Lake | Fisher et al., 2009 |
| Beta-194056 | **9660 ± 40** | 11200-10792 | Wood | Crescent Lake | Fisher et al., 2009 |
| ETH-30174 | **9595 ± 70** | 11175-10725 | Wood | Crescent Lake | Fisher et al., 2009 |
| ETH-28527 | **9335 ± 70** | 10717-10296 | Wood | Crescent Lake | Fisher et al., 2009 |
| ETH-28528 | **9295 ± 70** | 10664-10268 | Wood | Crescent Lake | Fisher et al., 2009 |
| ETH-29209 | **9290 ± 70** | 10660-10264 | Wood | Crescent Lake | Fisher et al., 2009 |
| ETH-29210 | **9180 ± 70** | 10520-10225 | Wood | Crescent Lake | Fisher et al., 2009 |
| ETH-29208 | **9090 ± 70** | 10494-9970 | Wood | Crescent Lake | Fisher et al., 2009 |
| ETH-29219 | **10020 ± 75** | 11918-11249 | Wood | Hook Lake | Fisher et al., 2009 |
| ETH-30177 | **10030 ± 75** | 11931-11257 | Wood | Hook Lake | Fisher et al., 2009 |
| Beta-194058 | **10270 ± 50** | 12377-11811 | Wood | Deep Hole Lake | Fisher et al., 2009 |
| Beta-194059 | **10080 ± 40** | 11938-11396 | Wood | Deep Hole Lake | Fisher et al., 2009 |
| ETH-30187 | **9910 ± 75** | 11696-11200 | Wood | Deep Hole Lake | Fisher et al., 2009 |
| ETH-28535 | **9820 ± 70** | 11596-11094 | Wood | Deep Hole Lake | Fisher et al., 2009 |
| ETH-28536 | **9795 ± 70** | 11394-10882 | Wood | Deep Hole Lake | Fisher et al., 2009 |
| ETH-30587 | **9510 ± 70** | 11099-10587 | Wood | Richardson Lake | Fisher et al., 2009 |
| ETH-30588 | **8330 ± 60** | 9475-9137 | Wood | Esker Kettle Lake | Fisher et al., 2009 |
| ETH-32165 | **10310 ± 75** | 12414-11817 | Wood | Mariana Lake | Fisher et al., 2009 |
| ETH-30594 | **9860 ± 65** | 11601-11173 | Wood | Sick Hill Lake | Fisher et al., 2009 |
| ETH-30585 | **10210 ± 65** | 12161-11616 | Wood | Don's Lake | Fisher et al., 2009 |
| ETH-30586 | **10460 ± 65** | 12568-12099 | Wood | Don's Lake | Fisher et al., 2009 |
| ETH-32166 | **12780 ± 95** | 15610-14895 | Organics | Dipper Lake | Fisher et al., 2009 |
| ETH-30590 | **9850 ± 65** | 11599-11164 | Wood | Survive Lake | Fisher et al., 2009 |
| ETH-30591 | **9730 ± 65** | 11256-10794 | Wood | Survive Lake | Fisher et al., 2009 |
| ETH-32323 | **10150 ± 70** | 12070-11405 | Seed Pods | White Cow Lake | Fisher et al., 2009 |
| ETH-32324 | **10140 ± 70** | 12046-11404 | Seed Pods | White Cow Lake | Fisher et al., 2009 |

# Chapter 4: Conclusions

## 4.1 Summary and significance of research

The overarching aim of this thesis was to investigate the geological and temporal relationships between the basin of glacial Lake Agassiz and meltwater routing through its northwestern outlet. This is demonstrated in this thesis by the thorough examination of previously published radiocarbon dates from the Agassiz basin, along with new ages constraining a revised stratigraphic architecture of the northwestern outlet.

*Chronology of the Agassiz basin and occupation northwestern outlet*

The history of glacial Lake Agassiz has been disputed and revised for over a century, with various models of lake development and evolution put forward as chronological constrains improve and new data comes to light. Perhaps the most contentious period of lake progression is the time surrounding the Moorhead Phase, where lake levels abruptly and significantly dropped and drained to an unknown outlet before gradually rebounding. In Chapter 2, previously published radiocarbon dates for the Moorhead and subsequent Emerson Phases were collated and scrutinized for quality control both manually and statistically using a Bayesian approach. Some ages, including the date that traditionally linked the onset of the Moorhead Low with the onset of Younger Dryas cold reversal (ca. 11 ka), is from when radiocarbon was in its infancy. As such, the procedures employed in Chapter 2 produce a robust, vetted dataset of radiocarbon ages from the Lake Agassiz basin, and subjects those ages to a Bayesian model to produce probability age ranges from the start and demise of the Moorhead and Emerson Phases, respectively. Results from Chapter 2 suggest that, at present, the radiocarbon data does not sufficiently define the onset of the Moorhead Low, and the ages previously linking the low stand to the start of the Younger Dryas could be attributed as outlying dates. More high-quality ages from the Agassiz basin are required to further constrain the timing of these lake Phases.

Chapter 3 provides a suite of new radiocarbon dates from deltaic sands associated with the northwestern outlet in the Fort McMurray area. The abundance of bituminous material (i.e. reworked or *in situ* oil sands) in the region can have adverse affects on radiocarbon measurements. To mitigate this, a pre-treatment method involving refluxing bitumen solvents was developed. Results show that contamination within organics in the region is prevalent and precautions should be employed hereafter. The new ages provide direct chronological control on the availability of the northwestern outlet. Ages spanning approximately 10.2 to 9.6 ka are consistent and constrain the development of a distal braid delta complex. They show that the outlet was operational ca. 700 years before the currently presented radiocarbon chronology, during at least during the later part of the Younger Dryas cold reversal.

*Geological context of the northwestern outlet*

A re-examination of glacial Lake Agassiz's northwestern outlet stratigraphy in the lower Athabasca River valley was undertaken in Chapter 3. Three principal depositional zones were identified, with sediments relating to: pre-flood, and Laurentide Ice Sheet dynamics, catastrophic flooding, and a post-flood, stable flow phase of Lake Agassiz. A new conceptual depositional model is proposed in Chapter 3 that suggests Lake Agassiz flooding graded into a low stand of glacial Lake McConnell – as shown in the LiDAR profiling slopes and sedimentological assemblages – before a transgression in Lake McConnell enabled the deposition of the distal braid delta. This model, if validated, would imply that the braid delta complex for which the aforementioned radiocarbon dates are derived, would post-date catastrophic flooding, with the implication that the flood occurred some time earlier, perhaps at the onset of the Younger Dryas as some authors suggest (e.g. Murton et al., 2010; Keigwin et al., 2018).

### 4.2 Suggestions for future research

More questions and insights have arisen since scratching the surface on proglacial lake drainage and its role in influencing climatic changes during the end of the last Ice Age. Some suggestions for future work expanding off this thesis include:

1) An increase in radiocarbon constraints on the initiation of the Moorhead Phase in the Lake Agassiz basin. Modern radiocarbon dates within a well-documented stratigraphic context will only improve the understanding of lake level dynamics during the low stand. Other dating techniques (e.g. OSL) currently have too great error uncertainties to resolve lake fluctuations at centennial time scale.
2) More robust temporal constrains on the catastrophic flood sedimentation in the Fort McMurray area. At present, there are no radiocarbon ages and too few luminescence ages directly dating the flood deposits (Chapter 3; unit 3) in the lower Athabasca valley. It is unlikely to retrieve quality organic materials in a late-glacial, flood-dominated setting but relatively little work has been undertaken in this regard. New mining exposures south of the Firebag Moraine will provide kilometers of exposed sections and the potential for adequate dating programmes.
3) Tracking catastrophic flooding throughout the Mackenzie River valley using geochemical tracers or provenance signatures. Unit 3 in Chapter 3 is the only documented unequivocal flood sedimentation associated with the northwestern outlet at present, ~ 2000 km away from documented flooding in the Mackenzie Rive delta region (c.f. Murton et al., 2010; Keigwin et al., 2018). Perhaps a geochemical signature in deep-water glacial Lake McConnell sediments evidencing punctuated erosion in the Fort McMurray area can link Lake Agassiz drainage to the Arctic Ocean.
4) Additional chronological and sedimentological work on the other deltas of glacial Lake McConnell – specifically in the Peace and Liard Rivers – would further test the validity of the conceptual depositional model presented in

Chapter 3. Comparisons between all deltas would provide a more robust framework for Lake McConnell evolution and the influence of catastrophic flooding.

5) The most direct way to test the conceptual model of Chapter 3, and inherently the most expensive, would be to core the distal braid delta in the Athabasca valley and gather a complete stratigraphic profile of the sequence. It would become rather apparent if buried flood sediments were underlying the 'highstand' Lake McConnell muds (unit 9; Chapter 3).
6) The continued contamination of bitumen into the modern Athabasca River became apparent when documenting the stratigraphy of the pebble braided river sands in the distal reaches (unit 11; Chapter 3). Reworked bitumen balls erode out of the unit and often accumulate at the foot of the sections, degrading into the river. Quantifying the amount and effects of the reworked contaminants would provide a unique and significant perspective on the Quaternary influence on the environmental well-being of the modern river.

## References


Keigwin, L.D., Klotsko, S., Zhao, N., Reilly, B., Giosan, L., Driscoll, N.W., 2018. Deglacial floods in the Beaufort Sea preceded Younger Dryas cooling. Nat. Geosci. https://doi.org/10.1038/s41561-018-0169-6

Murton, J.B., Bateman, M.D., Dallimore, S.R., Teller, J.T., Yang, Z., 2010. Identification of Younger Dryas outburst flood path from Lake Agassiz to the Arctic Ocean. Nature 464, 740–743. https://doi.org/10.1038/nature08954

## Bibliography


Aharon, P., 2003. Meltwater flooding events in the Gulf of Mexico revisited: Implications for rapid climate changes during the last deglaciation. Paleoceanography 18, 1–14. https://doi.org/10.1029/2002PA000840

Andriashek, L.D., Atkinson, N., 2007. Buried channels and glacial-drift aquifers in the Fort McMurray Region, northeast Alberta, Alberta Geological Survey, Earth Sciences Report 2007-01.

Arnaud, F., Lignier, V., Revel, M., Desmet, M., Beck, C., Pourchet, M., Charlet, F., Trentesaux, A., Tribovillard, N., 2002. Flood and earthquake disturbance of Pb geochronology. Terra Nov. 14, 225–232. https://doi.org/10.1046/j.1365-3121.2002.00413.x

Ashley, G.M., Southard, J.B., Boothroyd, J.C., 1982. Deposition of climbing-ripple beds: a flume simulation. Sedimentology 29, 67–79. https://doi.org/10.1111/j.1365-3091.1982.tb01709.x

Ashmore, P., 1991. How do gravel-bed rivers braid? Can. J. Earth Sci. 28, 326–341. https://doi.org/10.1139/e91-030

Ashworth, A., Clayton, L., Bickley, W., 1972. The Mosbeck Site: a Paleoenvironmental Interpretation of the Late Quaternary History of Lake Agassiz Based on Fossil and Mollusk Remains. Quat. Res. 188, 176–188.

Bajc, A.F., Schwert, D.P., Warner, B.G., Williams, N.E., 2000. A reconstruction of Moorhead and Emerson Phase environments along the eastern margin of glacial Lake Agassiz, Rainy River basin, northwestern Ontario. Can. J. Earth Sci. 37, 1335–1353. https://doi.org/10.1139/e00-051

Bayrock, L.A., 1971. Surficial geology Bitumount, NTS 74E. Alberta Res. Counc. Alberta Geol. Surv. Map 34, scale 1:250 000.

Bayrock, L.A., Reimchen, T.H.F., 1973. Surficial geology, Waterways, NTS 74D. Alberta Res. Counc. Alberta Geol. Surv. Map 34, scale 1:250 000.

Benn, D.I., Evans, D.J.A., 1996. The Interpretation and Classification of Subglacially-deformed Materials 15, 23–52.

Benn, D.I., Evans, D.J.A., 2010. Glaciers and Glaciation, 2nd ed. Hopper Education, London.

Bennett, M.R., Huddart, D., Thomas, G.S.P., 2002. Facies architecture within a regional glaciolacustrine basin: Copper River, Alaska. Quat. Sci. Rev. 21, 2237–2279. https://doi.org/10.1016/S0277-3791(02)00027-6

Björck, S., Keister, C.M., 1983. The Emerson Phase of Lake Agassiz, independently registered in northwestern Minnesota and northwestern Ontario. Can. J. Earth

Sci. 20, 1536–1542. https://doi.org/10.1139/e83-143

Blaauw, M., Christen, J.A., 2011. Flexible paleoclimate age-depth models using an autoregressive gamma process. Bayesian Anal. 6, 457–474. https://doi.org/10.1214/11-BA618

Blockley, S.P.E., Pinhasi, R., 2011. A revised chronology for the adoption of agriculture in the Southern Levant and the role of Lateglacial climatic change. Quat. Sci. Rev. 30, 98–108. https://doi.org/10.1016/j.quascirev.2010.09.021

Boyd, M., 2007. Early postglacial history of the southeastern Assiniboine Delta , glacial Lake Agassiz basin. J. Paleolimnol. 37, 313–329. https://doi.org/10.1007/s10933-006-9044-3

Brand, U., McCarthy, F.M.G., 2005. The Allerød-Younger Dryas-Holocene sequence in the west-central Champlain Sea, eastern Ontario: A record of glacial, oceanographic, and climatic changes. Quat. Sci. Rev. 24, 1463–1478. https://doi.org/10.1016/j.quascirev.2004.11.002

Breckenridge, A., 2015. The Tintah-Campbell gap and implications for glacial Lake Agassiz drainage during the Younger Dryas cold interval. Quat. Sci. Rev. 117, 124–134. https://doi.org/10.1016/j.quascirev.2015.04.009

Brock, F., Ramsey, C.B., Higham, T.G., 2007. Quality assurance of ultrafiltred bone dating. Radiocarbon 49, 187–192.

Broecker, W.S., Denton, G.H., Edwards, R.L., Cheng, H., Alley, R.B., Putnam, A.E., 2010. Putting the Younger Dryas cold event into context. Quat. Sci. Rev. 29, 1078–1081. https://doi.org/10.1016/j.quascirev.2010.02.019

Broecker, W.S., Kennett, J.P., Flower, B.P., Teller, J.T., Trumbore, S., Bonani, G., Wolfli, W., 1989. Routing of meltwater from the Laurentide Ice Sheet during the Younger Dryas cold episode. Nature 341, 318–321. https://doi.org/10.1038/341318a0

Bronk Ramsey, C., 2009a. Bayesian Analysis of Radiocarbon Dates. Radiocarbon 51, 337–360. https://doi.org/10.1017/S0033822200033865

Bronk Ramsey, C., 2009b. Dealing with outliers and offsets in radiocarbon dating. Radiocarbon 51, 1023–1045. https://doi.org/10.1017/S0033822200034093

Buck, C.E., Christen, J.A., James, G.N., 1999. BCal: an online Bayesian radiocarbon calibration tool. Internet Archaeol. 7.

Burns, J.A., Young, R.R., 2017. A Tale of Two Floods. How the End of the Ice Age Enhanced Oil Sands Recovery-and Decimated the Fossil Record. In: Alberta's Lower Athabasca Basin: archaeology and palaeoenvironments. Edited by B.M. Rogaghan. AU Press, Edmonton. 25–43. https://doi.org/10.15215/aupress/9781926836904.01 43

Cant, D.J., Walker, R.G., 1978. Fluvial processes and facies sequences in the sandy braided South Saskatchewan River, Canada. Sedimentology 25, 625–648. https://doi.org/10.1111/j.1365-3091.1978.tb00323.x

Carlson, A.E., Clark, P.U., 2012. Ice Sheet Sources of Sea Level Rise and Freshwater Discharge During the Last Deglaciation. Rev. Geophys. 50, https://doi:10.1029/2011RG000371.

Carlson, A.E., Clark, P.U., Haley, B.A., Klinkhammer, G.P., Simmons, K., Brook, E.J., Meissner, K.J., 2007. Geochemical proxies of North American freshwater routing during the Younger Dryas cold event. Proc. Natl. Acad. Sci. 104, 6556-6561. https://doi.org/10.1073/pnas.0611313104

Carlson, A.E., Clark, P.U., Hostetler, S.W., 2009. Comment : Radiocarbon deglaciation chronology of the Thunder Bay , Ontario area and implications for ice sheet retreat patterns. Quat. Sci. Rev. 28, 2546–2547. https://doi.org/10.1016/j.quascirev.2009.05.005

Cheel, R.J., 1982. The depositional history of an esker near Ottawa, Canada. Can. J. Earth Sci. 19, 1417–1427.

Christiansen, E.A., 1979. The Wisconsinan deglaciation of southern Saskatchewan and adjacent areas. Can. J. Earth Sci. 17, 913–938. https://doi.org/10.1139/e80-052

Clark, P.U., Dyke, A.S., Shakun, J.D., Carlson, A.E., Clark, J., Wohlfarth, B., Mitrovica, J.X., Hostetler, S.W., and McCabe, A.M., 2006. the Last Glacial Maximum. Science 325, 710–714. https://doi.org/10.1029/2005GC001226

Clark, P.U., Marshall, S.J., Clarke, G.K.C., Hostetler, S.W., Licciardi, J.M., Teller, J.T., 2001. Freshwater forcing of abrupt climate change during the last glaciation. Science. 293, 283–287. https://doi.org/10.1126/science.1062517

Clayton, L., 1983. Chronology of Lake Agassiz drainage to Lake Superior, In: Teller, J. T. and Clayton, L. Eds, Glacial Lake Agassiz. pp. 291–307.

Clayton, L., Moran, S.R., 1982. Chronology of late wisconsinan glaciation in middle North America. Quat. Sci. Rev. 1, 55–82. https://doi.org/10.1016/0277-3791(82)90019-1

Condron, A., Winsor, P., 2012. Meltwater routing and the Younger Dryas. Proc. Natl. Acad. Sci. 109, 1–6. https://doi.org/10.1073/pnas.1207381109

Cronin, T.M., Rayburn, J.A., Guilbault, J.P., Thunell, R., Franzi, D.A., 2012. Stable isotope evidence for glacial lake drainage through the St. Lawrence Estuary, eastern Canada, ~13.1-12.9 ka. Quat. Int. 260, 55–65. https://doi.org/10.1016/j.quaint.2011.08.041

Davies, L.J., Appleby, P., Jensen, B.J.L., Magnan, G., Mullan-Boudreau, G., Noernberg, T., Shannon, B., Shotyk, W., van Bellen, S., Zaccone, C., Froese, D.G., 2018. High-resolution age modelling of peat bogs from northern Alberta, Canada, using pre- and post-bomb $^{14}C$, $^{210}Pb$ and historical cryptotephra. Quat. Geochronol. 47, 138–162. https://doi.org/10.1016/j.quageo.2018.04.008

Davies, L.J., Jensen, B.J.L., Froese, D.G., Wallace, K.L., 2016. Late Pleistocene and Holocene tephrostratigraphy of interior Alaska and Yukon: Key beds and chronologies over the past 30,000 years. Quat. Sci. Rev. 146, 28–53. https://doi.org/10.1016/j.quascirev.2016.05.026

de Vernal, A., Hillaire-Marcel, C., Bilodeau, G., 1996. Reduced meltwater outflow from the Laurentide ice margin during the Younger Dryas. Nature 381, 774.

Desloges, J.R., Church, M., 1987. Channel and floodplain facies in a wandering gravel-bed river. Recent Dev. Fluv. Sedimentol. - Contrib. from Third Int. Fluv. Sedimentol. Conf. Special P, 99–109.

Domack, E.W., 1984. Rhythmically bedded glaciomarine sediments on Whidbey Island, Washington. J. Sediment. Res. 54, 589–602. https://doi.org/10.1306/212F847C-2B24-11D7-8648000102C1865D

Dyke, A.S., 2004. An outline of North American deglaciation with emphasis on central and northern Canada. Dev. Quat. Sci. 2, 373–424. https://doi.org/10.1016/S1571-0866(04)80209-4

Elson, J.A., 1967. Geology of glacial Lake Agassiz. In: Mayer-Oakes, W.J. (ed.), Life, Land, and Water. University of Manitoba Press, Winnipeg, pp. 37-95. 1967.

Evans, D.J.A., Phillips, E.R., Hiemstra, J.F., Auton, C.A., 2006. Subglacial till: Formation, sedimentary characteristics and classification. Earth-Science Rev. 78, 115–176. https://doi.org/10.1016/j.earscirev.2006.04.001

Evans, D.J.A., Rother, H., Hyatt, O.M., Shulmeister, J., 2013. The glacial sedimentology and geomorphological evolution of an outwash. Sediment. Geol. 284–285, 45–75. https://doi.org/10.1016/j.sedgeo.2012.11.005

Eyles, N., Clark, B.M., Clague, J.J., 1987. Coarse-grained sediment gravity flow facies in a large supraglacial lake. Sedimentology 34, 193–216. https://doi.org/10.1111/j.1365-3091.1987.tb00771.x

Fenton, M.M., Moran, S.R., Teller, J.T., Clayton, L., 1983. Quaternary stratigraphy and history in the southern part of the Lake Agassiz Basin, In: In J.T. Teller & L. Clayton (Eds.), Glacial Lake Agassiz. The Geological Association of Canada. pp. 49–74.

Fisher, T.G., 1996. Sand-wedge and Ventifact Palaeoenvironmental Indicators in Northwest Saskatchewan, Canada, 11 ka to 9.9 ka BP. Permafrost and Periglacial Processes 7, 391–408. https://doi.org/10.1002/(SICI)1099-1530(199610)7:4<391::AID-PPP229>3.0.CO;2-W

Fisher, T.G., 2003. Chronology of glacial Lake Agassiz meltwater routed to the Gulf of

Mexico. Quat. Res. 59, 271–276. https://doi.org/10.1016/S0033-5894(03)00011-5

Fisher, T.G., Lowell, T. V, 2006. Questioning the age of the Moorhead Phase in the glacial Lake Agassiz basin. Quat. Sci. Rev. 25, 2688–2691. https://doi.org/10.1016/j.quascirev.2006.05.007

Fisher, T.G., Lowell, T. V., 2012. Testing northwest drainage from Lake Agassiz using extant ice margin and strandline data. Quat. Int. 260, 106–114. https://doi.org/10.1016/j.quaint.2011.09.018

Fisher, T.G., Lowell, T. V., 2017. Glacial Geology and land-forming events in the Fort McMurray region. Alberta's Low. In: Alberta's Lower Athabasca Basin: archaeology and palaeoenvironments. Edited by B.M. Rogaghan. AU Press, Edmonton, 45–68. https://doi.org/10.15215/aupress/9781926836904.01

Fisher, T.G., Smith, D.G., 1993. Exploration for Pleistocene aggregate resources using process-depositional models in the Fort Mcmurray region, NE Alberta, Canada. Quat. Int. 20, 71–80. https://doi.org/10.1016/1040-6182(93)90037-G

Fisher, T.G., Smith, D.G., 1994. Glacial Lake Agassiz: Its northwest maximum extent and outlet in Saskatchewan (Emerson Phase). Quat. Sci. Rev. 13, 845–858. https://doi.org/10.1016/0277-3791(94)90005-1

Fisher, T.G., Smith, D.G., Andrews, J.T., 2002. Preboreal oscillation caused by a glacial Lake Agassiz flood. Quat. Sci. Rev. 21, 873–878. https://doi.org/10.1016/S0277-3791(01)00148-2

Fisher, T.G., Waterson, N., Lowell, T. V., Hajdas, I., 2009. Deglaciation ages and meltwater routing in the Fort McMurray region, northeastern Alberta and northwestern Saskatchewan, Canada. Quat. Sci. Rev. 28, 1608–1624. https://doi.org/10.1016/j.quascirev.2009.02.003

Fisher, T.G., Yansa, C.H., Lowell, T. V., Lepper, K., Hajdas, I., Ashworth, A., 2008. The chronology, climate, and confusion of the Moorhead Phase of glacial Lake Agassiz: new results from the Ojata Beach, North Dakota, USA. Quat. Sci. Rev. 27, 1124–1135. https://doi.org/10.1016/j.quascirev.2008.02.010

Froese, D., Smith, D., Woywitka, R., 2013. Susan Lake Gravel Pit Catastrophic Flood Deposits and stratigraphy of the lower Athabasca valley, In: Froese, D., Woywitka, R., Andriashek, L. Smith, D. and Atkinson, N. (Eds.) Field Trip Guide to the Quaternary Geology and Geoarchaeology of the Oil Sands Region , NE Alberta. CANQUA Field Trip Guidebook. pp. 23–27.

Grimm, E.C., Maher, L.J., Nelson, D.M., 2009. The magnitude of error in conventional bulk-sediment radiocarbon dates from central North America. Quat. Res. 72, 301–308. https://doi.org/10.1016/j.yqres.2009.05.006

Hamilton, W.D., Kenney, J., 2015. Multiple Bayesian modelling approaches to a suite of radiocarbon dates from ovens excavated at Ysgol yr Hendre, Caernarfon, North Wales. Quat. Geochronol. 25, 72–82. https://doi.org/10.1016/j.quageo.2014.10.001

Hjellbakk, A., 1997. Facies and Fluvial Architecture Of a High-Energy Braided River - the Upper Proterozoic Seglodden Member, Varanger Peninsula, Northern Norway. Sediment. Geol. 114, 131-. https://doi.org/10.1016/S0037-0738(97)00075-4

Howard, J.L., 2010. Late Pleistocene glaciolacustrine sedimentation and paleogeography of southeastern Michigan, USA. Sediment. Geol. 223, 126–142. https://doi.org/10.1016/j.sedgeo.2009.10.006

Johnson, R.G., McClure, B.T., 1976. A model for Northern Hemisphere continental ice sheet variation. Quat. Res. 6, 325–353. https://doi.org/10.1016/0033-5894(67)90001-4

Kehew, A.E., Teller, J.T., 1994. History of late glacial runoff along the southwestern margin of the Laurentide Ice Sheet. Quat. Sci. Rev. 13, 859–877. https://doi.org/10.1016/0277-3791(94)90006-X

Keigwin, L.D., Klotsko, S., Zhao, N., Reilly, B., Giosan, L., Driscoll, N.W., 2018. Deglacial floods in the Beaufort Sea preceded Younger Dryas cooling. Nat. Geosci. https://doi.org/10.1038/s41561-018-0169-6

Klassen, R.W., 1967. Stratigraphy and chronology of Quaternary deposits of Assiniboine River valley and its tributaries. Report of Activities Part B, November 1966 to April 1967; Geol. Surv. of Canada Pap. no. 67-1B, 55–60. https://doi.org/10.4095/106424.

Klassen, R.W., 1983. Lake Agassiz and the late glacial history of northern Manitoba. In: Teller, J. T. and Clayton, L. Eds, Glacial Lake Agassiz, pp. 97-115, Geological Association of Canada Special Paper 26. 97–115.

Klassen, R.W., 1969. Quaternary Stratigraphy and Radicarbon Chronology in Southwestern Manitoba. Geol. Surv. Canada., Paper 69-27, 1-19.

Kuehn, S.C., Froese, D.G., Carrara, P.E., Foit, F.F., Pearce, N.J.G., Rotheisler, P., 2009. Major- and trace-element characterization, expanded distribution, and a new chronology for the latest Pleistocene Glacier Peak tephras in western North America. Quat. Res. 71, 201–216. https://doi.org/10.1016/j.yqres.2008.11.003

Lee, S., Ramsey, C.B., 2012. Development and Application of the Trapezoidal Model for Archaeological Chronologies. Radiocarbon 54, 107–122.

Lemmen, D.S., Duk-Rodkin, A., Bednarski, J.M., 1994. Late glacial drainage systems along the northwestern margin of the Laurentide Ice Sheet. Quat. Sci. Rev. 13, 805–828. https://doi.org/10.1016/0277-3791(94)90003-5

Lepper, K., Buell, A.W., Fisher, T.G., Lowell, T. V., 2013. A chronology for glacial Lake Agassiz shorelines along Upham's namesake transect. Quat. Res. 80, 88–98. https://doi.org/10.1016/j.yqres.2013.02.002

Lepper, K., Gorz, K.L., Fisher, T.G., Lowell, T.V., 2011. Age determinations for glacial Lake Agassiz shorelines west of Fargo, North Dakota, USA. Can. J. Earth Sci. 48, 1199–1207. https://doi.org/10.1139/E11-025

Levac, E., Lewis, M., Stretch, V., Duchesne, K., Neulieb, T., 2015. Evidence for meltwater drainage via the St. Lawrence River Valley in marine cores from the Laurentian Channel at the time of the Younger Dryas. Glob. Planet. Change 130, 47–65. https://doi.org/10.1016/j.gloplacha.2015.04.002

Leverington, D.W., Mann, J.D., Teller, J.T., 2000. Changes in the bathymetry and volume of glacial Lake Agassiz between 11,000 and 930014C yr B.P. Quat. Res. 54, 174–181. https://doi.org/10.1006/qres.2000.2157

Lewis, T., Francus, P., Bradley, R.S., 2009. Recent occurrence of large jökulhlaups at Lake Tuborg, Ellesmere Island, Nunavut. J. Paleolimnol. 41, 491–506. https://doi.org/10.1007/s10933-008-9240-4

Leydet, D.J., Carlson, A.E., Teller, J.T., Breckenridge, A., Barth, A.M., Ullman, D.J., Sinclair, G., Milne, G.A., Cuzzone, J.K., Caffee, M.W., 2018. Opening of glacial Lake Agassiz's eastern outlets by the start of the Younger Dryas cold period. Geology 46, 155–158. https://doi.org/10.1130/G39501.1

Livingstone, S.J., Piotrowski, J.A., Bateman, M.D., Ely, J.C., Clark, C.D., 2015. Discriminating between subglacial and proglacial lake sediments: An example from the Dänischer Wohld Peninsula, northern Germany. Quat. Sci. Rev. 112, 86–108. https://doi.org/10.1016/j.quascirev.2015.01.030

Lønne, I., 1995. Sedimentary facies and depositional architecture of ice-contact glaciomarine systems. Sediment. Geol. 98, 13–43. https://doi.org/10.1016/0037-0738(95)00025-4

Lord, M.L., Kehew, A.E., 1987. Sedimentology and paleohydrology of glacial-lake outburst deposits in southeastern Saskatchewan and northwestern North Dakota. Geol. Soc. Am. Bull., 99, 663–673.

Lowell, T. V, Applegate, P.J., Fisher, T.G., Lepper, K., 2013. What caused the low-water phase of glacial Lake Agassiz ? Quat. Res. 80, 370–382. https://doi.org/10.1016/j.yqres.2013.06.002

Lowell, T. V, Fisher, T.G., Hajdas, I., Glover, K., Loope, H., Henry, T., 2009. Radiocarbon deglaciation chronology of the Thunder Bay , Ontario area and implications for ice sheet retreat patterns. Quat. Sci. Rev. 28, 1597–1607. https://doi.org/10.1016/j.quascirev.2009.02.025

Lowell, T., Waterson, N., Fisher, T., Loope, H., Glover, K., Comer, G., Hajdas, I., Denton, G., Schaefer, J., Rinterknecht, V., Broecker, W., Teller, J., 2009. Reply to comments by Carlson et al ., (2009) on Radiocarbon deglaciation chronology of the Thunder Bay , Ontario area and implications for ice sheet retreat patterns 28, 2548–2550. https://doi.org/10.1016/j.quascirev.2009.06.022

McPherson, J.G., 1987. Fan-deltas and braid deltas: Varieties of coarse-grained deltas. Geol. Soc. Am. Bull. 7606, 331–340. https://doi.org/10.1130/0016-7606(1987)99<331

Miall, A.D., 1977. A review of the braided river depositional environment. Earth-Sciences Rev. 13, 1–62.

Miall, A.D., 1978. Lithofacies types and vertical profile models in braided river deposits: a summary. Fluv. Sedimentol. 5, 597–600.

Miall, A.D., 1985. Architectural-Element Analysis: A New Method of Facies Analysis Applied to Fluvial Deposits. Earth-Science Rev. 22, 261–308. https://doi.org/10.1016/0012-8252(85)90001-7

Moran, S., Clayton, L., Cvancara, A., 1971. New sedimentological and paleontological evidence for history of Lake Agassiz: Snake Curve Section, Red Lake County, Minnesota. Proceedings of the North Dakota Academy of Science 24, 61-73.

Moran, S.R., Clayton, L., Scott, M., Brophy, J., 1973. Catalog of North Dakota radiocarbon dates. North Dakota Geol. Surv. Misc. Ser. 53, 1–51.

Morlan, R.E., McNeely, R., Wolfe, S.A., Schreiner, B.T., 2000. Manitoba radiocarbon dates. Manitoba Ind. Trade, Mines. Manitoba Geol. Surv. Open File Rep. OF2000-1. 198.

Munyikwa, K., Rittenour, T.M., Feathers, J.K., 2017. Temporal constraints for the Late Wisconsinan deglaciation of western Canada using eolian dune luminescence chronologies from Alberta. Palaeogeogr. Palaeoclimatol. Palaeoecol. 470, 147–165. https://doi.org/10.1016/j.palaeo.2016.12.034

Murton, J.B., Bateman, M.D., Dallimore, S.R., Teller, J.T., Yang, Z., 2010. Identification of Younger Dryas outburst flood path from Lake Agassiz to the Arctic Ocean. Nature 464, 740–743. https://doi.org/10.1038/nature08954

Murton, J.B., French, H.M., 1993. Thaw modification of frost-fissure wedges, Richards Island, Pleistocene Mackenzie Delta, Western Arctic Canada. J. Quat. Sci. 8, 185–196. https://doi.org/10.1002/jqs.3390080302

Nielsen, E., Gryba, E.M., Wilson, M.C., 1984. Bison Remains From a Lake Agassiz Spit Complex in the Swan River Valley, Manitoba - Depositional Environment and Paleoecological Implications. Can. J. Earth Sci. 21, 829–842. https://doi.org/10.1139/e84-089

Noakes, J.E., Stipp, J.J., Hood, D.W., 1964. Texas A & M University radiocarbon dates

1. Radiocarbon 6, 189–193.

Ó Cofaigh, C., Dowdeswell, J.A., 2001. Laminated sediments in glacimarine environments: Diagnostic criteria for their interpretation. Quat. Sci. Rev. 20, 1411–1436. https://doi.org/10.1016/S0277-3791(00)00177-3

Owen, G., Moretti, M., 2011. Identifying triggers for liquefaction-induced soft-sediment deformation in sands. Sediment. Geol. 235, 141–147. https://doi.org/10.1016/j.sedgeo.2010.10.003

Pettapiece, W.W., 1986. Physiographic subdivision of Alberta; Agriculture Canada, physiographic map, scale 1:500 000.

Piotrowski, J.A., 2007. Groundwater Under Ice Sheets and Glaciers. Glacier Sci. Environ. Chang. 50–60. https://doi.org/10.1002/9780470750636.ch9

Post, R.., 2003. Stratigraphy and Sedimentology of the Athabasca Group in the Net Lake-Maybelle River Area , Northeastern Alberta. EUB/AGS Earth Sciences Report 2003-01, 1-96.

Rayburn, J.A., Cronin, T.M., Franzi, D.A., Knuepfer, P.L.K., Willard, D.A., 2011. Timing and duration of North American glacial lake discharges and the Younger Dryas climate reversal. Quat. Res. 75, 541–551. https://doi.org/10.1016/j.yqres.2011.02.004

Reimer, P.J., Bard, E., Bayliss, A., Beck, J.W., Blackwell, P.G., Ramsey, C.B., Buck, C.E., Cheng, H., Edwards, R.L., Friedrich, M., Grootes, P.M., Guilderson, T.P., Haflidason, H., Hajdas, I., Hatté, C., Heaton, T.J., Hoffmann, D.L., Hogg, A.G., Hughen, K.A., Kaiser, K.F., Kromer, B., Manning, S.W., Niu, M., Reimer, R.W., Richards, D.A., Scott, E.M., Southon, J.R., Staff, R.A., Turney, C.S.M., van der Plicht, J., 2013. IntCal13 and Marine13 Radiocarbon Age Calibration Curves 0–50,000 Years cal BP. Radiocarbon 55, 1869–1887. https://doi.org/10.2458/azu_js_rc.55.16947

Renssen, H., Mairesse, A., Goosse, H., Mathiot, P., Heiri, O., Roche, D.M., Nisancioglu, K.H., Valdes, P.J., 2015. Multiple causes of the Younger Dryas cold period. Nat. Geosci. 8, 946–949. https://doi.org/10.1038/ngeo2557

Reyes, A. V, Cooke, C.A., 2011. Northern peatland initiation lagged abrupt increases in deglacial atmospheric $CH_4$. Proc. Natl. Acad. Sci. USA. 108, 4748-4753. https://doi.org/10.1073/pnas.1013270108.

Reyes, A. V., Froese, D.G., Jensen, B.J.L., 2010. Permafrost response to last interglacial warming: Field evidence from non-glaciated Yukon and Alaska. Quat. Sci. Rev. 29, 3256–3274. https://doi.org/10.1016/j.quascirev.2010.07.013

Rhine, J.L., 1984. Sedimentological and Geomorphilogical Reconstruction of the Late Pleistocene Athaasca Fan-Delta, Northwast Alberta. Msc. Thesis, University of Calgary, Canada.

Rhine, J.L., Smith, D.G., 1988. The late Pleistocene Athabasca braid delta of northeastern Alberta, Canada. In: W. Nemec, R. Steel Eds, Fan Deltas: Sedimentology and Tectonic Settings, Blackie and Son Ltd, Glasgow, U.K. 159-169.

Rodrigues, C.G., Vilks, G., 1994. The impact of glacial lake runoff on the goldthwait and champlain seas: The relationship between glacial lake agassiz runoff and the younger dryas. Quat. Sci. Rev. 13, 923–944. https://doi.org/10.1016/0277-3791(94)90009-4

Rooth, C., 1982. Hydrology and ocean circulation. Prog. Oceanogr. 11, 131–149. https://doi.org/10.1016/0079-6611(82)90006-4

Roy, S.K., 1972. Fossil wood of Taxaceae from the Mc Murray formation (Lower Cretaceous) of Alberta, Canada. Can. J. Bot. 50, 349–352.

Rubin, M., Alexander, C., 1960. U.S. Geological Survey Radiocarbon Dates V 2, 129–185.

Russell, H. a J., Arnott, R.W.C., 2003. Hydraulic-Jump and Hyperconcentrated-Flow Deposits of a Glacigenic Subaqueous Fan: Oak Ridges Moraine, Southern Ontario, Canada. J. Sediment. Res. 73, 887–905. https://doi.org/10.1306/041103730887

Schillereff, D.N., Chiverrell, R.C., Macdonald, N., Hooke, J.M., 2014. Flood stratigraphies in lake sediments: A review. Earth-Science Rev. 135, 17–37. https://doi.org/10.1016/j.earscirev.2014.03.011

Shotton, F.W., 1972. An example of hard-water error in radiocarbon dating of vegetable matter. Nature 240, 460–461. https://doi.org/10.1038/240460a0

Small, D., Clark, C.D., Chiverrell, R.C., Smedley, R.K., Bateman, M.D., Duller, G.A.T., Ely, J.C., Fabel, D., Medialdea, A., Moreton, S.G., 2017. Devising quality assurance procedures for assessment of legacy geochronological data relating to deglaciation of the last British-Irish Ice Sheet. Earth-Science Rev. 164, 232–250. https://doi.org/10.1016/j.earscirev.2016.11.007

Smith, D.G., 1994. Glacial lake McConnell: Paleogeography, age, duration, and associated river deltas, mackenzie river basin, western Canada. Quat. Sci. Rev. 13, 829–843. https://doi.org/10.1016/0277-3791(94)90004-3

Smith, D.G., Fisher, T.G., 1993. Glacial Lake Agassiz: The northwest outlet and paleoflood. Geol. 21. 9–12.

Smith, N.D., 1978. Sedimentation processes and patterns in a glacier-fed lake with low sediment input. Can. J. Earth Sci. 15, 741–756. https://doi.org/10.1139/e78-081

Sproule, J.C., 1939. The Pleistocene geology of the Cree Lake region, Saskatchewan. R. Soc. Canada Trans. 33, 101–109.

Stipp, J.J., Davis, E.M., Noakes, J.E., Hoover, T.E., 1962. University of Texas

Radiocarbon Dates 1. Radiocarbon 4, 43-50.

Talling, P.J., Masson, D.G., Sumner, E.J., Malgesini, G., 2012. Subaqueous sediment density flows: Depositional processes and deposit types. Sedimentology 59, 1937–2003. https://doi.org/10.1111/j.1365-3091.2012.01353.x

Tarasov, L., Peltier, W.R., 2005. Arctic freshwater forcing of the Younger Dryas cold reversal. Nature, 435, 662–665. https://doi.org/10.1038/nature03617

Taylor, R.S., 1960. Some Pleistocene Lakes of Northern Alberta and Adjacent Areas. J. Alberta Soc. Pet. Geol. 8, 167–178.

Teller, J.T., 1980. Radiocarbon dates in Manitoba. Manitoba Miner. Resour. Div. Geol. Rep. GR80-4. 1–61.

Teller, J.T., 1989. Importance of the Rossendale site in establishing a deglacial chronology along the southwestern margin of the Laurentide ice sheet. Quat. Res. 32, 12–23. https://doi.org/10.1016/0033-5894(89)90028-8

Teller, J.T., 2001. Formation of large beaches in an area of rapid differential isostatic rebound: The three-outlet control of Lake Agassiz. Quat. Sci. Rev. 20, 1649–1659. https://doi.org/10.1016/S0277-3791(01)00007-5

Teller, J.T., 2013. Lake Agassiz during the Younger Dryas. Quat. Res.80, 361–369. https://doi.org/10.1016/j.yqres.2013.06.011

Teller, J.T., Boyd, M., 2006. Two possible routings for overflow from Lake Agassiz during the Younger Dryas. A Reply to Comment by T. Fisher, T. Lowell, H. Loope on “Alternative routing of Lake Agassiz overflow during the Younger Dryas: new dates, paleotopography, a re-evaluation.” Quat. Sci. Rev. 25, 1142–1145. https://doi.org/10.1016/j.quascirev.2006.01.011

Teller, J.T., Boyd, M., Yang, Z., Kor, P.S.G., Fard, A.M., 2005. Alternative routing of Lake Agassiz overflow during the Younger Dryas: New dates, paleotopography, and a re-evaluation. Quat. Sci. Rev. 24, 1890–1905. https://doi.org/10.1016/j.quascirev.2005.01.008

Teller, J.T., Clayton, L., 1983. Glacial Lake Agassiz. Geological Association Canada Special Paper. p. 451.

Teller, J.T., Leverington, D.W., 2004. Glacial Lake Agassiz: A 5000 yr history of change and its relationship to the δ18O record of Greenland. Bull. Geol. Soc. Am. 116, 729–742. https://doi.org/10.1130/B25316.1

Teller, J.T., Leverington, D.W., Mann, J.D., 2002. Freshwater outbursts to the oceans from glacial Lake Agassiz and their role in climate change during the last deglaciation. Quat. Sci. Rev. 21, 879–887. https://doi.org/10.1016/S0277-3791(01)00145-7

Teller, J.T., Riseberg, J., Gaywood, M., Zoltai, S., 2000. Postglacial history and paleoecology of Wampum , Manitoba , a former lagoon in the Lake Agassiz basin. GSA Bulletin 112, 943–958.

Teller, J.T., Thorleifson, L.H., 1983. The Lake Agassiz – Lake Superior connection, In: Teller, J.T. and Clayton, L. Eds, Glacial Lake Agassiz, pp. 261–290.Geological Association Canada, Special Paper, 26.

Thorleifson, L.H., 1996. Review of Lake Agassiz History. In: Teller, J.T., Thorleifson, L.H., Matile, G., and Brisbin, W.C., Eds, Sedimentology, geomorphology and histroy of the central Lake Agassiz basin: Winnipeg, Manitoba, Field Trip Guidebook B2, Geological Association of Canada/Mineralogical Association of Cannada Annual Meeting, May 27-29, 55-84.

Upham, W., 1895. The Glacial Lake Agassiz. U.S. Geol. Surv. Monogr. 25, 658.

van der Meer, J.J.M., Kjær, K.H., Krüger, J., Rabassa, J., Kilfeather, A.A., 2009. Under pressure: clastic dykes in glacial settings. Quat. Sci. Rev. 28, 708–720. https://doi.org/10.1016/j.quascirev.2008.07.017

Vance, R.E., 1986. Pollen stratigraphy of Eaglenest Lake , northeastern Alberta. Can. J. Earth Sci. 23, 11–20. https://doi.org/10.1139/e86-002

Wickert, A.D., Mitrovica, J.X., Williams, C., Anderson, R.S., 2013. Gradual demise of a thin southern Laurentide ice sheet recorded by Mississippi drainage. Nature 502, 668–671. https://doi.org/10.1038/nature12609

Winsemann, J., Lang, J., Polom, U., Loewer, M., Ingel, J., Pollok, L., Brandes, C., 2018. Ice-marginal forced regressive deltas in glacial lake basins: geomorphology, facies variability and large-scale depositional architecture. Boreas.

Wolfe, S. a., Huntley, D.J., Ollerhead, J., 2004. Relict Late Wisconsinan Dune Fields of the Northern Great Plains, Canada. Géographie Phys. Quat. 58, 323. https://doi.org/10.7202/013146ar

Woywitka, R.J., Froese, D.G., Wolfe, S.A., 2017. Raised Landforms in the East-Central Oil Sands Region: Origin, Age, and Archaeological Implications. In: Alberta's Lower Athabasca Basin: archaeology and palaeoenvironments. Edited by B.M. Rogaghan. AU Press, Edmonton. 69–82. doi: 10.15215/aupress/9781926836904.01

Yansa, C.H., Ashworth, A.C., 2005. Late Pleistocene Palaeoenvironments of the Southern Lake Agassiz Basin. J. Quat. Sci, 20, 255–267. https://doi.org/10.1002/jqs.905